https://doi.org/10.15388/vu.thesis.950
https://orcid.org/0009-0003-6476-8721

VILNIUS UNIVERSITY

Karolis Bartkus

Changed Segment Tests on Functional Data

DOCTORAL DISSERTATION

NATURAL SCIENCES,

Mathematics (N 001)

VILNIUS 2026

The dissertation was written between 2019–2025 at Vilnius University.

Academic Supervisor – Prof. Habil. Dr. Alfredas Račkauskas (Vilnius University, Natural Sciences, Mathematics, N 001).

This Doctoral Dissertation will be Defended in a Public Meeting of the Dissertation Defence Panel:
Chairman: Prof. Dr. Jurgita Markevičiūtė (Vilnius University, Natural Sciences, Mathematics, N 001).
Members:

Dr. Jolita Bernatavičienė *(Vilniaus Universitetas, Natural Sciences, Informatics, N 009).*

Prof. Habil. Dr. Vydas Čekanavičius *(Vilniaus Universitetas, Natural Sciences, Mathematics, N 001).*

Assoc. Prof. Dr. Viktor Skorniakov *(Vilniaus Universitetas, Natural Sciences, Mathematics, N 001).*

Prof. Dr. Martin Wendler *(Otto von Guericke University, Germany, Natural Sciences, Mathematics, N 001).*

The dissertation shall be defended at a public meeting of the Dissertation Defence Panel on August 28th, 2026, at 10:00 a.m. in Room 201 of the Faculty of Mathematics and Informatics at Vilnius University.
Address: Naugarduko str. 24, LT03225, Vilnius, Lithuania
Tel. +37052193050: e-mail mif@mif.vu.lt.

https://doi.org/10.15388/vu.thesis.950
https://orcid.org/0009-0003-6476-8721

VILNIAUS UNIVERSITETAS

Karolis Bartkus

Pasikeitusio segmento testai funkcinėje duomenų analizėje

DAKTARO DISERTACIJA

Gamtos mokslai,

Matematika (N 001)

VILNIUS 2026

Disertacija rengta 2019–2025. metais Vilniaus universitete.

Mokslinis vadovas – prof. habil. dr. Alfredas Račkauskas (Vilniaus universitetas, gamtos mokslai, matematika, N 001).

Gynimo taryba:
Pirmininkė – Prof. dr. Jurgita Markevičiūtė *(Vilniaus universitetas, gamtos mokslai, matematika, N 001).*

Nariai:

Dr. Jolita Bernatavičienė *(Vilniaus universitetas, gamtos mokslai, informatika, N 009).*

Prof. habil. dr. Vydas Čekanavičius *(Vilniaus universitetas, gamtos mokslai, matematika, N 001).*

Doc. dr. Viktor Skorniakov *(Vilniaus universitetas, gamtos mokslai, matematika, N 001).*

Prof. dr. Martin Wendler *(Otto von Guericke University, Vokietija, gamtos mokslai, matematika, N 001).*

Disertacija ginama viešame Gynimo tarybos posėdyje 2026 m. rugpjūčio 28 d. 10:00 val. Vilniaus universiteto fakulteto Matematikos ir informatikos fakultete 201 auditorijoje.
Adresas: Naugarduko g. 24, LT03225, Matematikos ir informatikos fakultetas, Vilnius, Lietuva, tel. +37052193050: el. paštas mif@mif.vu.lt.

Contents

Summary

Many modern data sets arrive as ordered sequences: measurements collected over time, observations indexed by space, or records produced by monitoring systems. A central statistical task in such settings is to decide whether the mechanism generating the data remains stable or whether it changes at some point. In numerous applications, deviations are not permanent: the system may depart from its baseline behaviour for a limited period and then return to its original regime. Examples include transient anomalies in sensor networks, temporary shifts in financial or energy markets, short-lived changes in biomedical signals, and classical "epidemics" in public health time series. Such patterns motivate *changed segment* (or *epidemic*) models, where the distribution differs from baseline only on an unknown contiguous interval.

Changed segment model. Let $(\mathbb{S}, \mathcal{S})$ be a measurable space and $X_1, \ldots, X_n$ independent $\mathbb{S}$-valued random elements with distributions $P_{X_1}, \ldots, P_{X_n}$. The starting point is the hypothesis test

$$H_0 : \quad P_{X_1} = \cdots = P_{X_n} = P,$$

against the epidemic alternative

$$H_1 : \quad \exists\, I^* = \{k^* + 1, \ldots, k^* + \ell^*\} \subset \{1, \ldots, n\} \text{ such that}$$
$$P_{X_i} = \begin{cases} P, & i \notin I^*, \\ Q, & i \in I^*, \end{cases} \quad \text{with } P \neq Q.$$

Under H_1, the observations on I^* form a contiguous segment generated from a different distribution. If k^* and ℓ^* were known, the problem would reduce to a two-sample test comparing the "inside" and "outside" samples. In practice, however, both the location and the length of the changed segment are unknown, and an effective procedure must search across many candidate intervals while remaining valid under H_0.

Background and motivation. Classical work on change-point analysis was predominantly parametric, but nonparametric approaches became essential as applications moved beyond simple mean or variance shifts and beyond low-dimensional observations. Early nonparametric contributions include rank-based procedures [36], consistency results under minimal assumptions [12],

and methods based on cumulative sums or empirical likelihood ideas [26, 21, 34]. Epidemic-type alternatives have a long tradition as well [31, 14, 46, 23, 1, 15, 7, 48, 35] and remain an active topic in modern research, including high-dimensional efficiency considerations, multiple epidemic changes, and structured nuisance changes [4, 28, 16, 17].

Two further developments are particularly relevant for this thesis. First, *integral probability metrics* and related discrepancies have become a standard way to compare distributions in a fully nonparametric manner; prominent examples include the Kolmogorov–Smirnov family [43, 10, 41] and kernel-based distances such as maximum mean discrepancy (MMD) [24, 25]. Second, the growth of *functional data analysis* (FDA) has shifted attention to random objects living in infinite-dimensional spaces, such as curves, surfaces, and trajectories. In many applications the observations are naturally functional, or become functional after smoothing and registration, and the ability to detect distributional changes for such data is increasingly important. At the same time, functional observations amplify the methodological challenges of distributional testing: one must control Type I error under complex dependence structures induced by dimension, while retaining power against subtle alternatives.

Aim and guiding questions. This dissertation develops nonparametric methods for detecting epidemic changes in distribution, with a particular emphasis on procedures that

- are formulated on general sample spaces, without restrictive parametric assumptions,
- handle unknown segment locations and lengths via scan-type constructions, and
- extend naturally to Hilbert-space-valued and functional observations.

The work is driven by the following questions:

1. How can one build powerful and provably valid tests for an unknown changed segment when the change may affect the entire distribution (not only moments)?
2. How can two-sample discrepancies (e.g. L_p-type or RKHS distances) be adapted to the epidemic framework across a wide range of segment lengths?

3. How can such procedures be implemented and analysed for functional data living in an infinite-dimensional Hilbert space?

A unifying viewpoint: scanning integral-type discrepancies. A recurring theme of the thesis is that epidemic detection can be formulated as maximising, over all candidate intervals $I(k,\ell) = \{k+1,\dots,k+\ell\}$, a suitably normalised discrepancy between the empirical distributions inside and outside the interval. Writing

$$P_n^I = \frac{1}{|I|}\sum_{i\in I}\delta_{X_i}, \qquad \widehat{P}_n := P_n^{\{1,\dots,n\}},$$

a natural heterogeneity measure is the distance (or seminorm) between $P_n^{I(k,\ell)}$ and $P_n^{I^c(k,\ell)}$. This leads to scan statistics of the form

$$\max_{k,\ell} \frac{\mathcal{N}\Big(\sum_{i=k+1}^{k+\ell}(\delta_{X_i} - \widehat{P}_n)\Big)}{\rho(\ell/n)},$$

where $\mathcal{N}$ is a seminorm on signed measures (possibly random and depending on n) and ρ is a weight controlling how different segment lengths contribute to the limiting distribution and to power. By selecting $\mathcal{N}$ appropriately, this framework covers a broad class of nonparametric two-sample distances and transports them into the epidemic setting. In particular, integral-type semimetrics induced by a function class $\mathcal{F}$,

$$\zeta_{\mathcal{F}}(P,Q) = \sup_{f\in\mathcal{F}} |Pf - Qf|,$$

connect the epidemic problem to a large and well-studied literature on two-sample testing, while raising new technical questions due to the maximisation over (k,ℓ) and the dependence of the outside sample on (k,ℓ).

From finite to infinite dimension: Wilcoxon statistics and Brownian projections. A second main theme concerns functional and Hilbert-space-valued observations. While many classical procedures are naturally formulated for $\mathbb{R}^d$, modern applications often require methods that remain meaningful when d is large or even infinite. In this thesis, we develop Wilcoxon-type statistics built from antisymmetric kernels, extending ideas that connect rank-based testing, U-statistics, and change-point analysis. To obtain robust procedures for functional data, we further employ *Brownian projections* as a principled device to reduce infinite-dimensional objects to informative one-dimensional summaries while retaining nonparametric validity. This projection approach is designed to complement scan statistics: it yields implementable tests for distributional epidemic changes in Hilbert spaces and provides asymptotic theory under the null as well as consistency results under changed segment alternatives.

Contributions of the thesis. The dissertation is based on two published papers and their extensions. Its contributions can be summarised as follows:

- **A general nonparametric epidemic testing framework.** We develop scan statistics based on seminorms of empirical measure differences and weighted normalisation, covering short and long changed segments in a single construction.
- **Extensions of two-sample distances to the changed segment setting.** We show how L_p-type distances and RKHS-based kernel distances can be embedded into the scan framework, and we study their asymptotic behaviour and empirical performance for epidemic alternatives.
- **Distributional epidemic detection for functional data.** We construct Wilcoxon-type tests for Hilbert-space-valued samples using antisymmetric kernels and introduce Brownian projection methodology tailored to epidemic changes in distribution, thereby providing robust procedures for functional time series applications.
- **Practical implementation and applications.** We complement the theory with simulation studies and data examples, including an application to electricity balancing prices, illustrating how distributional changed segments can be detected and interpreted in practice.

Aim and objectives

The aim of this doctoral thesis is to develop and analyse nonparametric methods for detecting *changed segments* (epidemic change-points) in sequences of independent observations, with a particular focus on changes in the *entire distribution* and on extensions to Hilbert-space-valued and functional data. The proposed methodology builds on scan-type constructions that maximise two-sample discrepancies over all candidate intervals, and on robust rank- and projection-based techniques suitable for infinite-dimensional settings.

To achieve this aim, the following objectives are pursued:

1. Formalise the epidemic change-point problem as testing homogeneity of distributions against an unknown contiguous segment of distributional

shift, and relate the task to nonparametric two-sample testing.

2. Develop scan statistics based on seminorms of empirical measure differences, including weighting schemes for a broad range of segment lengths and ensuring valid asymptotic behaviour under the null hypothesis.

3. Extend integral-type and two-sample distances to the changed segment setting, with particular emphasis on L_p-type discrepancies and reproducing kernel Hilbert space (RKHS) distances, and derive their asymptotic properties and consistency under epidemic alternatives.

4. Construct distribution-free, Wilcoxon-type test procedures for Hilbert-space-valued samples using antisymmetric kernels, and study their limiting behaviour under the null and power properties under distributional changes.

5. Introduce and investigate Brownian projection methodology for functional observations, providing implementable procedures for epidemic changes in distribution in a functional time series context.

6. Assess the finite-sample performance of the proposed tests via simulation studies, investigating the effect of segment length, change magnitude, and data dimension/functional complexity on size and power.

7. Demonstrate the practical utility of the methods on real data, including an application to electricity balancing prices, and discuss interpretation of detected changed segments in an applied setting.

Practical and scientific novelty

This doctoral thesis contributes new theory and methodology for *nonparametric* detection of *changed segments* (epidemic change-points) in sequences of independent observations, with emphasis on changes in the *entire distribution* rather than only in moments. The developed procedures unify scan-type epidemic testing with modern two-sample discrepancies and extend naturally to Hilbert-space-valued and functional data.

From the **scientific** perspective, the novelty of the thesis lies in:

1. **A unified scan framework based on seminorms of empirical measure differences.** The epidemic testing problem is formulated via maximising, over all candidate intervals, normalised seminorms of partial-sum signed measures $\sum_{i\in I(k,\ell)}(\delta_{X_i} - \widehat{P}_n)$, leading to a general class of test

statistics that cover multiple nonparametric distances within a single construction.

2. **Extension of integral-type and kernel two-sample distances to the epidemic setting.** The thesis adapts L_p-type discrepancies and RKHS-based distances (including kernel-induced integral probability metrics) from two-sample testing to changed segment detection, and provides asymptotic justification and consistency results under epidemic alternatives.

3. **Wilcoxon-type changed-segment tests in Hilbert spaces.** Building on antisymmetric-kernel constructions, the thesis develops rank-based (Wilcoxon) procedures for Hilbert-space-valued observations, yielding robust nonparametric tests for high-dimensional and functional data.

4. **Brownian projection methodology for functional epidemic changes in distribution.** A further methodological contribution is the use of Brownian projections to obtain implementable and robust procedures for detecting temporary distributional changes in functional samples, connecting functional data methodology with epidemic change-point testing in a new way.

From the **practical** perspective, the novelty is that the proposed methods:

1. **Detect temporary distributional departures without parametric models.** The tests apply when the change is unknown and may affect the full distribution; they suit complex data where mean- or variance-based methods fall short.

2. **Handle unknown segment location and length.** The scan statistics are designed to search across all contiguous candidate intervals and employ weighting schemes to remain effective for a broad range of changed segment lengths, including short epidemic events.

3. **Extend to functional observations encountered in modern applications.** By working in Hilbert spaces and using projection-based implementations, the procedures are applicable to curve-valued data and other infinite-dimensional objects arising in areas such as energy markets, biomedical monitoring, environmental studies, and finance.

4. **Are accompanied by implementable algorithms and empirical validation.** The thesis provides practical guidance for implementation, investigates finite-sample size and power through simulations, and illustrates applicability on real data, including electricity balancing prices.

Overall, the thesis advances epidemic change-point methodology by combining rigorous nonparametric theory with practical procedures that remain effective in high-dimensional and functional settings and are directly applicable to real-world monitoring problems.

Layout of the doctoral thesis

The dissertation consists of a summary and introductory material, eight main chapters, and a bibliography. The structure reflects the methodological flow of the thesis: first introducing the functional and probabilistic framework, then developing projection tools for functional observations, then presenting three complementary classes of nonparametric changed-segment tests, and finally collecting simulation studies, the real-data application, and concluding remarks.

* **Chapter 1: Introduction.** This chapter introduces the main statistical setting and reviews background material needed throughout the thesis. It includes (i) a brief introduction to Functional Data Analysis, with emphasis on functional data reconstruction and smoothing (including the Faber–Schauder basis), (ii) an overview of changed segment (epidemic) detection and its links to nonparametric two-sample testing, and (iii) the weight class $\mathcal{R}$ used to balance segment length.

* **Chapter 2: Dimensionality reduction.** This chapter develops projection and dimensionality-reduction tools that enable implementable procedures for functional observations. It presents Brownian projections as a key device for robust reduction of infinite-dimensional data, and introduces an additional projection approach (the C-projection) used later in the construction of functional test statistics.

* **Chapter 3: Changed segment tests based on antisymmetric kernels.** This chapter develops Wilcoxon-type tests built from antisymmetric kernels in Hilbert spaces. After introducing the statistics and the main theoretical results, it proposes Brownian-projection variants and discusses their structural properties; the corresponding finite-sample power studies are reported in Chapter 6.

* **Chapter 4: Changed segment tests based on L_p-type statistics.** This chapter extends L_p-type integral discrepancies from the two-sample setting to the epidemic framework. It establishes the main theoretical results under the null and under changed segment alternatives; the simulation studies illustrating the impact of segment length and change magnitude on power are collected in Chapter 6.

* **Chapter 5: Changed segment tests based on RKHS.** This chapter investigates RKHS-based procedures, including kernel distances and scan statistics motivated by maximum mean discrepancy ideas. It provides the theoretical underpinning of the proposed tests; numerical comparisons of kernel choices and the strengths of RKHS methods for distributional changes are reported in Chapter 6.

* **Chapter 6: Simulation studies.** This chapter centralises the Monte Carlo evaluation of the three families of tests proposed in Chapters 3–5. It documents the simulation design, the scalar and functional alternatives, the segment-length regimes, and the resulting empirical levels and powers.

* **Chapter 7: Application to Lithuanian electricity balancing prices.** This chapter demonstrates the practical applicability of the methodology on real data. It describes the data and motivation, outlines functional representation and pre-processing steps, presents the testing framework used in the application, and discusses the empirical results and their interpretation.

* **Chapter 8: Concluding remarks and future work.** The final chapter summarises the main theoretical and empirical conclusions of the dissertation and outlines potential directions for further research, including methodological extensions and additional application domains.

Maintaining statements

1. The proposed projections extend classical methods to functional data analysis framework.

2. The limit distributions of the test statistics are established.

3. Statistical tests for detecting an epidemic-type change are developed.

4. Application of the tests to Lithuanian electricity balancing prices demonstrates their practical utility.

Dissemination of results

Publications

A1 Bartkus, K.; Račkauskas, A. Changed segment tests via norm and Brownian projection. *Lith Math J* **2025**, *65*, 481–499.
doi.org/10.1007/s10986-025-09699-7.

A2 Bartkus, K.; Račkauskas, A. Nonparametric changed segment detection in functional data. *Nonlinear Analysis: Modelling and Control* **2026**, *31(1)*, 194–211.
doi.org/10.15388/namc.2026.31.44489.

Conferences

C1 Bartkus, K. Change segment detection in functional sample via projections to Wiener process. *64th Conference of Lithuanian Mathematical Society, (Vilnius)* **2023 June**.

C2 Bartkus, K. Nonparametric changed segment detection in functional data. *66th Conference of Lithuanian Mathematical Society, (Klaipėda)* **2025 June**.

C3 Bartkus, K. Changed segment tests via norm and Brownian projection. *1st Int. Vilnius Conference on Statistics and Its Applications (ICSA 2025)* **27–29 August 2025**.

C4 Bartkus, K. Changed segment tests via C-type projection. *25th European Young Statisticians Meeting (EYSM 2026), Vilnius* **7–10 July 2026**.

Main results

The dissertation develops nonparametric procedures to detect *changed segments* (epidemic alternatives) in ordered scalar-, vector-, and function-valued samples. The main theoretical contributions are summarised as follows.

1. **Kernel-type scan statistics and Brownian-bridge limits.** For a finite collection of antisymmetric kernels $h : \mathcal{S} \times \mathcal{S} \to \mathbb{R}$ and scan statistics based on associated U–process increments over candidate intervals, we establish weak convergence under H_0 and derive the asymptotic null

distribution of the maximised scan statistic as a functional of a (possibly multivariate) Brownian bridge. This yields a general limit theory that covers distribution-free rank-type constructions as special cases.

2. **Wilcoxon-type changed-segment tests via projections and norms.** For functional observations $X_i \in C[0,1]$, we introduce Wilcoxon-type scan tests that combine (i) projections of functional data onto low-dimensional directions (including Brownian-type projection schemes) with (ii) aggregation by either a Euclidean norm or a coordinate-wise maximum. Under H_0, the resulting statistics admit tractable Brownian-bridge limits; under changed-segment alternatives they are consistent when the projected signal is non-degenerate.

3. **L_p-type (Cramér–von Mises) scan tests.** We construct L_p-type scan statistics that quantify distributional deviations via integrated empirical-process increments. Under H_0 the weak limits are functionals of a two-parameter Gaussian process (Brownian sheet / bridge-type). The procedure stays sensitive across short and long segments through an explicit scan range and a stabilising weight ρ.

4. **RKHS distance scan tests.** Using reproducing kernel Hilbert space (RKHS) embeddings, we propose scan statistics based on kernel mean (and related) distances. Under moment and tail conditions, we prove weak convergence under H_0 to functionals of a Q–Wiener process in the RKHS, yielding a nonparametric tool that is sensitive to general changes in distribution (not restricted to mean shifts).

5. **Localisation of the changed segment.** For each family of scan statistics, maximising over candidate intervals yields an endpoint estimator. Under fixed alternatives, it localises the true epidemic segment in probability (up to scan-grid constraints used in implementation).

Simulation and application results

The finite-sample performance of the proposed changed-segment procedures is investigated by Monte Carlo experiments and illustrated on a real functional time series of Lithuanian electricity balancing prices.

Simulation results. The simulation study has two goals: (i) to assess calibration under the null hypothesis H_0 (empirical size), and (ii) to compare power under a range of epidemic alternatives that vary by segment length, signal strength, and the type of distributional departure. In all considered settings, rejection probabilities increase with the effect size and with the length of the changed segment. The scan-range restriction (and the stabilising weight function ρ, where applicable) governs the trade-off between sensitivity to short epidemic intervals and stability for long intervals: too wide a scan range can dilute power against short segments, whereas too narrow a scan range reduces sensitivity to longer segments.

The experiments further indicate that different statistics excel for different alternatives. Projection- and norm-based Wilcoxon scans are competitive when the change has a pronounced low-dimensional structure and tend to be robust in heavy-tailed settings. L_p-type statistics provide stable power over a broad class of alternatives, including moderate deviations spread over many coordinates or time points. RKHS-based distances are particularly effective for general distributional changes that are not well described by mean shifts or a small number of principal directions. Overall, the simulated size is close to the nominal level after the proposed normalisation and critical-value calibration, with the largest deviations occurring for very small samples and extremely heavy-tailed designs.

Application results. A real-data analysis of Lithuanian electricity balancing prices demonstrates the practical use of the methodology in functional settings. After reconstructing daily price curves and applying a mild smoothing / basis representation to obtain functional observations in $C[0, 1]$, the scan statistics identify time intervals consistent with an epidemic-type departure. The detected segments are interpretable in terms of market behaviour and remain qualitatively stable under reasonable changes of preprocessing choices (e.g., smoothing level, basis truncation, and projection dimension), and the conclusions are supported by several complementary test families.

1. Introduction

This thesis studies nonparametric detection of *changed segments* (also called *epidemic change-points*) in ordered samples. The statistical goal is to test whether the distribution is stable throughout the sample, or whether it differs on an unknown contiguous interval and then returns to baseline. While classical epidemic tests often target changes in moments (mean/covariance), our focus is on *distributional* changes and on methods that remain applicable when observations are functions.

The chapter is organised as follows. Section 1.1 recalls the functional-data setting and the reconstruction step for obtaining curves in $C[0,1]$ from noisy grid data. Section 1.2 introduces the changed-segment testing problem, fixes the standing hypotheses (1.1)–(1.2), and reviews the relevant nonparametric literature. Section 1.3 introduces the weight class $\mathcal{R}$ used to scale the scan statistics in subsequent chapters.

1.1. Functional Data Analysis

Next, we define Faber-Schauder basis, which will be used to reconstruct functional data.

1.1.1. Functional data reconstruction

A random functional sample is a collection of stochastic processes

$$X_i = \big(X_i(t),\, t \in [0,1]\big), \qquad i = 1, \ldots, n,$$

defined on a probability space $(\Omega, \mathcal{F}, P)$. In practice, one cannot observe an entire stochastic process. The data usually have the form

$$x_i(j/m) = X_i(j/m, \omega) + \varepsilon_{ij}, \qquad j = 1, \ldots, m;\ i = 1, \ldots, n,$$

with sample paths $X_1(\omega), \ldots, X_n(\omega)$ and measurement errors ε_{ij}. Smoothing reconstructs the paths $(X_i(t,\omega),\, t \in [0,1])$, reducing noise and improving test power.

1.1.2. Smoothing with Faber–Schauder basis

We use the Faber–Schauder basis to reconstruct the observations. Path-wise Brownian projection requires the paths to lie in the Hölder-type space $H_\alpha^o[0,1]$, $\alpha \in [0, 1/2)$ (precise definition see in Section 3.2). The Faber–Schauder basis is a basis in any such Hölder space.

Definition of the Faber–Schauder Basis Functions

At level $n = 0$ we include the constant and the identity function

$$\psi_{0,0}(t) = 1, \quad \psi_{0,1}(t) = t, \quad t \in [0, 1].$$

For $n \geq 1$ and $k = 1, \dots, 2^n$, define

$$\psi_{n,k}(t) = \begin{cases} 2^n\big(t - \frac{k-1}{2^n}\big), & t \in \big[\frac{k-1}{2^n}, \frac{k}{2^n}\big), \\ 2^n\big(\frac{k+1}{2^n} - t\big), & t \in \big[\frac{k}{2^n}, \frac{k+1}{2^n}\big), \\ 0, & \text{otherwise.} \end{cases}$$

These piecewise linear functions form a Schauder basis for $C([0, 1])$; hence every $f \in C([0, 1])$ admits the expansion

$$f(t) = \alpha_{0,0}\, \psi_{0,0}(t) + \alpha_{0,1}\, \psi_{0,1}(t) + \sum_{n=1}^{\infty} \sum_{k=1}^{2^n} \alpha_{n,k}\, \psi_{n,k}(t).$$

This representation captures different levels of detail through simple linear "hats."

Expansion of the Functional Observations

Given a random sample $\{X_1, \dots, X_n\}$ from a stochastic process on $[0, 1]$ observed at $\{t_j\}_{j=1}^m$, approximate $X_i(t)$ by

$$X_i(t) \approx \beta_{i,0,0}\, \psi_{0,0}(t) + \beta_{i,0,1}\, \psi_{0,1}(t) + \sum_{n=1}^{N} \sum_{k=1}^{2^n} \beta_{i,n,k}\, \psi_{n,k}(t),$$

where $\beta_{i,n,k}$ are coefficients and N controls the resolution. As $N \to \infty$, the series converges to X_i in the strong topology of $C([0, 1])$, and hence also in all Hölder spaces $H^\alpha[0, 1]$ with $\alpha \in (0, 1)$. A finite N retains key features while suppressing high-frequency noise.

Estimating the Faber–Schauder Coefficients

Since the functions $X_i(t)$ are observed at discrete points $\{t_j\}$, let $X_i(t_j)$ denote the measured values. The coefficients $\beta_{i,n,k}$ can be found by minimising the standard least squares objective

$$\min_{\{\beta_{i,n,k}\}} \sum_{j=1}^{m} \Big(X_i(t_j) - \beta_{i,0,0}\, \psi_{0,0}(t_j) - \beta_{i,0,1}\, \psi_{0,1}(t_j) \\ - \sum_{n=1}^{N} \sum_{k=1}^{2^n} \beta_{i,n,k}\, \psi_{n,k}(t_j) \Big)^2.$$

Increasing the resolution level N captures finer features, but may also introduce more observation noise. It can be seen in Figure 1.1 how different N levels are able to approximate

$$f_\alpha(x) = \left(1 - \left|x - \frac{1}{2}\right|^\alpha\right)^{\frac{1}{\alpha}}, \quad x \in [0,1], \quad \alpha \in [0, 1/2).$$

Choice of resolution in practice. The literature on wavelet-like orthogonal series smoothers offers several practical rules for choosing N, and the Faber–Schauder basis inherits most of them because it is a classical Schauder basis with the same dyadic scaling as the Haar wavelet (see [13, 29]). Two guidelines suffice in the present work. *(i) Sampling budget.* With m observations per curve, the number of free coefficients is at most 2^{N+1}; to avoid exact interpolation of noise, practitioners choose N so that $2^{N+1} \ll m$. The rule of thumb $N = \lfloor \log_2 m \rfloor - c$ with $c \in \{1, 2, 3\}$ is widely used in wavelet smoothing (cf. [18]). *(ii) Smoothness of the target.* When the unknown curve belongs to a Hölder ball H^α_∞ with $\alpha \in [0, 1/2)$ (the regime relevant for Brownian-projection arguments on rough paths), the projection onto the first N levels has mean-squared error of order $2^{-2N\alpha}$; balancing this bias against the $O(2^N/m)$ variance suggests $N \asymp \log_2(m^{1/(2\alpha+1)})$, which matches the usual minimax trade-off for Besov-type classes. In the simulations and the real-data study of this dissertation we use small fixed $N \in \{3, 4, 5\}$, which empirically keeps reconstruction noise low while retaining enough resolution for Brownian-projection arguments on Hölder paths.

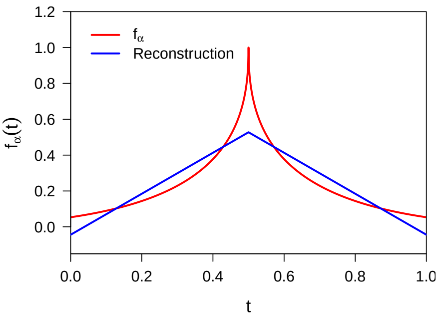

(a) $N = 1$

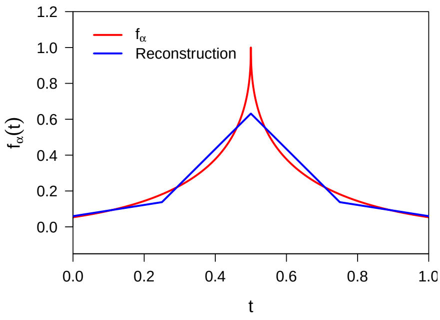

(b) $N = 2$

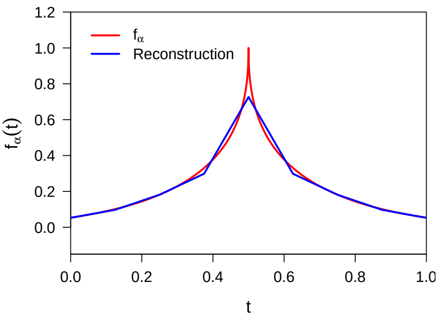

(c) $N = 3$

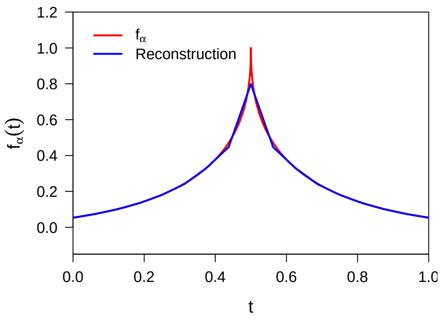

(d) $N = 4$

Figure 1.1: Smoothing the spike function f_α with $\alpha = 0.45$ via the Faber–Schauder basis at resolution levels $N \in \{1, 2, 3, 4\}$.

Reconstruction of Functional Data

Once the coefficients $\widehat{\beta}_{i,n,k}$ are obtained, the reconstructed function $\tilde{X}_i(t)$ is given by the partial sum:

$$\tilde{X}_i(t) \;=\; \widehat{\beta}_{i,0,0}\,\psi_{0,0}(t) + \widehat{\beta}_{i,0,1}\,\psi_{0,1}(t) + \sum_{n=1}^{N}\sum_{k=1}^{2^n} \widehat{\beta}_{i,n,k}\,\psi_{n,k}(t).$$

The reconstruction step converts each observational unit into a single curve, so the data become an ordered sample in a function space. Once in this form, the changed-segment problem can be posed at the level of distributions on the function space: we test whether all curves are generated from the same distribution, versus a temporary distributional departure on an unknown interval.

1.2. Changed segment detection

Let $X_1, X_2, \ldots, X_n$ be independent random elements in a sample space $(\mathbb{S}, \mathcal{S})$ with distributions $P_{X_1}, P_{X_2}, \ldots, P_{X_n}$. We test the null hypothesis

$$H_0 : P_{X_1} = P_{X_2} = \cdots = P_{X_n} = P, \tag{1.1}$$

versus the alternative

$$\begin{aligned} H_1 :\ & \text{there is a segment} \\ & \quad I^* := \{k^*+1, \ldots, m^*\} \subset I_n := \{1, 2, \ldots, n\} \\ & \text{such that} \\ & P_{X_i} = \begin{cases} P & \text{for } \ i \in I_n \setminus I^* \\ Q & \text{for } \ i \in I^*, \end{cases} \quad \text{and } \ P \neq Q. \end{aligned} \tag{1.2}$$

In other words, under (1.2) there is a contiguous segment I^* (of length $\ell^* = m^* - k^*$) on which the distribution changes to $Q \neq P$. Such epidemic change models, in which the process reverts to the baseline P after a temporary shift to Q, frequently arise in epidemiological contexts. The hypothesis pair (1.1)–(1.2) is the standing problem of this dissertation; subsequent chapters reuse these labels rather than restating the hypotheses.

Early work on change point analysis was largely parametric. In the non-parametric framework, Pettitt [36] adapted the Mann-Whitney test to detect a single change in a univariate setting, while Carlstein [12] introduced non-parametric methods for strong consistency of estimated change points under minimal assumptions. Approaches involving cumulative sums of squares (Inclan and Tian [26]) or empirical likelihood techniques (Einmahl and McKeague [21]; Ning [34]) further expanded nonparametric change point tools. In an epidemic setting, Levin and Kline [31] studied a two-phase mean change that returns later to baseline, and Commenges, Seal, and Pinatel [14] introduced epidemic-type models in neurophysiology. Subsequent parametric and nonparametric research includes Lombard [32], Gombay [23], Siegmund [42], Yao [46], Antoch and Hušková [1], Csörgö and Horváth [15], Avery [7], Avery and Henderson [6], Zuokas [48], and others. Ning et al. [35] proposed a distribution-free epidemic test based on empirical likelihood ratio statistics, estimating start and end points of the temporary distributional departure.

In the last decade, works on epidemic change models remain an active area of research across both parametric and nonparametric frameworks. Aston and Kirch [4] introduced the concept of high-dimensional efficiency to compare change-point tests, including extensions to epidemic alternatives. Zhao and Yau [47] developed alternating pruned dynamic programming for multiple epidemic change-points. Juodakis and Marsland [28] proposed a two-level detector handling epidemic segments in the presence of nuisance changes. Diop and Kengne [16, 17] extended epidemic detection to causal and integer-valued time series via QMLE-based statistics. Other recent contributions include Fisch et al. [22] on collective anomaly detection and application in astronomical data, and Jin, Han and Wu [27] on simultaneous estimation of epidemic changes. Closest to the present work in setting and language, Birbilas [11] developed an epidemic-change test $E_{n,\beta,\gamma}$ for functional data based on weighted partial sums of recentred curves; we adopt his FAR(1) data-generating process as the F4 benchmark scenario in Section 6.1.2 and compare against $E_{n,\beta,\gamma}$ directly. However, these epidemic change tests focus on mean or covariance changes. To our knowledge, there are no established nonparametric epidemic tests designed for *distributional* changes in functional data. We are inspired to use dimensionality reduction by the recent line of work on functional change-point analysis (Berkes et al.[8], Aue et al.[5], Aston and Kirch[3]). Although we do not exhaustively review all functional change point literature, the references above illustrate this framework's development in both parametric and nonparametric forms.

1.3. The weight class $\mathcal{R}$

The asymptotic theory developed in this and the following chapters relies on a fixed family of weighting functions $\rho : (0, 1) \to \mathbb{R}$. We collect this family into a class $\mathcal{R}$ and use $\mathcal{R}$ as the standing notation throughout the dissertation.

Definition 1 (Weight class $\mathcal{R}$)**.** *The class $\mathcal{R}$ consists of all functions $\rho : (0, 1) \to \mathbb{R}$ that satisfy*

i) for some $0 < \alpha \leq 1/2$ and some function L which is normalised slowly varying at infinity,

$$\rho(s) = s^{\alpha} L(1/s), \quad 0 < s \leq 1;$$

ii) $\theta(t) = t^{1/2}\rho(1/t)$ is C^1 on $[1, \infty)$;

iii) there exist $\beta > 1/2$ and $a > 0$ such that $\theta(t) \log^{-\beta}(t)$ is non-decreasing on $[a, \infty)$.

Unless stated otherwise, throughout the remainder of the dissertation ρ denotes a function belonging to the class $\mathcal{R}$.

The class $\mathcal{R}$ includes, in particular, the polynomial weights $\rho_\gamma(t) = t^\gamma$ with $0 \leq \gamma < 1/2$ and the boundary-logarithmic weights $\rho_{0.5,\beta}(t) = t^{1/2} \log^{\beta}(c/t)$, $t \in (0, 1)$, with $\beta > 1/2$.

On the role and lineage of ρ. The class $\mathcal{R}$ and the ρ_γ weighting are not introduced here for the first time: they originate in the Hölder-norm scan literature and, in the epidemic setting, go back to [40, 37], where they served to control short and long segments uniformly and to yield a non-degenerate weak limit in Hölder space. The role of ρ in those works is dual. First, it re-scales candidate segments of very different lengths so that the scan statistic is not dominated by the longest windows, which makes the test sensitive to short epidemic segments (and hence, for example, γ close to $1/2$ is preferred when the change is localised). Second, the condition $\rho \in \mathcal{R}$ is precisely what is needed for the functional CLT in the corresponding Hölder space (class condition (iii) rules out the critical $\beta = 1/2$ logarithmic rate that would place ρ on the boundary of the Hölder modulus). The contribution of this dissertation is therefore not the weighting mechanism itself, but rather the application of the class $\mathcal{R}$ weighting to new scan statistics (antisymmetric-kernel and RKHS-based tests) for which the corresponding functional CLT in $\mathcal{H}^o_\rho$ had not been established.

2. Dimensionality reduction

Most scan statistics for changed-segment detection are formulated for real-valued or low-dimensional vector observations. In functional applications, however, each X_i is a curve observed on a grid with noise, so two additional steps are needed before distributional scan statistics become implementable.

Classical functional principal component analysis (FPCA) is widely used for L_2-based functional models (see, e.g., [30]). In this dissertation we primarily work with representations compatible with $C[0,1]$ and with projection schemes that lead to tractable weak limits for the scan statistics developed later.

This chapter provides the reduction tools used throughout the thesis. First, we reconstruct smooth curves in $C[0,1]$ from discrete measurements. Second, we map curves to informative low-dimensional summaries using projection devices. These summaries serve as inputs to the scan statistics developed in subsequent chapters: antisymmetric-kernel Wilcoxon scans (Chapter 3), L_p-type empirical-process scans (Chapter 4), and RKHS-based scans (Chapter 5).

Two complementary strategies used in this manuscript.

1. *Basis representations and truncation* (e.g., multiresolution bases) convert curves into coefficient vectors that retain local features while enabling robust estimation and fast computation.

2. *Projection methods* map curves to $\mathbb{R}$ or $\mathbb{R}^d$ via point evaluations or random (Brownian-type) projections, enabling univariate or multivariate scan statistics.

2.1. Brownian projections

Let $\mathbb{H}$ be a real separable Hilbert space with an inner product $\langle x, y\rangle$ and the norm $||x|| = \sqrt{\langle x, x\rangle}$, $x, y \in \mathbb{H}$.

Recall that an $\mathbb{H}$-isonormal Gaussian process is a family $\mathrm{W} = \{\mathrm{W}(x)\colon\ x \in \mathbb{H}\}$ of real-valued random variables, defined on a common probability space $(\Omega, \mathcal{F}, \mathrm{P})$, such that $\mathrm{W}(x)$ is a Gaussian random variable for all $x \in \mathbb{H}$ and, for $x, y \in \mathbb{H}$, we have $E(\mathrm{W}(x)\mathrm{W}(y)) = \langle x, y\rangle$. It is well known that such process exists and it is linear in a sense that $\mathrm{W}(ah + bg) = a\mathrm{W}(h) + b\mathrm{W}(g)$ in distribution.

Definition 2 (Brownian projection)**.** *Let $\mathbb{H}$ be a real separable Hilbert space and let $\mathrm{W} = \{\mathrm{W}(x)\colon\ x \in \mathbb{H}\}$ be an $\mathbb{H}$-isonormal Gaussian process. For a* *fixed* $x \in \mathbb{H}$*, the* Brownian projection *of* x *is the real Gaussian random variable* $\mathrm{W}(x)$*. For a finite sample* $x_1, \ldots, x_n \in \mathbb{H}$*, a Brownian projection of the sample is the jointly Gaussian vector* $(\mathrm{W}(x_1), \ldots, \mathrm{W}(x_n))$ *with mean zero and covariance* $\mathrm{Cov}(\mathrm{W}(x_i), \mathrm{W}(x_j)) = \langle x_i, x_j \rangle$*. In the implementation, independent projections are obtained by drawing independent copies* $\mathrm{W}_1, \ldots, \mathrm{W}_d$ *of the isonormal process. In infinite-dimensional* $\mathbb{H}$ *this construction should be understood through the finite collection of evaluated sample points rather than as a single almost-surely continuous linear functional on all of* $\mathbb{H}$*.*

Example 1. *In the case where* $\mathbb{H} = L_2([0,1], \lambda)$*, one takes*

$$\mathrm{W}(x) = \int_0^1 x \mathrm{d}W, \quad x \in L_2([0,1], \lambda),$$

where $W = (W(t), t \in [0,1])$ *is a standard Wiener process and the integral is in the Itô sense, and so* $\mathrm{W} = \{\mathrm{W}(x) : x \in L_2([0,1], \lambda)\}$ *is the isonormal Gaussian process on the Hilbert space* $L_2([0,1], \lambda)$ *[19]. If* $x \in H^o_\alpha[0,1]$ *with* $\alpha \in (1/2, 1)$*, then the integral can be defined path-wise (see Proposition 1.3, [20] for details.)*

Relation to the next example. Although both constructions yield isonormal Gaussian processes on an L_2-type Hilbert space, they should not be conflated. In Example 1 the integral is the deterministic-integrand Wiener–Itô integral with respect to a standard Wiener process on $[0,1]$. In particular, for $A \in \mathcal{B}([0,1])$,

$$\mathrm{W}(\mathbf{1}_A) = \int_0^1 \mathbf{1}_A(t)\,\mathrm{d}W(t)$$

is a centred Gaussian random variable with variance $\lambda(A)$, where λ denotes Lebesgue measure. In Example 2 one starts instead from an independently scattered Gaussian random measure G on a general measure space $(\mathbb{S}, \mathcal{S}, \mu)$; then $G(A)$ is centred Gaussian with variance $\mu(A)$. Thus, in the special case $\mathbb{S} = [0,1]$ and $\mu = \lambda$, the random variables $\mathrm{W}(\mathbf{1}_A)$ and $G(A)$ have the same distribution, and they may be identified if G is constructed from the same Wiener process. The second example is stated separately because it also covers general Polish spaces $\mathbb{S}$.

Example 2. *Consider the Polish measure space* $(\mathbb{S}, \mathcal{S}, \mu)$*, where* $\mathbb{S}$ *is a Polish space,* $\mathcal{S}$ *is the associated Borel* σ*-algebra and the measure* μ *is positive,* σ*-finite and non-atomic. In this setting* $\mathbb{H} = L_2(\mathbb{S}, \mathcal{S}, \mu)$ *is separable Hilbert space. Let* G *be a Gaussian random measure over* $(\mathbb{S}, \mathcal{S})$ *with control measure*

μ. For every $h \in L_2(\mathbb{S}, \mathcal{S}, \mu)$ define

$$\mathrm{W}(h) := \int_{\mathrm{S}} h(s)\mathrm{d}G(s).$$

Then $\mathrm{W} = (\mathrm{W}(h), h \in L_2(\mathbb{S}, \mathcal{S}, \mu))$ is an isonormal Gaussian process.

Example 3. *Isonormal Gaussian process derived from covariances might be an interesting example. Construction is as follows. Consider $Y = (Y_t, t \geq 0)$ a centred real-valued Gaussian process with covariance*

$$R_Y(s,t) = E(Y_s Y_t), \quad s,t \in [0,\infty).$$

Let $\mathcal{E}$ be a collection of all finite linear combinations of indicators $\mathbf{1}_{[0,t]}, t \geq 0$. Define $\mathbb{H}$ to be the Hilbert space given by the closure of $\mathcal{E}$ with respect to the inner product

$$\langle f, g \rangle = \sum_{i,j} a_i b_j R_Y(s_i, t_j),$$

where $f = \sum_i a_i \mathbf{1}_{[0,s_i]}$, $g = \sum_j b_j \mathbf{1}_{[0,t_j]}$. Now for $h = \sum_j c_j \mathbf{1}_{[0,t_j]}$ set

$$\mathrm{W}(h) = \sum_j c_j Y_{t_j}$$

whereas for $h \in \mathbb{H}$ set $\mathrm{W}(h)$ to be the L_2 limit of any sequence $(\mathrm{W}(h_n))$, where $(h_n) \subset \mathcal{E}$ converge to h in $\mathbb{H}$. Then $(\mathrm{W}(h), h \in \mathbb{H})$ is an isonormal Gaussian process.

2.2. Point evaluation projections in $C[0,1]$

Let $X_1, \ldots, X_n$ be a sample of continuous curves, $X_i \in C[0,1]$. A simple projection maps each function to a real number by evaluation at a fixed location $t_0 \in (0,1)$:

$$P_{t_0} : C[0,1] \to \mathbb{R}, \qquad P_{t_0}(f) = f(t_0).$$

Consequently, the functional sample $\{X_i\}_{i=1}^n$ is transformed into the univariate sample $\{X_i(t_0)\}_{i=1}^n$ and classical univariate scan statistics become applicable. Point evaluations are particularly informative when the change is localised in time (e.g., spike-type changes).

Choice of the evaluation point. In applications we choose t_0 to maximise empirical variability, which is a simple data-driven proxy for locations where a change may be most detectable. Define the empirical mean and pointwise empirical variance

$$\bar{X}(t) = \frac{1}{n}\sum_{i=1}^{n} X_i(t), \qquad V_n(t) = \frac{1}{n}\sum_{i=1}^{n}\big(X_i(t) - \bar{X}(t)\big)^2, \qquad t \in [0,1].$$

We set

$$t_0 \in \arg\max_{t\in[0,1]} V_n(t).$$

In practice curves are observed on a grid $0 \le t_1 < \cdots < t_m \le 1$, and we use the discrete maximiser $t_0 = t_{j^*}$ where $j^* \in \arg\max_{1\le j\le m} V_n(t_j)$, breaking ties (if any) uniformly at random.

Remark. The same idea extends to multiple evaluation points $t_{0,1}, \ldots, t_{0,d}$ (e.g., the top-d maximisers of V_n separated by a minimum distance), producing a low-dimensional vector sequence suitable for multivariate scan statistics.

3. Change segment tests based on antisymmetric kernels

This chapter develops Wilcoxon-type changed-segment tests built from *antisymmetric kernels*. Rather than comparing distributions through parametric summaries, we construct scan statistics from U-process increments that remain distribution-free under the null and are robust in heavy-tailed settings.

The key input is a measurable antisymmetric kernel $h : \mathbb{S} \times \mathbb{S} \to \mathbb{R}$. For each candidate interval $I(k, m) = \{k+1, \ldots, m\}$ we form a two-sample-type contrast between the observations inside and outside the interval, and then maximise over all (k, m). To extend the construction to Hilbert-space-valued and functional samples, we combine the Wilcoxon kernel with projection features, including Brownian projections introduced in Chapter 2.

The chapter is organised as follows. Section 3.1 defines the kernel scan statistics. Section 3.2 establishes the weak limits under H_0, drawing on the weight class $\mathcal{R}$ from Section 1.3. Section 3.3 discusses projection choices and implementation details. Empirical evaluation is conducted alongside the other proposed tests in Chapter 6 (functional-data scenarios in Section 6.1).

3.1. Definitions of kernel type statistics

Let $I_n := \{1, 2, \ldots, n\}$. For a subsample $(X_i,\ i \in I)$ with $I \subset I_n$, set

$$P_n^I = \frac{1}{|I|} \sum_{j \in I} \delta_{X_j}.$$

where δ_x denotes the Dirac measure at point x. We abbreviate $P_n^{I_n}$ to $\widehat{P}_n$. Note that $\widehat{P}_n$ is the empirical distribution of the sample $X_1, \ldots, X_n$.

To detect a changed segment in the sample, we use kernel-type statistics that measure heterogeneity between empirical distributions of two segments.

$$(X_i, i \in I(k, m)) \text{ and } (X_i, i \in I^c(k, m)),\ \ 0 \le k < m \le n,$$

where $I(k, m) = \{k + 1, \ldots, m\}$ and $I^c(k, m) = I_n \setminus I(k, m)$. Following [39], for a measurable function $h : \mathbb{S} \times \mathbb{S} \to \mathbb{R}$ we set

$$\begin{aligned}\Delta_{n,h}(k, m) &= \sum_{i \in I(k,m)} \sum_{j \in I_n \setminus I(k,m)} h(X_i, X_j) \\ &= (m - k)(n - (m - k)) \int_{\mathbb{S}} \int_{\mathbb{S}} h(x, y) P_n^{I(k,m)}(\mathrm{d}x) P_n^{I^c(k,m)}(\mathrm{d}y)\end{aligned}$$

and define the statistics

$$T_{n,\rho}(h; X_1, \ldots, X_n) := \max_{0 \le k < m \le n} \frac{|\Delta_{n,h}(k,m)|}{\rho((m/n - k/n)(1 - (m/n - k/n)))},$$

which we shall use to test the presence of a changed segment in the sample (X_i), where, as throughout, $\rho \in \mathcal{R}$ is the weighting function used to smooth over the influence of very short and very long candidate windows. Although a systematic and data-driven study of optimal selection rules for ρ lies beyond the scope of this dissertation, our simulations (Section 6.1) illustrate how different specifications affect performance.

Next we assume that $n = dN$ and divide the sample $X_1, \ldots, X_n$ into d sub-samples of length N each:

$$X_{(i-1)N+1}, \ldots, X_{iN}, \quad i = 1, \ldots, d,$$

thus obtaining d sub-samples $X_{i,1}, \ldots, X_{i,N}$, $i = 1, \ldots, d$, where $X_{i,k} = X_{(i-1)N+k}$, $k = 1, \ldots, N$, and d statistics

$$T_{N,\rho}(h; X_{i,1}, \ldots, X_{i,N}), \quad i = 1, \ldots, d.$$

The idea is that under an epidemic alternative with change duration $\ell^* < n/d$, the change appears in one sub-sample or in two adjacent ones only. Hence at least one of the statistics above differs from its null hypothesis behaviour.

Recall that a kernel $h : \mathbb{S} \times \mathbb{S} \to \mathbb{R}$ is symmetric if $h(x,y) = h(y,x)$, and antisymmetric if $h(x,y) = -h(y,x)$ for all $x, y \in \mathbb{S}$. Moreover, h is antisymmetric if and only if $E[h(X,Y)] = 0$ for any i.i.d. pair when the expectation exists (see [39]). We consider a set $\mathcal{H} = \{h_1, \ldots, h_d\}$ of d antisymmetric kernels $h_i : \mathbb{S} \times \mathbb{S} \to \mathbb{R}$ and define two test statistics:

$$T_{n,\rho}(\mathcal{H}) := \max_{h \in \mathcal{H}} T_{n,\rho}(h; X_1, \ldots, X_n)$$

and

$$T_{n,\rho}^{(d)}(\mathcal{H}) = \max_{1 \le i \le d} T_{N,\rho}(h_i; X_{i,1}, \ldots, X_{i,N}).$$

As a leading example of antisymmetric kernels, we use a class generated by a kernel $h : \mathbb{R} \times \mathbb{R} \to \mathbb{R}$ and a set of features $\mathcal{F} = \{f_1, \ldots, f_d\} : \mathbb{S} \to \mathbb{R}^d$ in such a way:

$$h_i(x,y) = h(f_i(x), f_i(y)), \quad x, y \in \mathbb{S}; \ i = 1, \ldots, d.$$

Wilcoxon kernel

$$h(x,y) := \mathbf{1}\{x-y \le 0\} - \mathbf{1}\{y-x \le 0\}, \ \ x,y \in \mathbb{R},$$

will be used as a leading example in our simulation study. As for the set $\mathcal{F}$, its choice depends on the sample space $\mathbb{S}$. In the case where $\mathbb{S} = \mathbb{H}$ is a separable Hilbert space, we consider Brownian projections (see Section 3.3), and the norm as a feature of a Hilbert-space-valued sample. Of course, some other projections, e.g., on principal components, may be used as well.

The weighting function ρ above is constrained to belong to a class $\mathcal{R}$ formalised in Section 1.3; see Definition 1.

3.2. Theoretical results

Consider a finite set $\mathcal{H} = \{h_1, \ldots, h_d\}$ of antisymmetric measurable kernels $h_i : \mathbb{S}\times\mathbb{S} \to \mathbb{R}$ such that $\int\int h_i^2(x,y)P(\mathrm{d}x)P(\mathrm{d}y) < \infty$ for each $i = 1,\ldots,d$. Throughout this section we assume that the weighting function ρ belongs to the class $\mathcal{R}$ introduced in Definition 1. Our main results are the following two theorems.

Theorem 1. *Let $\rho \in \mathcal{R}$. If X, $(X_i, i \ge 1)$ are i.i.d. random variables with values in the measurable space $(\mathbb{S}, \mathcal{S})$ and satisfies for any $A > 0$,*

$$\lim_{t\to\infty} tP(\max_{1\le i\le d} |\overline{h}_i(X)| > A\theta(t)) = 0,$$

where $\overline{h}(y) = Eh(X,y), y \in \mathbb{S}$, then

$$\lim_{n\to\infty} P(n^{-3/2}T_{n,\rho}(\mathcal{H}) \le x) = P(\max_{h\in\mathcal{H}} T_\rho(h) \le x), \ \ x \ge 0,$$

where

$$T_\rho(h) = \max_{0\le s<t\le 1} \frac{|B_h(t) - B_h(s)|}{\rho((t-s)(1-(t-s)))},$$

and $(B_h(t), t \in [0,1], h \in \mathcal{H})$ is a d-dimensional Brownian bridge, that is a Gaussian process with mean zero and covariance

$$E(B_h(t)B_g(s)) = E(\overline{h}(X)\overline{g}(X))[\min\{t,s\} - ts], \ \ h,g \in \mathcal{H}, s,t \in [0,1].$$

Theorem 2. *Let $\rho \in \mathcal{R}$ and let $h : \mathbb{S}\times\mathbb{S} \to \mathbb{R}$ be a measurable antisymmetric kernel. If X, $(X_i, i \ge 1)$ are i.i.d. random variables with values in the* *measurable space* $(\mathbb{S}, \mathcal{S})$ *and satisfies for any* $A > 0$*,*

$$\lim_{t\to\infty} tP(|\overline{h}(X)| > A\theta(t)) = 0,$$

where $\overline{h}(y) = Eh(X, y), y \in \mathbb{S}$*, then*

$$\lim_{n\to\infty} P(n^{-3/2}\sigma_h^{-1} T_{n,\rho}^{(d)}(\mathcal{H}) \le x) = P^d(T_\rho \le x), \;\; x \ge 0,$$

where $\sigma_h^2 = \mathrm{var}(\overline{h}(X))$*,*

$$T_\rho := \max_{0\le s<t\le 1} \frac{|B(t) - B(s)|}{\rho((t-s)(1-(t-s)))},$$

and $(B(t), t \in [0,1])$ *is a standard Brownian bridge.*

The proof of both theorems is based on a functional central limit theorem which we provide after some preparation.

For any anti-symmetric measurable kernel $h : \mathbb{S} \times \mathbb{S} \to \mathbb{R}$ consider the double partial sums

$$U_{h,0} = U_{h,n} = 0, \;\; U_{h,k} = \sum_{i=1}^{k} \sum_{j=k+1}^{n} h(X_i, X_j), \;\; 1 \le k < n$$

and the corresponding *polygonal line process* $\mathcal{U}_{h,n} = (\mathcal{U}_{h,n}(t), t \in [0,1])$ defined by

$$\mathcal{U}_{h,n}(t) := U_{h,\lfloor nt\rfloor} + (nt - \lfloor nt\rfloor)(U_{h,\lfloor nt\rfloor+1} - U_{h,\lfloor nt\rfloor}), \;\; t \in [0,1], \quad (3.1)$$

where for a real number $a \ge 0$, $\lfloor a\rfloor := \max\{k\colon\, k \in \mathbb{N}, k \le a\}$, $\mathbb{N} = \{0, 1, \dots\}$, is the floor function. So $\mathcal{U}_{h,n} = (\mathcal{U}_{h,n}(t), t \in [0,1])$, is the random polygonal line with vertices $(k/n, U_{h,k})$, $k = 0, 1, \dots, n$. As a functional framework for the process $(\mathcal{U}_{h,n}, h \in \mathcal{H})$ we consider Banach spaces of Hölder functions. Recall the space $C(\mathbb{R}^d) = C([0,1], \mathbb{R}^d)$ of continuous functions $x : [0,1] \to \mathbb{R}^d$ is endowed with the norm

$$|x| = \max_{0\le t\le 1} \|x(t)\|_d,$$

where $\|\cdot\|_d$ is any norm in $\mathbb{R}^d$. For $\rho \in \mathcal{R}$ the Hölder space $\mathcal{H}_\rho^o(\mathbb{R}^d) =$

$\mathcal{H}_\rho^o([0,1],\mathbb{R}^d)$, of functions $x \in C(\mathbb{R}^d)$ such that

$$\omega_\rho(x,\delta) := \sup_{0<s<t\leq\delta} \frac{|x(t)-x(s)|}{\rho(|t-s|)} \to 0 \ \text{ as } \ \delta \to 0,$$

is endowed with the norm

$$||x||_\rho := |x(0)| + \omega_\rho(x,1).$$

Both $C(\mathbb{R}^d)$ and $\mathcal{H}_\rho^o(\mathbb{R}^d)$ are separable Banach spaces. The space $\mathcal{H}_\rho^o(\mathbb{R}^d)$ is isomorphic to $C(\mathbb{R}^d)$.

Let D_j be the set of dyadic numbers of level j in $[0,1]$, that is $D_0 := \{0,1\}$ and for $j \geq 1$, $D_j := \{(2l-1)2^{-j};\ 1 \leq l \leq 2^{j-1}\}$. For $r \in D_j$ set $r^- := r - 2^{-j}$, $r^+ := r + 2^{-j}$, $j \geq 0$. For $f : [0,1] \to \mathbb{R}^d$ and $r \in D_j$ define

$$\lambda_r(f) := \begin{cases} f(r^+) + f(r^-) - 2f(r) & \text{if } j \geq 1, \\ f(r) & \text{if } j = 0. \end{cases}$$

If $\rho \in \mathcal{R}$, then the following sequential norm on $\mathcal{H}_\rho^o([0,1],\mathbb{R}^d)$ defined by

$$||f||_\rho^{\text{seq}} := \sup_{j\geq 0} \frac{1}{\rho(2^{-j})} \max_{r\in D_j} |\lambda_r(f)|,$$

is equivalent to the norm $||f||_\rho$, see [13]: there is a constant $c_\rho \geq 1$ such that

$$c_\rho^{-1}||f||_\rho^{\text{seq}} \leq ||f||_\rho \leq c_\rho ||f||_\rho^{\text{seq}}, \quad f \in \mathcal{H}_\rho^o([0,1],\mathbb{R}^d). \tag{3.2}$$

Set $\mathcal{D}_j := \{k2^{-j},\ 0 \leq k \leq 2^j\}$. In what follows, we denote by log the logarithm with basis 2 ($\log 2 = 1$).

Lemma 1. *For any $\rho \in \mathcal{R}$, there is a constant $c_\rho > 0$ such that, if V_n is a polygonal line function with vertices $(0,0), (k/n, V_n(k/n)), k = 1,\dots,n$, then*

$$||V_n||_\rho \leq c_\rho \max_{0\leq j\leq \log n} \frac{1}{\rho(2^{-j})} \max_{r\in\mathcal{D}_j} \Big| V_n(\lfloor nr + n2^{-j}\rfloor/n) - V_n(\lfloor nr\rfloor/n)\Big|.$$

Proof. The proof goes along the lines of the proof of Lemma 8 in [39]. □

Recall the definition of $(B_h, h \in \mathcal{H})$ in theorem 3.1.

Theorem 3. *Assume that* $(X, X_i, i \geq 1)$ *are i.i.d. random elements in* $\mathbb{S}$ *and let* $\mathcal{H}$ *be a finite set of measurable antisymmetric kernels* $h : \mathbb{S} \times \mathbb{S} \to \mathbb{R}$*, with* $d = \#(\mathcal{H})$*. Then for any* $\rho \in \mathcal{R}$*,*

$$n^{-3/2}(\mathcal{U}_{h,n}, h \in \mathcal{H}) \xrightarrow{\mathscr{D}} (B_h, h \in \mathcal{H}) \text{ in the space } \mathcal{H}^o_\rho([0,1], \mathbb{R}^d),$$

if the following condition holds: for any $A > 0$*,*

$$\lim_{t\to\infty} tP(\max_{h\in\mathcal{H}} |\overline{h}(X)| > A\theta(t)) = 0,$$

where $\overline{h}(x) := E[h(x, X')]$ *is the Hoeffding linear projection of the kernel* h *(cf.* (3.3) *below).*

Proof. In order to make use of results for partial sum processes, we decompose the U-statistics under consideration into a linear part and a so-called degenerate part. Hoeffding's decomposition of the kernel h reads

$$h(x, y) = \overline{h}(x) - \overline{h}(y) + q_h(x, y), \quad x, y \in \mathbb{S},$$

where

$$\overline{h}(x) = \int_{\mathbb{S}} h(x, y) P_X(\mathrm{d}y), \text{ and } q_h(x, y) := h(x, y) - \overline{h}(x) + \overline{h}(y), \quad x, y \in \mathbb{S},$$

and leads to the splitting

$$\mathcal{U}_{h,n}(t) = n[W_{\overline{h},n}(t) - tW_{\overline{h},n}(1)] + \mathcal{U}_{q_h,n}(t), \quad t \in [0,1], \tag{3.3}$$

where

$$W_{\overline{h},n}(t) = \sum_{i=1}^{\lfloor nt \rfloor} \overline{h}(X_i) + (nt - \lfloor nt \rfloor)\overline{h}(X_{\lfloor nt \rfloor + 1}), \quad t \in [0,1],$$

is the polygonal line process defined by partial sums of the random variables $(\overline{h}(X_i), i \geq 1)$. Next we check that for each $h \in \mathcal{H}$,

$$||n^{-3/2}\mathcal{U}_{q_h,n}||_\rho = o_P(1) \tag{3.4}$$

for any $\rho \in \mathcal{R}$. To this aim we repeat arguments of the proof of Lemma 6 in [39]. First we observe that $Eq_h(X_i, X_j)q_h(X_{i'}, X_{j'}) = 0$ if either $i \neq i'$ or

$j \neq j'$. Indeed, it is enough to check that $Eq_h(X_1, x) = 0$ for each x:

$$\begin{aligned} Eq_h(X_1, x) &= E[h(X_1, x) - \overline{h}(X_1) + \overline{h}(x)] \\ &= E[-h(x, X_1) - \overline{h}(X_1) + \overline{h}(x)] \\ &= E\overline{h}(X_1) = Eh(X_1, X_2) = 0. \end{aligned}$$

Now, if $i \neq i'$, $j = j'$ then we have

$$Eq_h(X_i, X_j)q_h(X_{i'}, X_{j'}) = \int_{\mathbb{S}} Eq_h(X_i, x)Eq_h(X_{i'}, x)P_X(\mathrm{d}x) = 0.$$

Hence,

$$\begin{aligned} E\Big(\sum_{i=m_1+1}^{n_1}\sum_{j=m_2+1}^{n_2} q_h(X_i, X_j)\Big)^2 &= \sum_{i=m_1+1}^{n_1}\sum_{j=m_2+1}^{n_2} Eq_h^2(X_i, X_j) \\ &= (n_1 - m_1)(n_2 - m_2)Eq_h^2(X_1, X_2) \\ &\leq c(n_1 - m_1)(n_2 - m_2). \end{aligned} \tag{3.5}$$

By Lemma 1 we have with some constant $C > 0$,

$$\begin{aligned} E||\mathcal{U}_{q_h,n}||_\rho^2 \leq C \sum_{j=0}^{\log n} & \frac{1}{\rho^2(2^{-j})} 2^j \\ & \times \max_{r \in \mathcal{D}_j} E\Big(\mathcal{U}_{q_h,n}(\lfloor nr + n2^{-j} \rfloor/n) - \mathcal{U}_{q_h,n}(\lfloor nr \rfloor/n)\Big)^2. \end{aligned}$$

From (3.5) we deduce

$$E\Big(\mathcal{U}_{q_h,n}(m/n) - \mathcal{U}_{q_h,n}(k/n)\Big)^2 \leq C(m-k)(n-(m-k)).$$

Indeed, by antisymmetry, for $m > k$,

$$\begin{aligned} \mathcal{U}_{q_h,n}\big(\tfrac{m}{n}\big) - \mathcal{U}_{q_h,n}\big(\tfrac{k}{n}\big) &= \sum_{i=k+1}^{m}\sum_{j=m+1}^{n} q_h(X_i, X_j) \\ &\quad + \sum_{i=k+1}^{m}\sum_{j=1}^{k} q_h(X_i, X_j), \end{aligned}$$

so (3.5) gives

$$E\left(\mathcal{U}_{q_h,n}\left(\tfrac{m}{n}\right)-\mathcal{U}_{q_h,n}\left(\tfrac{k}{n}\right)\right)^2 \le 2C\big[(m-k)(n-m)+(m-k)(k-1)\big]$$
$$\le 2C(m-k)(n-(m-k)).$$

This yields, taking into account that $\lfloor nr+n2^{-j}\rfloor-\lfloor nr\rfloor \le n2^{-j}$ for $r\in\mathcal{D}_j$,

$$\begin{aligned}E||n^{-3/2}\mathcal{U}_{q_h,n}||_\rho^2 &\le C_\rho n^{-3}\sum_{j=1}^{\log n}\frac{1}{\rho^2(2^{-j})}2^j[n2^{-j}(n-n2^{-j})]\\ &\le C_\rho n^{-1}\sum_{j=0}^{\log n}\frac{1}{\rho^2(2^{-j})}(1-2^{-j})\\ &\le \frac{C_\rho}{n}\sum_{j=0}^{\log n}\frac{1}{\rho^2(2^{-j})}.\end{aligned}$$

Fix $m\in\mathbb{N}$. Split the sum into head and tail:

$$\frac{1}{n}\sum_{j=0}^{\lfloor\log n\rfloor}\rho(2^{-j})^{-2}=\underbrace{\frac{1}{n}\sum_{j=0}^{m}\rho(2^{-j})^{-2}}_{\to 0\text{ as }n\to\infty}+\frac{1}{n}\sum_{j=m+1}^{\lfloor\log n\rfloor}\rho(2^{-j})^{-2}.$$

By the definition of $\mathcal{R}$, there exist $\beta>\frac{1}{2}$ and $c>0$ such that for all sufficiently small u, $\rho(u)\ \ge\ c\,u^{1/2}\,(\log\frac{1}{u})^\beta$. Hence for j large,

$$\rho(2^{-j})^{-2}\ \le\ C\,\frac{2^j}{j^{2\beta}}\qquad\text{with } C=C(c,\beta).$$

Therefore, for every n and $m<\lfloor\log n\rfloor$,

$$\begin{aligned}\frac{1}{n}\sum_{j=m+1}^{\lfloor\log n\rfloor}\rho(2^{-j})^{-2} &\le \frac{C}{n}\sum_{j=m+1}^{\lfloor\log n\rfloor}\frac{2^j}{j^{2\beta}}=C\sum_{j=m+1}^{\lfloor\log n\rfloor}\frac{2^{j-\lfloor\log n\rfloor}}{j^{2\beta}}\\ &\le C\sum_{j=m+1}^{\infty}\frac{1}{j^{2\beta}}.\end{aligned}$$

Since $\beta>\frac{1}{2}$, the tail $\sum_{j=m+1}^\infty j^{-2\beta}\to 0$ as $m\to\infty$. Combining this with the vanishing head term yields

$$\frac{1}{n}\sum_{j=0}^{\lfloor \log n\rfloor} \rho(2^{-j})^{-2} \;=\; o(1),$$

this completes the proof of (3.4). By (3.3),

$$n^{-3/2}(\mathcal{U}_{h,n}, h\in\mathcal{H}) = n^{-1/2}(B_{\overline{h},n}, h\in\mathcal{H}) + n^{-3/2}(\mathcal{U}_{q_h,n}, h\in\mathcal{H}),$$

where $B_{\overline{h},n} = (W_{\overline{h},n}(t) - tW_{\overline{h},n}(1),\ t\in[0,1])$. By (3.4),

$$\max_{h\in\mathcal{H}} \|n^{-3/2}\mathcal{U}_{q_h,n}\|_\rho = o_P(1).$$

Hence, the limit in distribution of $n^{-3/2}(\mathcal{U}_{h,n}, h\in\mathcal{H})$ coincides with that of $n^{-1/2}(B_{\overline{h},n}, h\in\mathcal{H})$. By Theorem 8 in [37],

$$n^{-1/2}(W_{\overline{h},n}, h\in\mathcal{H}) \xrightarrow{\mathscr{D}} (W_h, h\in\mathcal{H}) \ \text{ in the space }\ \mathcal{H}_\rho^o(\mathbb{R}^d),$$

where $(W_h, h\in\mathcal{H})$ is a $\mathbb{R}^d$-dimensional Wiener process with covariance

$$E(W_n(t)W_g(s)) = E(\overline{h}_i(X)\overline{h}_j(X))\min\{t,s\},\ \ t,s\in[0,1], i=1,\dots,d.$$

Since the mapping $T:\mathcal{H}_\rho^o(\mathbb{R}^d)\to\mathcal{H}_\rho^o(\mathbb{R}^d)$ defined by

$$(Tf)(t) = f(t) - tf(1),\quad t\in[0,1],$$

is continuous, the proof is completed by an application of the continuous mapping theorem. □

Proof of Theorem 1. By Lemma 13 and Lemma 14 of [40],

$$n^{-3/2}T_{n,\rho}(\mathcal{H}) = \max_{h\in\mathcal{H}} \Lambda\Big(n^{-3/2}\mathcal{U}_{h,n}\Big) + o_P(1),$$

where

$$\Lambda(f) = \sup_{0\le s<t\le 1} \frac{|f(t)-f(s)-(t-s)f(1)|}{\rho((t-s)(1-(t-s)))},\qquad f\in\mathcal{H}_\rho^o([0,1],\mathbb{R}^d).$$

This observation combined with Theorem 3 yields

$$n^{-3/2} T_{n,\rho}(\mathcal{H}) \xrightarrow{\mathscr{D}} \max_{h \in \mathcal{H}} \Lambda(B_h) = \max_{h \in \mathcal{H}} T_\rho(h).$$

□

Proof of Theorem 2. Observing that the random variables

$$T_{n,\rho}(h_i; X_{i,1}, \ldots, X_{i,N}), \;\; i = 1, \ldots, d$$

are independent and identically distributed, we have

$$P(T^{(d)}_{n,\rho} \leq x) = P^d(T_{n,\rho}(h_1; X_1, \ldots, X_N) \leq x)$$

and the result follows by Theorem 1, applied for $\mathcal{H} = \{h_1\}$. □

3.3. Wilcoxon type tests based on Brownian projections and norm

We consider $\mathcal{H} = \mathcal{H}_d = \{h_1, ..., h_d\}$ and $\mathcal{H} = \mathcal{H}_0 = \{h_0\}$ sets of Wilcoxon type kernels defined via Brownian projections and norm, as follows:

$$\begin{aligned} h_i(x, y) = \mathbf{1}\{f_i(x) - f_i(y) \leq 0\} - \mathbf{1}\{f_i(y) - f_i(x) \leq 0\}, \\ x, y \in \mathbb{H}, \; i = 1, \ldots, d, \end{aligned}$$

and

$$h_0(x, y) = \mathbf{1}\{\|x\| - \|y\| \leq 0\} - \mathbf{1}\{\|y\| - \|x\| \leq 0\}, \;\; x, y \in \mathbb{H},$$

where the scalar features $f_1, \ldots, f_d : \mathbb{H} \to \mathbb{R}$ are independent sample paths of the $\mathbb{H}$-isonormal Gaussian process $\mathrm{W} = \{\mathrm{W}(x) : x \in \mathbb{H}\}$, drawn once before the test is applied. Equivalently, fixing outcomes $\omega_1, \ldots, \omega_d \in \Omega$ from the underlying probability space $(\Omega, \mathcal{F}, \mathrm{P})$ on which W is defined, we set $f_i(x) := \mathrm{W}(x)(\omega_i)$. Here ω_i denotes a simulated sample trajectory of the underlying Wiener process: we draw d independent realisations once before the test is run, and these realisations parametrise the d projection features used throughout the testing procedure.

We compare tests based on $T^{(d)}_{n,\rho}(\mathcal{H}_d)$ and on $T^{(d)}_{n,\rho}(\mathcal{H}_0) = T_{n,\rho}(\mathcal{H}_0)$. Letting $T^{(d)}_{n,\rho}$ denote either, we define tests by

$$T^{(d)}_{n,\rho} \geq c_{\alpha,\rho} n^{\frac{3}{2}}, \tag{3.6}$$

where $c_{\alpha,\rho}$ satisfies

$$P(T_\rho > c_{\alpha,\rho}) = 1 - (1-\alpha)^{\frac{1}{d}}, \ \ d \geq 1.$$

This test has asymptotic significance level α, as follows from Theorem 2.

Below in Tables 3.1 and 3.2, we give the upper quantiles of distributions of $T_\gamma = T_{\rho_\gamma}$ and $T_{0.5,\beta} = T_{\rho_{0.5,\beta}}$, respectively.

The distribution was evaluated on a grid of size 10,000 and we ran a Monte Carlo simulation with 30,000 runs.

Table 3.1: Upper quantiles of T_γ.

	50%	20%	10%	5%	2.5%	1%	0.5%	0.25%	0.1%
$\gamma = 0$	1.213	1.460	1.612	1.741	1.857	2.012	2.104	2.195	2.311
$\gamma = 0.05$	1.314	1.573	1.732	1.862	1.987	2.143	2.242	2.334	2.476
$\gamma = 0.1$	1.423	1.708	1.876	2.016	2.148	2.306	2.417	2.501	2.638
$\gamma = 0.15$	1.544	1.839	2.017	2.172	2.309	2.485	2.596	2.720	2.859
$\gamma = 0.2$	1.684	1.995	2.175	2.344	2.498	2.677	2.812	2.947	3.085
$\gamma = 0.25$	1.846	2.172	2.357	2.527	2.684	2.862	2.998	3.104	3.219
$\gamma = 0.3$	2.042	2.372	2.572	2.748	2.906	3.122	3.262	3.372	3.562
$\gamma = 0.35$	2.294	2.621	2.825	3.017	3.196	3.387	3.541	3.695	3.860
$\gamma = 0.4$	2.654	2.961	3.150	3.330	3.499	3.695	3.852	4.002	4.208
$\gamma = 0.45$	3.268	3.529	3.697	3.852	4.011	4.216	4.362	4.486	4.627

Table 3.2: Upper quantiles of $T_{0.5,\beta}$.

	50%	20%	10%	5%	2.5%	1%	0.5%	0.25%	0.1%
$\beta = 1$	11.781	14.661	16.315	17.721	19.044	20.561	21.719	22.690	23.897
$\beta = 2$	62.710	78.686	87.845	95.459	102.694	111.740	117.406	123.767	129.379

3.4. Conclusions

This chapter established Wilcoxon-type scan statistics for epidemic change-point detection in functional data and proved their null limit distributions under

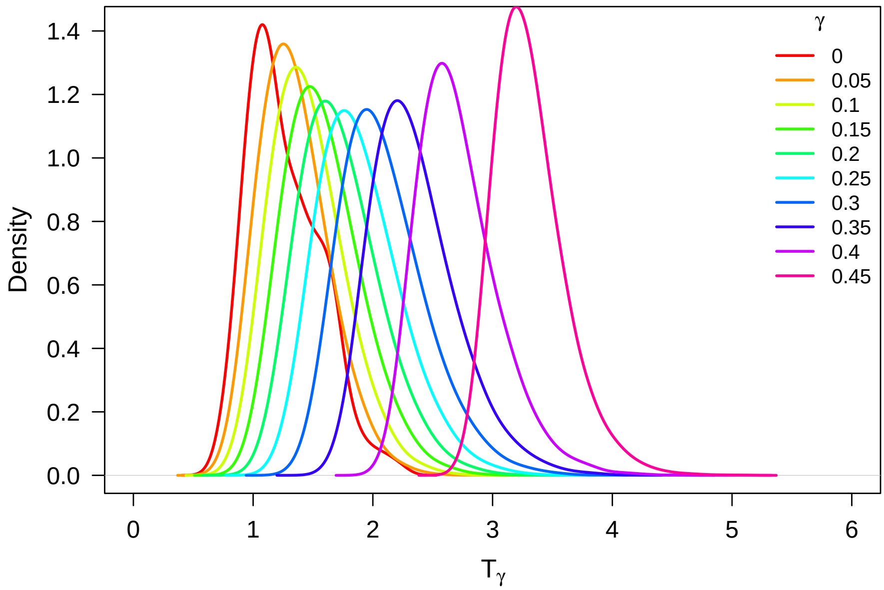

Figure 3.1: T_γ densities

i.i.d. assumptions. Brownian projections provide a distribution-free, rotation-invariant way to reduce Hilbert-space data to univariate margins. The finite-sample performance of these procedures is investigated in the simulation studies of Chapter 6, and the real-data illustration is given in Chapter 7; open problems (data-driven choice of ρ, dependence, minimax rates) are collected in Chapter 8.

4. Change segment tests based on L_p type statistics

4.1. Introduction

This chapter develops changed-segment (epidemic) tests via L_p-type functionals of empirical process increments. The idea is simple: for each candidate interval $I(k,\ell) = \{k+1,\dots,k+\ell\}$ we compare the empirical distribution inside the interval to that of the full sample, then *scan* over all intervals. The resulting statistic is of Cramér–von Mises type when $p = 2$, and more generally yields a family of integral discrepancies that remain sensitive to distributional changes beyond mean and variance shifts.

Throughout this chapter we consider independent real-valued observations $X_1,\dots,X_n$ with distribution functions $F_{X_1},\dots,F_{X_n}$ and collect them into the sample vector $\mathcal{X} := (X_1,\dots,X_n)$. We test the standing hypothesis pair (1.1)–(1.2), with the distributions P_{X_i} identified with their CDFs F_{X_i}.

4.2. Theoretical results

Write

$$F_n(x) := \frac{1}{n}\sum_{i=1}^{n} \mathbf{1}\{X_i \le x\}, \qquad x \in \mathbb{R},$$

for the empirical distribution function of $X_1,\dots,X_n$. The L_p-type statistic is defined as

$$T_{n,\rho,p}(\mathcal{X}) = \max_{1\le\ell<n}\max_{0\le k\le n-\ell} \frac{\left(\int_{-\infty}^{\infty}\left|\sum_{i=k+1}^{k+\ell}(\mathbf{1}\{X_i\le x\}-F_n(x))\right|^p \mathrm{d}F_n(x)\right)^{1/p}}{\rho(\ell/n)}.$$

If $p = 2$, this statistic is known as a Cramér–von Mises-type statistic. In the case where the distribution function F is continuous we reduce the statistic $T_{n,\rho,p}$ to

$$\widehat{T}_{n,\rho,p} = \max_{1\le\ell\le n/2}\max_{0\le k\le n-\ell} \frac{\left(\int_0^1\left|\sum_{i=k+1}^{k+\ell}(\mathbf{1}\{F(X_i)\le t\}-t)\right|^p \mathrm{d}t\right)^{1/p}}{\rho(\ell/n)}.$$

Relation to existing L_p-type changepoint tests. L_p-functionals of the empirical process have been used for (single-changepoint) testing by [15] and, in the epidemic setting with $p = 2$, by [40, 37]. The classical at-most-one-change (AMOC) statistics take the form $\max_k \int |F_{n,k}(x) - F_n(x)|^p\,\mathrm{d}F_n(x)$, where

$F_{n,k}(x) = k^{-1}\sum_{i=1}^{k} \mathbf{1}\{X_i \le x\}$ denotes the empirical distribution function of the first k observations; this corresponds to the special case $\ell = k$ of our two-dimensional scan (no varying window length). Our statistic $T_{n,\rho,p}$ extends this in two directions that are novel relative to the cited work: *(i)* the scan ranges jointly over start index k and window length ℓ, so the test is sensitive to temporary – rather than permanent – distributional departures; *(ii)* a weighting function $\rho(\ell/n)$ in the denominator rescales the contributions of intervals of different lengths, allowing the user to trade off sensitivity to short vs. long segments. The price paid for (i)–(ii) is a richer null limit: instead of a functional of Brownian bridge, the limit is expressed through a two-parameter Wiener sheet (see Theorem 2). In the one-dimensional case $\ell = n$, $\gamma = 0$ our statistic reduces to the classical Cramér–von Mises omnibus test, so published quantiles agree with ours (we verified this numerically for $p = 2$).

Why integrate with respect to F_n rather than F. If the baseline distribution function F were known, one could integrate against $\mathrm{d}F$ directly. In practice F is unknown, so we integrate against F_n; this keeps the test distribution-free under H_0 with continuous F (since $F_n \circ F^{-1}$ converges to the uniform empirical process), and reduces the integral to a finite sum $\int |\cdot|^p \mathrm{d}F_n = \frac{1}{n}\sum_{j=1}^{n} |\cdot(X_{(j)})|^p$ evaluated at the sample points.

Before we establish asymptotic distribution of the statistics $\widehat{T}_{n,\rho,p}(\mathcal{X})$ under null hypothesis we need some preparation.

Let $W^{(2)} := (W(s,t), (s,t) \in [0,1]^2)$ be a standard Wiener sheet. That is $W^{(2)}$ is a Gaussian zero mean random process with covariance

$$\mathrm{E}(W^{(2)}(s,t)W^{(2)}(s',t') = \min\{s,s'\}\min\{t,t'\}, \quad s,s',t,t' \in [0,1].$$

We use the same class $\mathcal{R}$ of weighting functions ρ as introduced in Definition 1; in particular $\rho_\gamma(t) = t^\gamma$ with $0 \le \gamma < 1/2$ and $\rho_{0.5,\beta}(t) = t^{1/2}\log^\beta(c/t)$ with $\beta > 1/2$ are the leading examples. Since the empirical process takes values in L_p, we need the Banach-space version of the Hölder space introduced in Section 3.1. For a separable Banach space $\mathbb{B}$ with the norm $\|x\|, x \in \mathbb{B}$, we denote by $C([0,1],\mathbb{B})$ a Banach space of continuous functions $x : [0,1] \to \mathbb{B}$ endowed with the norm $\|x\|_{\mathbb{B}} = \sup_{0\le t\le 1}\|x(t)\|$. Set

$$\mathcal{H}^o_\rho([0,1],\mathbb{B}) = \Big\{x \in C([0,1],\mathbb{B}) : \lim_{\delta\to 0} \sup_{0<t-s<1} \frac{\|x(t)-x(s)\|}{\rho(t-s)} = 0\Big\}.$$

With the norm

$$\|x\|_{\rho,\mathbb{B}} = \|x(0)\| + \sup_{0<t-s\leq 1} \frac{\|x(t)-x(s)\|}{\rho(t-s)}, \quad x \in \mathcal{H}_\rho^o([0,1],\mathbb{B}),$$

the set $\mathcal{H}_\rho^o([0,1],\mathbb{B})$ is a separable Banach space.

Theorem 2. *Let $\rho \in \mathcal{R}$ and $p \geq 2$. If $X_1,\dots,X_n$ are i.i.d. random variables with continuous distribution function F, then*

$$\lim_{n\to\infty} \mathbb{P}(n^{-1/2}\widehat{T}_{n,\rho,p}(\mathcal{X}) \leq x) = \mathbb{P}(T_{\rho,p} \leq x), \quad x \geq 0,$$

where

$$T_{\rho,p} = \sup_{0<t-s\leq 1/2} \frac{\left(\int_0^1 |\Delta_{t,s}(u)|^p \mathrm{d}u\right)^{1/p}}{\rho(t-s)}$$

with

$$\begin{aligned}\Delta_{t,s}(u) &= W(u,t) - W(u,s) - (t-s)W(u,1)\\ &\quad - u\big(W(1,t) - W(1,s) - (t-s)W(1,1)\big).\end{aligned}$$

Proof. Consider random functions $Z_k := (Z_k(t) = \mathbf{1}\{F(X_k) \leq t\} - t, t \in [0,1])$, $k = 1,\dots,n$. The random functions $Z_1,\dots,Z_n$ can be identified with a random sample of i.i.d. $L_p := L_p(0,1)$-valued random variables. Clearly $\mathrm{E}(Z_i) = 0$. Covariance operator $Q = \mathrm{E}(Z_i \otimes Z_i) : L_q \to L_p$. $1/p + 1/q = 1$ is defined by the covariance function

$$q(t,s) = \mathrm{E}Z_i(t)Z_i(s) = \min\{t,s\} - ts, \quad t,s \in [0,1]$$

via

$$Qh(g) = \int_0^1\int_0^1 h(t)g(s)q(t,s)\mathrm{d}t\mathrm{d}s, \quad h,g \in L_q.$$

With these notations the statistics $\widehat{T}_{n,\rho,p}$ takes the form

$$\widehat{T}_{n,\rho,p}(\mathcal{X}) = \max_{1\leq \ell<n} \frac{1}{\rho(\ell/n)} \max_{0\leq k<n-\ell} \Big\| \sum_{i=k+1}^{k+\ell} Z_i \Big\|_p.$$

Set

$$\zeta_n(t) = \sum_{i=1}^{\lfloor nt\rfloor} Z_i + (nt - \lfloor nt\rfloor)Z_{\lfloor nt\rfloor+1}, \quad t \in [0,1].$$

Random variables Z_i with values in L_p are bounded, therefore, they satisfy the central limit theorem and, as a result of Theorem 8 in [38]

$$n^{-1/2}\zeta_n \xrightarrow{\mathscr{D}} W_Q \text{ in the space } \mathcal{H}_\rho^o([0,1],L_p),$$

where $W_Q = (W_Q(t), t \in [0,1])$ is a Gaussian random process with values in L_p such that $W_Q(t) - W_Q(s)$ has the same distribution as $Y_Q|t-s|$ and Y_Q is zero mean Gaussian random variable in L_p with covariance Q. By continuous mapping theorem we get

$$n^{-1/2} \sup_{0<t\le 1/2} \frac{\|\zeta_n(t)-\zeta_n(s)\|}{\rho(t-s)} \xrightarrow{\mathscr{D}} \sup_{0<t-s\le 1/2} \frac{\|W_Q(t)-W_Q(s)\|}{\rho(t-s)}.$$

By Theorem 3 in [40],

$$\sup_{0<|t-s|\le 1/2} \frac{\|\zeta_n(t)-\zeta_n(s)\|}{\rho(t-s)} = \max_{1\le \ell\le n/2} \max_{0\le k\le n-\ell} \frac{\left\| \sum_{i=k+1}^{k+\ell} Z_i \right\|}{\rho(\ell/n)} = \widehat{T}_{n,\rho,p}.$$

Hence,

$$n^{-1/2}\widehat{T}_{n,\rho,p} \xrightarrow{\mathscr{D}} \max_{0<t-s\le 1/2} \frac{\|W_Q(t)-W_Q(s)-(t-s)W_Q(1)\|_p}{\rho(t-s)},$$

It is easy to see, that the random variable $\|W_Q(t)-W_Q(s)-(t-s)W_Q(1)\|_p^p$ has the same distribution as

$$\int_0^1 \big|W(u,t)-W(u,s)-(t-s)W(u,1)$$
$$-u\big(W(1,t)-W(1,s)-(t-s)W(1,1)\big)\big|^p \mathrm{d}u.$$

This completes the proof. □

Let $\alpha \in (0,1)$ be the preassigned asymptotic level of significance which controls the probability of falsely rejecting the hypothesis H_0 when it is true and define the test

$$\widehat{T}_{n,\rho,p} > \sqrt{n}C_\alpha, \tag{4.1}$$

where $C_\alpha > 0$ satisfies

$$\mathbb{P}(T_{\rho,p} > C_\alpha) = \alpha.$$

The quantiles C_α of $T_{\rho,p}$ are calculated in table 4.1.

Table 4.1: Estimated quantiles of $T_{\rho,p}$.

p	γ	2.5%	5%	25%	50%	75%	95%	97.5%
2	0	0.259	0.281	0.338	0.383	0.441	0.544	0.576
	0.25	0.391	0.406	0.477	0.526	0.585	0.683	0.709
	0.45	0.715	0.750	0.818	0.882	0.957	1.082	1.135
4	0	0.321	0.336	0.392	0.453	0.521	0.610	0.649
	0.25	0.465	0.479	0.552	0.618	0.671	0.775	0.796
	0.45	0.845	0.864	0.943	1.008	1.096	1.235	1.255
10	0	0.408	0.423	0.483	0.540	0.608	0.727	0.759
	0.25	0.567	0.600	0.672	0.736	0.821	0.994	1.065
	0.45	1.003	1.018	1.105	1.180	1.271	1.475	1.541

4.3. Conclusions

This chapter introduced the L_p-type scan statistic $\widehat{T}_{n,\rho,p}$ for changed-segment detection in real-valued samples, generalising the classical Cramér–von Mises functional ($p = 2$) to integral discrepancies of arbitrary order $p \geq 2$ rescaled by a weight $\rho \in \mathcal{R}$. The leading methodological choice — integrating against the empirical F_n rather than the unknown F — keeps the test distribution-free under H_0 with continuous baseline (Theorem 2) and reduces the integral to a finite sum at the order statistics, so a single Monte Carlo evaluation per (ρ, p) pair (Table 4.1) gives critical values for any sample. The asymptotic limit is a functional of a two-parameter Wiener sheet, which captures both the temporal scan and the integral over the F-axis simultaneously and is genuinely richer than the Brownian-bridge functionals that arise in the at-most-one-change literature. Finite-sample power on real-valued scenarios is reported in Section 6.2.3; a head-to-head comparison with the antisymmetric-kernel and RKHS scans on Birbilas's functional epidemic scenario is given in Section 6.1.2; the test is applied to Lithuanian electricity balancing prices in Chapter 7.

5. Change segment tests based on reproducing kernel Hilbert space

5.1. Introduction

Let $(\mathbb{S}, \mathcal{S})$ be a sample space and $\mathcal{P}(\mathbb{S})$ a set of all probability distributions on $(\mathbb{S}, \mathcal{S})$. Assume that we are given a random sample $\mathcal{X} = (X_1, X_2, \dots, X_n)$ of independent random variables defined on a probability space $(\Omega, \mathcal{F}, \mathbb{P})$, taking values in $(\mathbb{S}, \mathcal{S})$ and with distributions $P_{X_1}, P_{X_2}, \dots, P_{X_n}$ respectively. We test the standing hypothesis pair (1.1)–(1.2); under (1.2) the sample $\mathcal{X}_{I^*} = (X_i, i \in I^*)$ constitutes a changed segment of length ℓ^* starting at $k^* + 1$ and we have two samples $\mathcal{X}_{I^*}$ and $\mathcal{X}_{I_n \setminus I^*}$ taken from different distributions. If k^* and ℓ^* were known, we would face a two-sample problem that examines whether these two samples are from the same distribution or not. This indicates that test statistics for detecting epidemic change points can be based on two-sample tests, but have to account for the fact that neither the beginning nor the length of a changed segment is known.

For the broader nonparametric and epidemic change-point literature surveyed in this dissertation, see Section 1.2; here we recall only the kernel-specific developments most directly relevant to the construction below. Kernel methods are now standard for two-sample testing [24, 25] and have been extended to the epidemic/segment setting by maximising an RKHS two-sample discrepancy (MMD^2) over all contiguous interval candidates $I(k, \ell)$; see kernel segmentation via RKHS mean embeddings (KCP) and kernel scan statistics [2, 44]. In functional time series applications - such as household electricity consumption - combining changed segment testing with functional representations can improve pattern based grouping [33, 45].

To construct a test procedure, for any sub-sample $\mathcal{X}_I = \{X_i, i \in I\}$, where $I \subset I_n := \{1, 2, \dots, n\}$ we consider the probability

$$P_n^I := \frac{1}{|I|} \sum_{i \in I} \delta_{X_i},$$

where $|I|$ denotes the number of elements in the set I and δ_x is the Dirac probability. We abbreviate $P_n^{I_n}$ to $\widehat{P}_n$, which is the empirical distribution of the sample $\mathcal{X}$. To estimate heterogeneity in a sample $\mathcal{X}$ we consider a seminorm $\mathcal{N}$, defined in the space $\mathcal{M}(\mathbb{S}, \mathcal{S})$ of signed measures in $(\mathbb{S}, \mathcal{S})$, which may depend on n and may also be random. Next, as a measure of heterogeneity, consider $\mathcal{N}(P_n^I - P_n^{I^c})$, where $I^c = I_n \setminus I$.

For $1 \le \ell \le n, k = 0, 1, \ldots, n-\ell$, let $I(k,\ell) = \{k+1, \ldots, k+\ell\} \subset I_n$. The discrepancy between probabilities $P_n^{I(k,\ell)}$ and $P_n^{I^c(k,\ell)}$ is estimated then by

$$\mathcal{N}\Big(P_n^{I(k,\ell)} - P_n^{I^c(k,\ell)}\Big) = \frac{n}{\ell(n-\ell)} \mathcal{N}\Big(\sum_{i=k+1}^{k+\ell} (\delta_{X_i} - \widehat{P}_n)\Big).$$

Based on ideas in [37], the following statistic is suggested:

$$\max_{1 \le \ell < n} \max_{0 \le k \le n-\ell} \frac{\mathcal{N}\Big(\sum_{i=k+1}^{k+\ell} (\delta_{X_i} - \widehat{P}_n)\Big)}{\rho(\ell/n(1-\ell/n))}, \tag{5.1}$$

where $\rho : (0,1) \to \mathbb{R}$ is a weight function. This statistic takes into account both the small change segment where $\ell^*/n \to 0$ as $n \to \infty$ and the large one where $\ell^*/n \to 1$ as $n \to \infty$. If $\ell^*/n \to 0$ then the factor $1 - \ell/n$ does not contribute to the critical values of the test statistic, as well if $\ell^*/n \to 1$ then the factor ℓ/n does not contribute to the critical values of the test statistics. Observing that

$$\sum_{i \in I(k,\ell)} (\delta_{X_i} - \widehat{P}_n) = - \sum_{i \in I_n \setminus I(k,\ell)} (\delta_{X_i} - \widehat{P}_n)$$

we confine ourselves to the situation where under the alternative hypothesis $\ell^*/n \to 0$ as $n \to \infty$ and consider the statistic

$$T_{n,\rho}^{(\mathcal{N})}(\mathcal{X}) = \max_{1 \le \ell < \frac{n}{2}} \max_{0 \le k \le n-\ell} \frac{\mathcal{N}\Big(\sum_{i=k+1}^{k+\ell} (\delta_{X_i} - \widehat{P}_n)\Big)}{\rho(\ell/n)}. \tag{5.2}$$

A large class of seminorms $\mathcal{N}$ is obtained from integral-type probability semimetrics induced by a class $\mathcal{F}$ of measurable functions $f : \mathbb{S} \to \mathbb{R}$: for $P, Q \in \mathcal{P}(\mathbb{S})$,

$$\zeta_{\mathcal{F}}(P,Q) = \sup_{f \in \mathcal{F}} |Pf - Qf|,$$

where $Pf = \int_{\mathbb{S}} f(s)P(\mathrm{d}s)$.

In statistics, integral-type distances are widely employed in nonparametric two-sample testing, most notably in the Kolmogorov–Smirnov [43, 10, 41] and kernel tests [25, 24]. In this dissertation, we extend tests based on the L_p metric and kernel methods from the two–sample framework to the epidemic change setting.

Taking $\mathcal{N}(P-Q) = \zeta_{\mathcal{F}}(P,Q)$ in (5.2) leads to the statistic

$$T_{n,\rho}^{\mathcal{F}}(\mathcal{X}) := \max_{1\le\ell\le n/2}\max_{0\le k<n-\ell} \frac{\sup_{f\in\mathcal{F}}\left|\sum_{j=k+1}^{k+\ell}(f(X_j)-\overline{f(X)}_n)\right|}{\rho(\ell/n)}. \quad (5.3)$$

Throughout, we write $\overline{X}_n := \frac{1}{n}\sum_{i=1}^n X_i$ for the sample mean.

Example 4. *For a real-valued sample $\mathcal{X} = (X_1,\dots,X_n)$ the L_p-type test is obtained via the seminorm*

$$\mathcal{N}(\mu) = \Big(\int_{-\infty}^{\infty}|\mu((-\infty,x])|^p F_n(\mathrm{d}x)\Big)^{1/p}$$

where $p\ge 2$, $\mu\in\mathcal{M}(\mathbb{R},\mathcal{B}_{\mathbb{R}})$, and $F_n(x) = \widehat{P}_n((-\infty,x])$ is the empirical distribution function. This is a random semi-norm depending on n. The L_p-type test is discussed in detail in Section 4.2.

Example 5. *Reproducing kernel distance $\zeta_{\mathcal{F}}$ is obtained when $\mathcal{F} = \{f : \|f\|_{\mathcal{H}}\le 1\}$, where $\mathcal{H}$ represents a reproducing kernel Hilbert space (RKHS) with κ as its reproducing kernel. Section 5.2 is devoted to application of kernel-distance for testing epidemic change point.*

In Section 6.2.4 we report empirical power of the test on scalar scenarios. Finally in section 7 we apply defined tests to the electricity balancing prices.

5.2. Theoretical results

Following [25], we consider (5.3), where the function class $\mathcal{F}$ is the unit ball in a reproducing kernel Hilbert space defined via symmetric kernel. To be more precise, let $\kappa:\mathbb{S}\times\mathbb{S}\to\mathbb{R}$ be a symmetric positive definite function. According to the Moore-Aronszajn theorem [9], there is an associated reproducing kernel Hilbert space (RKHS) $H_\kappa(\mathbb{S})$, a separable Hilbert space of real-valued functions defined on $\mathbb{S}$ with the norm $\|x\|_\kappa$ and inner product $\langle x,y\rangle_\kappa$, $x,y\in H_\kappa(\mathbb{S})$ for which the function κ is a reproducing kernel that is

(i) for each $s\in\mathbb{S}$, $\kappa(\cdot;s) = (\kappa(t,s), t\in\mathbb{S})\in H_\kappa(\mathbb{S})$, and

(ii) for each $s\in\mathbb{S}$ and each $f\in H_\kappa(\mathbb{S})$,

$$\langle f,\kappa(\cdot,s)\rangle_\kappa = f(s).$$

The kernel embedding of a probability P on $(\mathbb{S}, \mathcal{S})$ into $H_\kappa(\mathbb{S})$ is $P \to \mu_\kappa(P) \in H_\kappa(\mathbb{S})$ and is defined by a Bochner integral

$$\mu_\kappa(P) = \int_{\mathbb{S}} \kappa(\cdot, s) P(\mathrm{d}s).$$

A sufficient condition for the existence of $\mu_\kappa(P)$ is that κ is Borel measurable and that $\int_{\mathbb{S}} \kappa^{1/2}(s; s) P(\mathrm{d}s) < \infty$. If δ_x is a Dirac measure on $(\mathbb{S}, \mathcal{S})$ then

$$\mu_\kappa(\delta_x) = \kappa(\cdot, x) = (\kappa(s, x), s \in \mathbb{S}).$$

Now consider the pseudo-distance $d_{\mathcal{F}}(P, Q)$, where $\mathcal{F} = \{f \in H_\kappa : \|f\|_\kappa = 1\}$ is the unit ball in RKHS $H_\kappa(\mathbb{S})$. We have

$$\begin{aligned}
d_{\mathcal{F}}(P, Q) &= \sup_{f \in \mathcal{F}} \Big| \int_{\mathbb{S}} f(s) P(\mathrm{d}s) - \int_{\mathbb{S}} f(s) Q(\mathrm{d}s) \Big| \\
&= \sup_{f \in \mathcal{F}} | \int_{\mathbb{S}} \langle f, \kappa(\cdot, s) \rangle P(\mathrm{d}s) - \int_{\mathbb{S}} \langle f, \kappa(\cdot, s) \rangle Q(\mathrm{d}s) \Big| \\
&= \sup_{f \in \mathcal{F}} |\langle f, \mu_\kappa(P) \rangle - \langle f, \mu_\kappa(Q) \rangle| = \sup_{f \in \mathcal{F}} |\langle f, \mu_\kappa(P) - \mu_\kappa(Q) \rangle| \\
&= \|\mu_\kappa(P) - \mu_\kappa(Q)\|_\kappa.
\end{aligned}$$

With this observation test statistic $T_{n,\rho}^{(\mathcal{F})}(\mathcal{X})$ becomes

$$T_{n,\rho}^{\kappa}(X_1, \ldots, X_n) = \max_{1 \le \ell \le n/2} \max_{0 \le k < n-\ell} \frac{\Big\| \sum_{j=k+1}^{k+\ell} [\mu_\kappa(\delta_{X_j}) - \mu_\kappa(\widehat{P}_n)] \Big\|_\kappa}{\rho(\ell/n)}.$$

If the distribution P is known, we may use instead the statistic

$$\widehat{T}_{n,\rho}^{\kappa}(X_1, \ldots, X_n) = \max_{1 \le \ell \le n/2} \max_{0 \le k < n-\ell} \frac{\Big\| \sum_{j=k+1}^{k+\ell} [\mu_\kappa(\delta_{X_j}) - \mu_\kappa(P)] \Big\|_\kappa}{\rho(\ell/n)}.$$

For any two distributions P, Q on $(\mathbb{S}, \mathcal{S})$

$$\begin{aligned}
\|\mu_\kappa(P) - \mu_\kappa(Q)\|_\kappa^2 = &\int_{\mathbb{S}}\int_{\mathbb{S}} \kappa(s, s') P(\mathrm{d}s) P(\mathrm{d}s') \\
&+ \int_{\mathbb{S}}\int_{\mathbb{S}} \kappa(s, s') Q(\mathrm{d}s) Q(\mathrm{d}s') \\
&- 2 \int_{\mathbb{S}}\int_{\mathbb{S}} \kappa(s, s') P(\mathrm{d}s) Q(\mathrm{d}s').
\end{aligned}$$

Hence,

$$
\begin{aligned}
\Delta^2_{k,\ell}(X_1,\dots,X_n) := \Big\| \sum_{j=k+1}^{k+\ell} [\mu_\kappa(\delta_{X_j}) - \mu_\kappa(\widehat{P}_n)] \Big\|^2_\kappa \\
= \sum_{i,j=k+1}^{k+\ell} \kappa(X_i, X_j) + (\ell/n)^2 \sum_{i,j=1}^{n} \kappa(X_i, X_j) \\
- 2(\ell/n) \sum_{i=k+1}^{k+\ell} \sum_{j=1}^{n} \kappa(X_i, X_j).
\end{aligned}
$$

This expression makes statistics $T^{\mathcal{F}}_{n,\rho}(\mathcal{X})$ easy to calculate:

$$
T^{(\kappa)}_{n,\rho}(X_1,\dots,X_n) = \max_{1\le \ell \le n/2} \max_{0 \le k < n-\ell} \frac{\Delta_{k,\ell}(X_1,\dots,X_n)}{\rho(\ell/n)}.
$$

Under H_0, $X_i, i = 1,\dots,n$ are independent and identically distributed with marginal distribution P. So $\mu_\kappa(\delta_{X_i}), i = 1,\dots,n$ are also identically distributed and independent. Its mean is

$$
\mathrm{E}(\mu_\kappa(\delta_{X_i})) = \mathrm{E}\kappa(\cdot, X_i) = \int_{\mathbb{S}} \kappa(\cdot, s) P(\mathrm{d}s) = \mu_\kappa(P),
$$

and covariance $Q : H_\kappa(\mathbb{S}) \to H_\kappa(\mathbb{S})$,

$$
\langle Qh, g\rangle_\kappa = \mathrm{E}(\langle \mu_\kappa(\delta_{X_i}), h\rangle \langle \mu_\kappa(\delta_{X_i}), g\rangle) = \mathrm{E}[f(X_i) g(X_i)], \quad f, g \in H_\kappa.
$$

Similarly,

$$
\widehat{T}^{(\kappa)}_{n,\rho}(X_1,\dots,X_n) = \max_{1\le \ell \le n/2} \max_{0 \le k < n-\ell} \frac{\widehat{\Delta}_{k,\ell}(X_1,\dots,X_n)}{\rho(\ell/n)},
$$

where

$$
\begin{aligned}
\widehat{\Delta}^2_{k,\ell}(X_1,\dots,X_n) := \Big\| \sum_{j=k+1}^{k+\ell} [\mu_\kappa(\delta_{X_j}) - \mu_\kappa(P)] \Big\|^2_\kappa \\
= \sum_{i,j=k+1}^{k+\ell} \kappa(X_i, X_j) + \ell^2 \int_{\mathbb{S}}\int_{\mathbb{S}} \kappa(s,t) P(\mathrm{d}s) P(\mathrm{d}t) \\
- 2\ell \sum_{i=k+1}^{k+\ell} \int_{\mathbb{S}} \kappa(X_i, s) P(\mathrm{d}s).
\end{aligned}
$$

Recall W_Q is a Gaussian $H_\kappa(\mathbb{S})$-valued random process such that $W_Q(t) - W_Q(s)$ has the same distribution as $Y_Q\sqrt{|t-s|}$, where Y_Q is a zero mean Gaussian random variable in $H_\kappa(\mathbb{S})$ with covariance Q.

Theorem 3. *Let $\rho \in \mathcal{R}$. Assume that the random variable X with distribution P satisfies*

$$\lim_{t\to\infty} t\mathbb{P}(\kappa^{1/2}(X,X) > A\theta(t)) = 0 \text{ for any } A > 0. \tag{5.4}$$

Then under H_0,

i) If P is known, then

$$n^{-1/2}\widehat{T}^{(\kappa)}_{n,\rho}(X_1,\ldots,X_n) \xrightarrow{\mathscr{D}} \sup_{0<t-s\le 1/2} \frac{\|W_Q(t)-W_Q(s)\|_\kappa}{\rho(t-s)},$$

ii) If P is unknown, then

$$\begin{aligned} &n^{-1/2}T^{(\kappa)}_{n,\rho}(X_1,\ldots,X_n) \\ &\xrightarrow{\mathscr{D}} \sup_{0<t-s\le 1/2} \frac{\|W_Q(t)-W_Q(s)-(t-s)W_Q(1)\|_\kappa}{\rho(t-s)}, \end{aligned}$$

where $W_Q = (W_Q(t), t\in[0,1])$ is a Q-Wiener process in $H_\kappa(\mathbb{S})$.

Proof. Consider $Z_j := \mu_\kappa(\delta_{X_j}) - \mu_\kappa(P), j = 1,\ldots,n$, as random variables with values in the space $H_\kappa(\mathbb{S})$. Set

$$\zeta_n(t) = \sum_{j=1}^{\lfloor nt\rfloor} Z_j + (nt - \lfloor nt\rfloor)Z_{\lfloor nt\rfloor+1}, \;\; t\in[0,1].$$

Under H_0, $(Z_j, j = 1,\ldots,n)$ are independent and identically distributed random variables with values in the space $H_\kappa(\mathbb{S})$ and satisfies for each $A > 0$,

$$\lim_{t\to\infty} t\mathbb{P}(\|Z_1\|_\kappa > A\theta(t)) = 0. \tag{5.5}$$

Since $\mu_\kappa(P)$ does not contribute to this condition, we have to check that

$$\lim_{t\to\infty} t\mathbb{P}(\|\mu_\kappa(\delta_{X_1})\|_\kappa > A\theta(t)) = 0. \tag{5.6}$$

Since

$$\|\mu_\kappa(\delta_{X_1})\|^2_\kappa = \kappa^{1/2}(X_1,X_1)$$

condition (5.6) follows by (5.4). By Theorem 8 in [38],

$$n^{-1/2}\zeta_n \xrightarrow{\mathscr{D}} W_Q \text{ in the space } \mathcal{H}_\rho^o([0,1], H_\kappa(\mathbb{S})). \tag{5.7}$$

Proof of (i). Let the function $\widehat{L} : \mathcal{H}_\rho^o([0,1], H_\kappa(\mathbb{S})) \to \mathbb{R}$ is defined by

$$\widehat{L}f = \sup_{0<t-s\le 1/2} \frac{\|f(s)-f(t)\|_\kappa}{\rho(t-s)}.$$

It is easy to check that $\widehat{L}$ is a continuous function. By the continuous mapping theorem and (5.7) it follows that

$$\widehat{L}(n^{-1/2}\zeta_n) \xrightarrow{\mathscr{D}} \widehat{L}W_Q.$$

Finally notice that $\widehat{L}(n^{-1/2}\zeta_n) = \widehat{T}_{n,\rho}^\kappa(X_1,\dots,X_n)$ by Theorem 3 in [40].

Proof of (ii). Now let the function $L : \mathcal{H}_\rho^o([0,1], H_\kappa(\mathbb{S})) \to \mathbb{R}$ is defined by

$$Lf = \sup_{0<t-s\le 1/2} \frac{\|f(t)-f(s)-(t-s)f(1)\|_\kappa}{\rho(t-s)}.$$

Again, it is easy to check that L is a continuous function. By the continuous mapping theorem and (5.7) it follows that

$$L(n^{-1/2}\zeta_n) \xrightarrow{\mathscr{D}} LW_Q. \tag{5.8}$$

Finally notice that $L(\zeta_n)$ is a polygonal process with vertexes at

$$(0,0), \quad \Big(k/n, \sum_{j=1}^k (Z_j - \overline{Z}_n)\Big), \quad k=1,\dots,n.$$

Hence, by Theorem 3 in [40], $L(n^{-1/2}\zeta_n) = T_{n,\rho}^\kappa(X_1,\dots,X_n)$, and (5.8) ends the proof of (ii). Now the proof of Theorem is complete. □

Example 6. *Let $\mathbb{S} \subset \mathbb{R}$ be any compact set. Suppose κ is a continuous positive semi-definite kernel on $\mathbb{S}$, and the integral operator $T_\kappa : L_2(\mathbb{S}) \to L_2(\mathbb{S})$ defined by*

$$(T_\kappa f)(\cdot) = \int_{\mathbb{S}} \kappa(\cdot,t) f(t)\mathrm{d}t$$

is positive semi-definite, that is,

$$\int_{\mathbb{S}} \kappa(u,v) f(u) f(v) \mathrm{d}u\mathrm{d}v \geq 0, \quad f \in L_2(\mathbb{S}),$$

Then according to Mercer's theorem, there is an orthonormal basis (e_i) *of* $L_2(\mathbb{S})$ *consisting of eigenfunctions of* T_κ *such that the corresponding sequence of eigenvalues* (λ_i) *are non-negative. The eigenfunctions corresponding to non-zero eigenvalues are continuous on* $\mathbb{S}$ *and* $\kappa(u,v)$ *has the representation*

$$\kappa(u,v) = \sum_{i=1}^{\infty} \lambda_i e_i(u) e_i(v), \quad u, v \in \mathbb{S},$$

where the convergence is absolute and uniform, that is,

$$\lim_{n\to\infty} \sup_{u,v\in\mathbb{S}} \left| \kappa(u,v) - \sum_{i=1}^{n} \lambda_i e_i(u) e_i(v) \right| = 0.$$

Define

$$L_{2,\lambda}(\mathbb{S}) = \{ f \in L_2(\mathbb{S}) : \sum_k \lambda_k^{-1} \langle f, e_k \rangle^2 < \infty \}$$

and endow this set with the inner product

$$\langle f, g \rangle_\kappa = \sum_{k=1}^{\infty} \frac{1}{\lambda_k} \langle f, e_k \rangle \langle g, e_k \rangle.$$

Then $L_{2,\lambda}(\mathbb{S})$ *is the RKHS associated with* κ*. Indeed, since* $\langle \kappa(\cdot, s), e_j \rangle = \lambda_j e_j(s)$*, for* $s \in [0,1]$ *we have*

$$\begin{aligned} \langle f, \kappa(\cdot, s) \rangle &= \sum_{k=1}^{\infty} \frac{1}{\lambda_k} \langle f, e_k \rangle \langle \kappa(\cdot, s), e_k \rangle \\ &= \sum_{k=1}^{\infty} \frac{1}{\lambda_k} \langle f, e_k \rangle \lambda_k e_k(s) = f(s). \end{aligned}$$

The quantiles in Table 5.1 were obtained by Monte Carlo simulation under the null hypothesis. For each kernel listed below, we generated 300 independent samples, each of size $n = 2000$, and estimated the sampling distribution of the test statistic:

(K1) $\kappa(x,y) = 2 - \max(x,y), \quad x,y \in [0,1]$, with data drawn from the $\mathrm{B}(1,9)$ distribution.

(K2) $\kappa(x,y) = \exp\{-\frac{(x-y)^2}{2}\}, \quad x,y \in \mathbb{R}$, with data drawn from the standard normal distribution.

(K3) $\kappa(x,y) = \min(x,y), \quad x,y \in \mathbb{R}^+$, with data drawn from a chi-squared distribution with $df = 1$.

Table 5.1: Estimated quantiles of $T_{n,\rho}^{(\kappa)}$.

$\kappa(x,y)$	γ	2.5%	5%	25%	50%	75%	95%	97.5%
$2-\max(x,y)$	0	1.809	1.858	1.918	1.938	1.946	1.948	1.949
	0.25	1.805	1.843	1.914	1.938	1.946	1.948	1.949
	0.45	1.820	1.860	1.916	1.938	1.947	1.949	1.950
$\exp\{-\frac{(x-y)^2}{2}\}$	0	0.795	0.864	1.031	1.137	1.174	1.193	1.203
	0.25	0.832	0.892	1.069	1.145	1.182	1.231	1.268
	0.45	1.332	1.352	1.439	1.527	1.635	1.857	1.939
$\min(x,y)$	0	0.622	0.641	0.781	0.942	1.126	1.355	1.382
	0.25	0.882	0.911	1.048	1.159	1.303	1.446	1.526
	0.45	2.069	2.110	2.292	2.442	2.577	2.822	2.903

5.3. Conclusions

This chapter introduced the RKHS scan statistic $T_{n,\rho}^{(\kappa)}$ for changed-segment detection on a general sample space $(\mathbb{S}, \mathcal{S})$ equipped with a positive-definite kernel κ, lifting the construction of the previous chapter from real-valued integral discrepancies to Hilbert-space-valued kernel mean embeddings. The leading methodological choice — the kernel κ — is the load-bearing modelling decision: it controls which features of the distribution the test is sensitive to and, through the implied RKHS norm, what notion of distance between distributions the scan maximises (Theorem 3, item (ii)). The construction connects the changed-segment problem to the established two-sample MMD literature [24, 25] and inherits the latter's flexibility: the same test applies to scalar samples, multivariate samples, and functional samples (with a function-space kernel) without modification of the asymptotics. A practical consequence of this generality is that critical values must be obtained per kernel from Monte Carlo simulation under the null (Table 5.1); we leave a data-driven kernel-selection rule for future work. Finite-sample power on real-valued scenarios is reported in Section 6.2.4; a head-to-head comparison with the antisymmetric-kernel and

L_p scans on Birbilas's functional epidemic scenario is given in Section 6.1.2; the test is applied to Lithuanian electricity balancing prices in Chapter 7.

6. Simulation studies

This chapter collects the Monte Carlo evaluation of all three proposed scan statistics under a common organisational scheme: the antisymmetric-kernel (Wilcoxon) test of Chapter 3, the L_p-type test of Chapter 4, and the RKHS test of Chapter 5. We split the evaluation by data type: Section 6.1 presents experiments on functional observations $X_j \in C[0,1]$, where the antisymmetric-kernel test is applied via Brownian projections; Section 6.2 presents experiments on real-valued samples, where the L_p and RKHS tests apply directly.

Throughout we examine the test statistics under a Monte Carlo simulation study. For each scenario we describe the simulated data and report the empirical rejection rate (statistical power) of the corresponding test as a function of the segment length, the weight exponent $\gamma \in \{0, 0.25, 0.45\}$, and any test-specific tuning parameter.

6.1. Functional data

We evaluate the proposed scan statistics on functional samples in two complementary studies. Section 6.1.1 reports a cross-method comparison on three Pareto-based functional scenarios that probe heavy-tailed alternatives across all three projections, the splitting parameter m, and the weight γ. Section 6.1.2 reports a cross-method comparison on the canonical functional epidemic scenario F4 of Birbilas, where the antisymmetric-kernel, L_p and RKHS scans developed in this dissertation are compared with each other and with Birbilas's $E_{n,\beta,\gamma}$ statistic.

6.1.1. Pareto-curve scenarios

This subsection evaluates all three proposed scans — the antisymmetric-kernel test of Theorem 2 (with the projection-based aggregation of Theorem 1), the L_p test of Theorem 2, and the RKHS test of Theorem 3 — under heavy-tailed alternatives, on functional samples whose marginal distributions can be tuned along a Pareto-shape parameter a.

Data

Let (ξ_{jk}) be i.i.d. random variables. Set

$$Y_j(t) = \sum_{k=1}^{d} \xi_{jk} \frac{\sqrt{2}\cos(k\pi t)}{k}, \quad t \in [0,1], \quad d \geq 1, \quad j \geq 1.$$

for scenarios F1 and F2 (defined below). For scenario F3 (also defined below), we set

$$Y_j(t) = \sum_{k=1}^{\lfloor dt \rfloor} \xi_{jk} + (dt - \lfloor dt \rfloor)\xi_{j,\lfloor dt \rfloor + 1}, \quad t \in [0,1], \quad d \geq 1, \quad j \geq 1.$$

We define the following scenarios:

(F1) *Normal vs centred Pareto* (cosine basis). Under the null hypothesis, we take $\xi_{jk} \sim \mathcal{N}(0,1)$ for $j = 1, \ldots, n$. Under the alternative, the in-window coefficients become a centred Pareto difference,

$$\xi_{jk} = Z^1_{jk} - Z^2_{jk}, \quad Z^1_{jk}, Z^2_{jk} \sim \text{Pareto}(1, a), \quad j \in I^*,$$

where $a \in \{1.5, 2, 2.5, 3, 5, 10\}$. There is no in-grid size check ($a = 0$ would recover H_0 but is omitted from the alternative grid by convention); empirical size is monitored separately at $a = 0$ when needed.

(F2) *Pareto vs Pareto* (cosine basis). Under the null hypothesis, we take $\xi_{jk} = Z^1_{jk} - Z^2_{jk}$ with $Z^1_{jk}, Z^2_{jk} \sim \text{Pareto}(1, 1.5)$ for $j = 1, \ldots, n$. Under the alternative, we replace the in-window shape with a,

$$\xi_{jk} = Z^1_{jk} - Z^2_{jk}, \quad Z^1_{jk}, Z^2_{jk} \sim \text{Pareto}(1, a), \quad j \in I^*,$$

where $a \in \{0.5, 1, 1.5, 2, 5\}$. The value $a = 1.5$ is the implicit size check (H_0 holds on I^* as well).

(F3) *Normal vs centred Pareto* (cumulative-sum / piecewise basis). Coefficient marginals are identical to F1 (Normal under H_0, Pa(1,a)−Pa(1,a) on I^*); only the basis differs. We use $a \in \{0.5, 1, 1.5, 2, 2.5, 5\}$.

Throughout the simulations we fixed the change segment as $I^* = \{2n/5 + 1, \ldots, 3n/5\}$. Discrete observations are converted to functional data $(X_j, j = 1, \ldots, n)$ using the Faber–Schauder basis.

Power analysis

We report empirical power for all three methods on the three Pareto-based scenarios, varying the projection (Itô, $\|\cdot\|_{L_2}$, C max-var), the splitting parameter $m \in \{1, 2, 4\}$ for the Wilcoxon scan, the segment-length regime ($\ell^* = \lfloor \log n \rfloor + 1$ short vs. $\ell^* = n/5$ long), and the weight exponent

$\gamma \in \{0, 0.25, 0.45\}$. The change-magnitude index a is scenario-specific: F1 (Normal-vs-centred-Pareto, cosine basis) uses $a \in \{1.5, 2, 2.5, 3, 5, 10\}$; F2 (Pareto-vs-Pareto, baseline shape $\theta = 1.5$) uses $a \in \{0.5, 1, 1.5, 2, 5\}$ with $a = 1.5$ as the implicit size check; F3 uses $a \in \{0.5, 1, 1.5, 2, 2.5, 5\}$. For F1 and F3 the approximate size check is $a = 2.5$. For the Wilcoxon scan the kernel is fixed at the canonical choice from Section 3.3; for the L_p scan we fix $p = 2$. For RKHS we use projection-kernel pairings — Itô / Gaussian, L_2-norm / min, C-max-var / Gaussian — and align the input distribution with the asymptotic null cache by passing each projected scalar series through the rank-CDF (T1) transform from the application Section 7.3; the Gaussian-kernel cells additionally apply the standard-normal quantile (T2) so the input is $N(0, 1)$, while the min-kernel cell uses the U(0,1) cache directly. This is the same calibration pipeline as in Chapter 7.

To keep each table to a glanceable size, we present results split by test (Wilcoxon / L_p / RKHS) and by segment length (short / long); each scenario F1, F2, F3 thus gets six small tables, all reported in Chapter 9.

Observations across scenarios. The pattern is consistent across F1–F3. At $\gamma = 0$ and the long segment regime ($\ell^* = n/5$), all three methods detect the change with high power once a moves away from the null shape: the L_p scan and the Wilcoxon scan with the L_2-norm projection are the most powerful in absolute terms, followed by the RKHS scan and the Wilcoxon scan with the Itô or C-max-var projection. Short segments ($\ell^* = \lfloor \log n \rfloor + 1$) are uniformly hard for every method-projection combination at the configured sample size $n = 400$. At $\gamma \in \{0.25, 0.45\}$ the Wilcoxon and (occasionally) RKHS rejection rates collapse to zero — a finite-sample calibration artefact of the conservative asymptotic critical values at non-zero γ already observed in the F4 study; Monte Carlo size adjustment per scenario is the appropriate remedy. The L_p scan retains comparatively high raw rejection rates across γ, but at the price of inflated empirical size at $a = 0$ (the same calibration gap noted in Section 6.1.2). Increasing the splitting parameter m for the Wilcoxon scan does not buy power, in line with the asymptotic invariance of Theorem 1; finite-sample power is dominated by the per-block effective sample size n/m.

6.1.2. F4 scenario: cross-method comparison

We now turn to a head-to-head comparison of the antisymmetric-kernel scan of Section 3.3, the L_p scan of Section 4.2, and the RKHS scan of Section 5.2, evaluated on the same functional epidemic scenario *F4* introduced by Birbilas in his doctoral dissertation [11]. The same scenario is also used to evaluate

Birbilas's own $E_{n,\beta,\gamma}$ statistic, providing an external benchmark.

Functional samples $X_1, \ldots, X_n \in C[0,1]$ are generated as a first-order functional autoregression FAR(1) under H_0, with a temporary departure on a contiguous interval $I^* = \{k^* + 1, \ldots, k^* + \ell^*\}$ under H_1.

The theoretical null limits established in Chapters 3–5 are derived under independence. The FAR(1) design used here is therefore not covered directly by those theorems; it is included as an external robustness benchmark and to enable comparison with Birbilas's functional epidemic scenario. Rejection rates in this subsection should be interpreted as finite-sample Monte Carlo performance under this dependent design, not as a consequence of the independence-based asymptotic theory.

The change magnitude is indexed by $a \in \{0,\ 0.25,\ 0.5,\ 1,\ 2,\ 4,\ 8\}$, with $a = 0$ recovering H_0. Two segment-length regimes are evaluated: a short segment ($\ell^* = \lfloor \log n \rfloor + 1$, used to expose detection in localised changes) and a long segment ($\ell^* = n/5$, used to expose detection in broader changes). Throughout we use $n = 400$, $N_{\text{rep}} = 100$ Monte Carlo replications, and nominal level $\alpha = 0.05$. Three projection schemes reduce functional samples to scalars: the Itô integral against an isonormal Gaussian process (Section 2.1), the L_2 norm of the sample path, and the $C[0,1]$ max-variance projection (Section 2.2).

Wilcoxon (antisymmetric-kernel) test

Tables 9.19 and 9.20 report power for the antisymmetric-kernel scan with the Wilcoxon kernel (Section 3.3), varying the splitting parameter $m \in \{1, 2, 4\}$, the projection and the weight exponent γ at the short and long segment-length regimes respectively.

The pattern is consistent across projections: the test gains substantial power as a grows for the long-segment regime, whereas in the short-segment regime power remains modest. At $\gamma \in \{0.25, 0.45\}$ the empirical rejection rate collapses to zero — a finite-sample artefact of the conservative critical-value adjustment used at non-zero γ even at $n = 400$, rather than a population-level statement. Increasing m does not improve power: in agreement with Theorem 1 the asymptotic distribution does not depend on m, and finite-sample power is dominated by the effective per-block sample size n/m.

L_p test

Tables 9.21 and 9.22 report power for the L_p scan of Theorem 2 at $p \in \{2, 4, 10\}$ at the short and long segment regimes respectively. $p = 2$ recovers the Cramér–von Mises specialisation; larger p progressively up-weights tail discrepancies between the inside-window and outside-window empirical distributions.

The L_p scan exhibits high power across all (p, projection, γ) settings, but also non-trivial empirical size at $a = 0$ (≈ 0.3–0.9) — the test is over-rejecting under H_0 at $n = 400$. Increasing p from 2 to 10 does not materially change the power profile on F4 (the row blocks are within sampling noise of each other), suggesting that for this scenario the change manifests primarily in the bulk rather than the tail of the empirical distribution; we expect $p \in \{4, 10\}$ to gain ground over $p = 2$ on heavier-tailed alternatives or under stronger tail contamination, which is left to a dedicated tail-targeted study. The size inflation across all p points to a finite-sample calibration gap relative to the asymptotic critical values of Table 4.1; size adjustment by Monte Carlo simulation is the appropriate remedy.

RKHS test

Tables 9.23 and 9.24 report power for the RKHS scan of Theorem 3 at the short and long segment regimes respectively, paired with the projection-fitting kernel choices: a Gaussian RBF for the (signed-real) Itô and C max-var projections, and the Brownian-bridge min kernel for the (non-negative) L_2-norm projection. The empirical H_0 quantiles of the test statistic at the matched (projection, kernel) pairs — which serve as the calibrated 5% critical values used to compute the rejection rates — are tabulated in Table 9.25.

Empirical size is well controlled in all three settings (≤ 0.10). Power is sharply kernel-dependent: the min kernel paired with the L_2-norm projection achieves near-perfect power on long segments at moderate a, while the Gaussian kernel applied to the Itô or C max-var projection shows much weaker detection. This confirms the message of Section 5.2 that the kernel choice is a load-bearing modelling decision; the quantile table additionally exposes the very different scales on which the test statistic operates under the three projection-kernel pairings, which directly explains the disparity in their power profiles.

Birbilas's epidemic statistic

Birbilas [11] introduced the epidemic-change test

$$E_{n,\beta,\gamma} = \max_{0 \le k < m \le n} \sup_{t \in [0,1]} \frac{\left|(I - \beta(t))\, S_{k,m}(t)\right|}{(m-k)^{\gamma}}, \tag{6.1}$$

where $S_{k,m}(t) = \sum_{i=k+1}^{m} \big(X_i(t) - \bar{X}_n(t)\big)$, $\bar{X}_n(t) = n^{-1} \sum_i X_i(t)$, $\beta : [0,1] \to \mathbb{R}$ is a Faber–Schauder-induced operator coefficient, and $\gamma \in [0, 1/2)$ plays the role of our weight exponent. He rejects H_0 at level α when $n^{-1/2+\gamma} E_{n,\beta,\gamma} > C''_{\alpha}$, where the asymptotic critical value C''_{α} is the $(1-\alpha)$-quantile of the corresponding Wiener-sheet limit; for moderate n his Algorithm 1 substitutes a finite-sample empirical quantile, which is what we use below.

Tables 9.26 and 9.27 report power for $E_{n,\beta_1,\gamma}$ with the canonical $\beta_1(t) = 0.7\sqrt{t}$ and the finite-sample critical-value adjustment, for the short and long segment regimes.

Birbilas's statistic is, on F4, the most powerful of the four against long-segment alternatives across every γ, attaining unit power already at $a = 1$. On short segments it is competitive with our Wilcoxon and L_p scans for $a \ge 4$ but notably weaker for moderate $a \in [0.5, 2]$, where the RKHS scan with the min kernel and our L_p scan are stronger.

Cross-method observations

On long segments at moderate-to-large a, all four methods detect the change, with Birbilas's statistic and the RKHS-min-kernel/L_2-norm pair the most powerful, followed closely by our L_p and Wilcoxon scans. On short segments the four methods diverge sharply: the L_p scan retains the highest raw rejection rate but at the cost of inflated size, the RKHS-Gaussian setup loses power outright, and Birbilas's statistic is competitive only at the largest a. The $\gamma \in \{0.25, 0.45\}$ Wilcoxon rejection rates of zero point to a finite-sample calibration mismatch that should be corrected by simulating critical values directly under F4 rather than reading them from the asymptotic distribution of T_γ in Table 3.1.

6.1.3. Investigating stability of random projections

The Itô-integral projector W of Section 2.1 depends on the realisation of the Wiener process $W = W(\omega)$, so the antisymmetric-kernel scan statistic $T_n =$

$T_n\big(\mathrm{W}(X_1),\ldots,\mathrm{W}(X_n)\big)$ of Section 3.3 is itself a random variable conditional on the data. A single evaluation of the test depends on ω, so the practical recipe is to repeat the test on N independent draws $\omega_1,\ldots,\omega_N$ and report the empirical rejection rate

$$\widehat{R}_N \;=\; \frac{1}{N}\sum_{i=1}^{N}\mathbf{1}\{T_n(\omega_i) > c_\alpha\}. \tag{6.2}$$

The two regimes that make this procedure consistent are

$$P\big(T_n(\omega) > c_\alpha \,\big|\, H_A\big) \xrightarrow[n\to\infty]{} 1, \tag{6.3}$$
$$P\big(T_n(\omega) > c_\alpha \,\big|\, H_0\big) \xrightarrow[n\to\infty]{} 0, \tag{6.4}$$

which by the law of large numbers (conditionally on the data) imply $\widehat{R}_N \to 1$ under H_A and $\widehat{R}_N \to 0$ under H_0 as n and N grow.

To investigate the finite-sample stability of $\widehat{R}_N$ we fix K independently drawn samples per scenario and compute $\widehat{R}_N$ on each over N independent Itô trajectories. We use the four functional scenarios already defined in this chapter, F1, F2, F3 of Section 6.1.1 and F4 of Section 6.1.2, at a representative grid of a that combines the implicit size check ($a \in \{2.5, 1.5, 2.5, 0\}$ for F1 / F2 / F3 / F4 respectively) with a few alternatives. All test parameters (kernel, weight, level, segment geometry) are inherited from the F1–F4 power tables of Sections 6.1.1 and 6.1.2 so that the only quantity varying within a cell is the realisation of the projector W. We use $n = 400$, $N = 100$ Itô draws per fixed sample, $K = 100$ independently drawn fixed samples per (scenario, a), $\gamma \in \{0, 0.25, 0.45\}$, and $\alpha = 0.05$. For each $(\text{scenario}, a, \gamma)$ Table 9.28 (Section 9.3) reports the mean, standard deviation, and coefficient of variation CV $=$ sd$/$mean of $\widehat{R}_N$ across the K fixed samples. Because absolute standard deviations are difficult to compare across cells with different mean rejection rates, the table also reports CV whenever the mean is bounded away from zero; for near-zero means the coefficient is undefined and we write "–" in that column, retaining the sd as the primary spread summary. The reported sd combines the within-X binomial Monte Carlo error $\sqrt{p(1-p)/N}$ with the genuine between-X spread of $E[\widehat{R}_N \mid X]$; on most cells the between-X component dominates.

Three observations emerge. First, at $\gamma = 0$ the mean of $\widehat{R}_N$ tracks the asymptotic targets (6.3)–(6.4): it sits within a few percent of α at the size-check a for F1, F2 and F3, and reaches values at or near 1 at the strongest alternatives in every scenario. The F4 size-check at $a = 0$ is the one exception, sitting at $\widehat{R}_N \approx 0.20$ with substantial between-sample spread (sd ≈ 0.16). At $\gamma = 0.25$ the size-check rate collapses to zero in every scenario; the strongest alternatives still attain rates at or near 1 in F1, F2 and F4, while in F3 the strongest alternative ($a = 5$) drops to 0.013. At $\gamma = 0.45$ the mean of $\widehat{R}_N$ is uniformly zero. The size collapse at $\gamma \in \{0.25, 0.45\}$ and the F3 power loss at $\gamma = 0.25$ are all instances of the same conservative-asymptotic-critical-value artefact described in Sections 6.1.1 and 6.1.2, and reflect calibration of c_α at non-zero γ rather than projection variability. Second, the standard deviation of $\widehat{R}_N$ across the K fixed samples is small on most cells, so a single random draw of X already gives a representative reading of the rejection rate; the spread is larger on boundary cells (notably F2 at $a = 2$, F4 at $a = 1$ for $\gamma = 0.25$, and the F3 and F4 size-checks at $\gamma = 0$), and is then dominated by the between-X variability of $E[\widehat{R}_N \mid X]$ rather than by within-X binomial error. Third, the randomness coming from W is handled by averaging over N projections at a fixed X, and the residual dependence on the realisation of X, surfaced by the sd column, is modest in the parameter ranges considered here.

6.2. Scalar data

We evaluate all three proposed tests on real-valued samples: the antisymmetric-kernel (Wilcoxon) scan of Chapter 3, the L_p test of Chapter 4, and the RKHS test of Chapter 5. The three tests share the same data scenarios, defined below; we then report the empirical power of each test in turn.

6.2.1. Data scenarios

We used the following scenarios:

(S1) *Normal.* Under H_0: $X_j \sim \mathcal{N}(0, 1)$, $j = 1, \ldots, n$. Under H_1: $X_j \sim \mathcal{N}(a, 1)$, $j \in I^*$.

(S2) *Non-central chi squared.* Under H_0: $X_j \sim {\chi'}^2_1(0)$, $j = 1, \ldots, n$. Under H_1: $X_j \sim {\chi'}^2_1(a)$, $j \in I^*$.

(S3) *Pareto.* Under H_0: $X_j \sim \mathrm{Pa}(1, 3)$, $j = 1, \ldots, n$. Under H_1: $X_j \sim \mathrm{Pa}(1 + a, 3)$, $j \in I^*$.

(S4) *Beta.* Under H_0: $X_j \sim \mathrm{B}(1, 9)$, $j = 1, \ldots, n$. Under H_1: $X_j \sim \mathrm{B}(1 + a, 9 - a)$, $j \in I^*$.

(S5) *Pareto shape change.* Under H_0: $X_j \sim \text{Pa}(1, 3)$, $j = 1, \dots, n$. Under H_1: $X_j \sim \text{Pa}(1, 3 + 10a)$, $j \in I^*$.

In all scenarios, we fix sample size $n = 400$ and place the epidemic interval $I^* = \{k^* + 1, \dots, k^* + l\}$ at $k^* = \lfloor n/2 \rfloor - \lfloor l/2 \rfloor$, with length $l \in \{\lfloor \log n \rfloor + 1,\, n/5\}$. The change magnitude $a \in \{0, \frac{1}{4}, \frac{1}{2}, 1, 2, 4, 8\}$ indexes the alternative, with $a = 0$ recovering the null hypothesis.

6.2.2. Wilcoxon test power

Tables 9.29 and 9.30 report power for the antisymmetric-kernel scan with the Wilcoxon kernel $h(x, y) = \mathbf{1}\{x - y \leq 0\} - \mathbf{1}\{y - x \leq 0\}$ (Section 3.3, $\beta = 0$), varying the splitting parameter $m \in \{1, 2, 4\}$, split by segment length.

For long segments ($\ell^* = n/5$, Table 9.30) the test detects shifts reliably already at $a \geq 1$, with size well controlled at $\gamma = 0$. For short segments ($\ell^* = \lfloor \log n \rfloor + 1$, Table 9.29) detection is much weaker and depends sharply on the scenario. As in the functional study, the rejection rates collapse to zero at $\gamma \in \{0.25, 0.45\}$: even at $n = 400$ the asymptotic critical values of Tables 3.1 and 3.2 are conservative at non-zero γ, and a Monte Carlo size adjustment is needed to recover power. Increasing m does not improve power, in line with Theorem 1 the asymptotic limit is invariant in m, and finite-sample power is dominated by the per-block effective sample size n/m.

6.2.3. L_p test power

Tables 9.31 and 9.32 report power for the L_p scan of Theorem 2 (at $p = 2$), split by segment length, and show that in all scenarios the setting $\gamma = 0.45$ provides the most attractive operating characteristics. Under the null hypothesis ($a = 0$) it gives the smallest type I error rate, while for every genuine departure ($a \geq 0.25$) and especially for $a \geq 2$ it matches or exceeds the power achieved by smaller γ values. The weaker performance observed for $\gamma < 0.45$ is largely explained by a slower convergence of the test statistic with its limit distribution, which inflates the rejection rate under the null hypothesis and, in turn, reduces the effective power. In short, $\gamma = 0.45$ offers the best trade-off: accurate type I error control combined with maximal sensitivity to meaningful changes.

6.2.4. RKHS test power

Tables 9.33 and 9.34 report power for the RKHS scan of Theorem 3, split by segment length, and reveal a different operating profile for the RKHS test than for its L_p counterpart. In scenarios S1 and S2, settings with $\gamma \leq 0.25$ achieve the desirable combination of a low type-I error rate and high power once $a \geq 1$. In scenario S4, however, the choice $\gamma = 0.45$ performs best. The sharp

0-to-1 power transition for S4 reflects the directional bias of the kernel $2 - \max(x, y)$ toward small values: under H_1 the in-window Beta marginal $\mathrm{B}(1 + a, 9 - a)$ shifts upward, so the within-window kernel sum *decreases* under mild alternatives and the scan statistic only exceeds the rejection threshold once the in-window data become substantially heavier-valued ($a \geq 4$ at $\gamma = 0.25$, $a \geq 2$ at $\gamma = 0.45$).

6.3. Conclusions

We observe in the Pareto-curve study of Section 6.1.1 a greatly diminished Wilcoxon-test power when γ is chosen close to $\frac{1}{2}$; this behaviour arises from the reduced convergence rate $n^{\frac{1}{2}-\gamma}$ and is also visible in the shift of distributions in Figure 3.1. The Brownian-projection approach (Itô vs. norm) provides complementary sensitivities for the Wilcoxon scan: the Itô integral aggregates evidence across multiple basis features and benefits from larger d when changes are broad, while the norm projection is more parsimonious and competitive when the alternative differs predominantly in tail behaviour. The L_p and RKHS scans are more γ-robust on F1–F3, frequently saturating at power one for $\gamma \in \{0.25, 0.45\}$ on long segments; among their three projections the L_2-norm wins the majority (roughly 60–80%) of long-segment cells across F1–F3, while Itô and C-max-var trail with broadly similar per-cell win counts and both exhibit non-monotone behaviour across a. On short segments at $n = 400$ no projection dominates and the per-cell ranking becomes mixed.

The F4 cross-method comparison of Section 6.1.2 reinforces these observations and adds a comparative perspective. On long segments all four methods detect the change with high power; on short segments and at intermediate change magnitudes, the methods fan out and the L_2 norm plus the RKHS scan with a problem-matched kernel offer the strongest detection. Birbilas's $E_{n,\beta,\gamma}$ remains a strong baseline. The current finite-sample size of the L_p scan and the calibration gap of the Wilcoxon scan at $\gamma > 0$ both point to Monte Carlo critical-value calibration as a practical refinement worth carrying through.

The scalar scenarios of Section 6.2 are deliberately scalar so that the power of the tests can be isolated from the choice of projection used to reduce functional observations to scalars. This is the cleanest setting in which to compare the kernels (K1)–(K3) defined in Section 5.2. Across all five scalar scenarios the L_p scan with $\gamma = 0.45$ reaches power one at $a \geq 2$ in every long-segment cell while keeping the type-I rate the lowest at $a = 0$, which makes it the most robust default among the three tests. The Wilcoxon scan calibrates well at $\gamma = 0$ on long segments but loses all power at $\gamma \in \{0.25, 0.45\}$, reinforcing the same Monte Carlo critical-value remedy already recommended for the functional case. The RKHS scan is sharply pairing-dependent: the (S1, Gaussian) and (S2, min) cells reach high power once $a \geq 1$ on long segments, while the (S4, $2 - \max$) cell only fires for extreme right-shifts because the kernel rewards co-occurrence at small values. The scalar study therefore isolates two practical lessons that the functional case obscures: $\gamma = 0.45$ is the right default for the L_p scan, and RKHS performance is contingent on aligning the kernel's directional emphasis with the alternative.

7. Application to Lithuanian electricity balancing prices

7.1. Motivation and Data

To illustrate the practical performance of the proposed tests, we apply them to the Lithuanian electricity balancing price data.[1] The three scans evaluated are the antisymmetric-kernel (Wilcoxon) scan of Chapter 3, the L_p-type scan of Chapter 4, and the RKHS scan of Chapter 5. Balancing prices are short-term market prices used to correct the imbalances between electricity supply and demand. They are known to exhibit abrupt changes due to shocks in demand, supply outages, or regulatory adjustments, and therefore provide a natural setting for changed segment models. We note that the balancing price data form a dependent time series rather than an i.i.d. sample; our analysis here is therefore exploratory, illustrating how the proposed methods can be applied in practice.

7.2. Functional Representation and Pre-processing

We used the hourly balancing price data from 2018 to 2024. For each week, we smoothed the hourly observations, 168 discrete points, into a continuous function on $[0, 1]$ using the Faber–Schauder basis expansion with truncation at $K = 4$. This yielded a sequence of functional observations $\{X_j(t) : j = 1, \ldots, n;\ t \in [0, 1]\}$ representing weekly price curves. Figure 7.1 shows the smoothed functional time series, which contained an outlier week (2021-11-20 – 2021-11-26) that, when removed, yielded a more stable dataset. Figure 7.2 shows the derived univariate inputs (L_2 norm, Itô projection, C projection).

7.3. Testing Framework

We apply some transformations before applying the L_p-type test (Theorem 2) and the RKHS test (Theorem 3), to satisfy the conditions of those theorems:

(T1) *L_p-type* For the observed sample $\{X_1, \ldots, X_n\}$, we define the empirical distribution function

$$\widehat{F}_n(x) = \frac{1}{n} \sum_{i=1}^{n} \mathbf{1}\{X_i \le x\}.$$

Then each observation X_i is transformed via

$$\widehat{F}_n(X_i) = \frac{1}{n} \sum_{j=1}^{n} \mathbf{1}\{X_j \le X_i\},$$

[1] Data provided by Litgrid, Lithuania's electricity grid operator: `https://baltic.transparency-dashboard.eu/`.

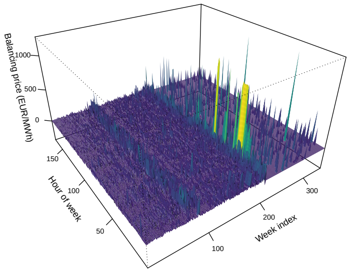

(a) Weekly functional observations, each curve representing one week of hourly balancing prices (168 points) smoothed using a Faber–Schauder basis expansion.

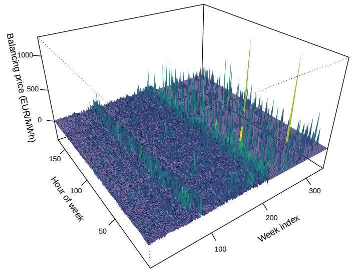

(b) Same as (a), omitting the outlier week.

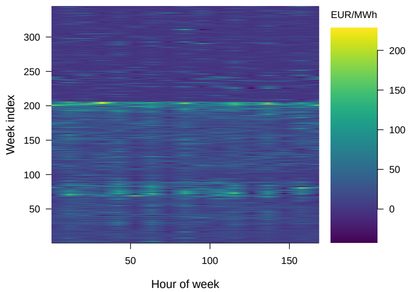

(c) Contour of the smoothed sample without the outlier. Colour indicates price level (EUR/MWh).

Figure 7.1: Visualisation of the electricity balancing price dataset.

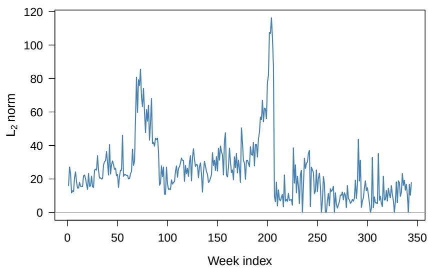

(a) L_2 norm

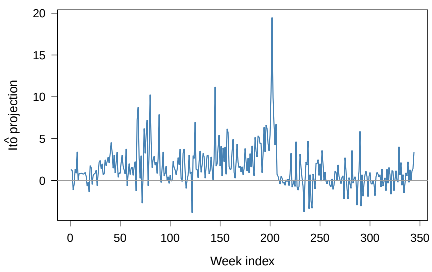

(b) Itô projection

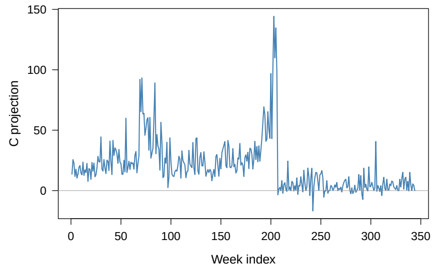

(c) C projection

Figure 7.2: Projections of the electricity balancing price dataset.

(T2) *RKHS* Next, we transform $\widehat{F}_n(X_i) \in [0,1]$ into the chi-square distribution with one degree of freedom through the quantile function $Q_{\chi^2_1}$. Define the transformed values

$$Y_i := Q_{\chi^2_1}\big(\widehat{F}_n(X_i)\big),$$

where $Q_{\chi^2_1}(u) = \inf\{x \in \mathbb{R} : F_{\chi^2_1}(x) \geq u\}$ denotes the inverse cumulative distribution function (CDF) of the χ^2_1 distribution. This transformation yields a sample $\{Y_1, \ldots, Y_n\}$ that is approximately chi-squared distributed and, therefore, can be used in the RKHS type test with the precalculated quantile values.

Consequently, we performed the proposed tests in two scenarios: (1) including the outlier week and (2) excluding it. In both cases, we applied the tests under three weighting parameters, $\gamma \in \{0.05, 0.25, 0.45\}$. The detected interval endpoints reported in the tables correspond to the values $(\frac{k}{n}, \frac{l}{n})$ at which the test statistic attains its maximum, i.e., the estimated start and end points of the epidemic segment.

7.4. Results

Table 7.1 reports the cross-method comparison on the no-outlier dataset: the Wilcoxon scan of Theorem 2, the L_p-type scan of Theorem 2 (at $p = 2$), and the RKHS scan of Theorem 3, each evaluated under all three projection schemes (Itô, $\|\cdot\|_{L_2}$, C max-var) and at $\gamma \in \{0.05, 0.25, 0.45\}$ (Wilcoxon) or $\gamma \in \{0, 0.25, 0.45\}$ (L_p / RKHS). At $\gamma \leq 0.25$ all nine method-projection combinations reject H_0 (the Itô-feature draws of the Wilcoxon and RKHS scans reject in $\geq 60\%$ of the 10 random-feature replicates) and locate the change interval to roughly $[0.08,\ 0.60]$ of the sample, i.e. the segment from approximately September 2018 to February 2022. At $\gamma = 0.45$, the Wilcoxon test statistics fall just below the asymptotic critical value across all three projections (no rejection), while the L_p and RKHS scans continue to reject across all three projections; this is consistent with the conservative finite-sample behaviour at large γ observed in the simulation studies of Sections 6.1 and 6.2. For the RKHS scan the kernel is paired with the projection so that the kernel-specific input distribution of (K1)–(K3) in Section 5.2 is matched after the rank-CDF (T1) and quantile (T2) transforms of Section 7.3: Gaussian kernel for Itô and C max-var (with Q_Φ as T2, so the transformed sample is approximately $\mathcal{N}(0, 1)$, matching K2), and min kernel for $\|\cdot\|_{L_2}$ (with $Q_{\chi_1^2}$ as T2, so the transformed sample is approximately χ_1^2, matching K3). The Itô projection was repeated 10 times to expose the variability induced by the random isonormal-Gaussian features; the reported T and interval endpoints are the corresponding means $\pm$ standard deviations, and the rejection column reports the rejection rate over the 10 draws.

The L_p and RKHS rows operate on the same three projections as the Wilcoxon rows; the rank-CDF transform T1 (with a kernel-matched quantile transform T2: Q_Φ for the Gaussian kernel and $Q_{\chi_1^2}$ for the min kernel) is applied before each RKHS scan so that the null distributions of Table 5.1 apply directly. The L_p rows use T1 only (the L_p asymptotic null is parameter-free under the empirical-CDF transform). The γ grid is $\{0,\ 0.25,\ 0.45\}$, matching the L_p and RKHS caches of Tables 4.1 and 5.1, whereas the Wilcoxon rows use the (Wilcoxon-cache-friendly) $\{0.05,\ 0.25,\ 0.45\}$ grid. Both grids are equally valid; the small offset at the lower end has no qualitative bearing on the rejection decisions.

Outlier-robustness check. Repeating the same battery on the full dataset (including the anomalous week) yields qualitatively the same conclusion: every method-projection-γ combination produces a rejection (or a near-miss at

Table 7.1: Cross-method comparison on the Lithuanian electricity balancing-price data (outlier week removed). For each test, projection (where applicable) and weight exponent γ, the table reports the test statistic T, the detected change-segment endpoints $(\hat{\ell}_-, \hat{\ell}_+)$ as fractions of the sample, and whether H_0 is rejected at the asymptotic critical value T_ρ given in parentheses. The Itô-projection entries are mean $\pm$ s.d. over 10 independent random-feature draws.

Test	**Projection**	γ	T	$\hat{\ell}_-$	$\hat{\ell}_+$	H_0 **rejection**
Wilcoxon (Ch. 3)	Itô	0.05	3.398 ± 1.052	0.126 ± 0.053	0.627 ± 0.051	100%
		0.25	3.048 ± 1.345	0.123 ± 0.060	0.666 ± 0.070	60%
		0.45	2.550 ± 0.529	0.135 ± 0.055	0.680 ± 0.067	0%
	$\|\cdot\|_{L_2}$	0.05	5.988	0.078	0.592	yes ($T_\rho = 1.862$)
		0.25	4.537	0.078	0.592	yes ($T_\rho = 2.527$)
		0.45	3.438	0.078	0.592	no ($T_\rho = 3.852$)
	C max-var	0.05	6.645	0.005	0.598	yes ($T_\rho = 1.862$)
		0.25	5.000	0.005	0.598	yes ($T_\rho = 2.527$)
		0.45	3.770	0.061	0.598	no ($T_\rho = 3.852$)
L_p ($p = 2$) (Ch. 4)	Itô	0.00	1.028 ± 0.527	0.249 ± 0.216	0.724 ± 0.159	90%
		0.25	1.288 ± 0.649	0.430 ± 0.190	0.780 ± 0.249	90%
		0.45	1.641 ± 0.715	0.513 ± 0.241	0.739 ± 0.302	70%
	$\|\cdot\|_{L_2}$	0.00	1.326	0.183	0.736	yes ($T_\rho = 0.545$)
		0.25	1.539	0.186	0.736	yes ($T_\rho = 0.683$)
		0.45	1.960	0.195	0.262	yes ($T_\rho = 1.082$)
	C max-var	0.00	2.364	0.003	0.599	yes ($T_\rho = 0.545$)
		0.25	2.913	0.599	0.997	yes ($T_\rho = 0.683$)
		0.45	3.502	0.599	0.997	yes ($T_\rho = 1.082$)
RKHS (Ch. 5)	Itô	0.00	1.760 ± 0.689	0.048 ± 0.062	0.718 ± 0.162	70%
		0.25	2.104 ± 0.883	0.411 ± 0.206	0.850 ± 0.151	90%
		0.45	2.613 ± 1.020	0.402 ± 0.209	0.654 ± 0.316	70%
	$\|\cdot\|_{L_2}$	0.00	2.322	0.183	0.730	yes ($T_\rho = 1.355$)
		0.25	2.701	0.183	0.730	yes ($T_\rho = 1.446$)
		0.45	4.859	0.552	0.596	yes ($T_\rho = 2.822$)
	C max-var	0.00	3.658	0.000	0.596	yes ($T_\rho = 1.193$)
		0.25	4.545	0.596	0.997	yes ($T_\rho = 1.231$)
		0.45	5.456	0.596	0.997	yes ($T_\rho = 1.857$)

$\gamma = 0.45$ for the Wilcoxon scan with the Itô and $\|\cdot\|_{L_2}$ projections, mirroring the trimmed dataset), and the located change segment is comparable. Table 7.2 mirrors the structure of Table 7.1 so that with- and without-outlier outcomes can be compared row-by-row; the $\|\cdot\|_{L_2}$ rows of the L_p and RKHS scans track their no-outlier counterparts to within the third decimal of T, confirming that the L_2-norm projection is essentially insensitive to the single outlying week.

Table 7.2: Cross-method outcomes on the Lithuanian electricity balancing-price data, full dataset (outlier week included). Same structure as Table 7.1.

Test	**Projection**	γ	$\boldsymbol{T}$	$\hat{\ell}_-$	$\hat{\ell}_+$	$\boldsymbol{H_0}$ **rejection**
Wilcoxon (Ch. 3)	Itô	0.05	3.966 ± 1.264	0.109 ± 0.048	0.639 ± 0.068	100%
		0.25	2.883 ± 0.824	0.110 ± 0.054	0.654 ± 0.075	70%
		0.45	3.369 ± 1.392	0.135 ± 0.064	0.645 ± 0.064	30%
	$\|\cdot\|_{L_2}$	0.05	6.162	0.078	0.595	yes ($T_\rho = 1.862$)
		0.25	4.668	0.078	0.595	yes ($T_\rho = 2.527$)
		0.45	3.537	0.078	0.595	no ($T_\rho = 3.852$)
	C max-var	0.05	6.695	0.073	0.599	yes ($T_\rho = 1.867$)
		0.25	5.071	0.073	0.599	yes ($T_\rho = 2.538$)
		0.45	3.841	0.073	0.599	no ($T_\rho = 3.851$)
L_p ($p = 2$) (Ch. 4)	Itô	0.00	1.033 ± 0.525	0.249 ± 0.216	0.727 ± 0.158	90%
		0.25	1.297 ± 0.650	0.431 ± 0.192	0.780 ± 0.247	90%
		0.45	1.652 ± 0.719	0.527 ± 0.230	0.755 ± 0.312	70%
	$\|\cdot\|_{L_2}$	0.00	1.340	0.183	0.738	yes ($T_\rho = 0.545$)
		0.25	1.555	0.183	0.602	yes ($T_\rho = 0.683$)
		0.45	1.952	0.195	0.262	yes ($T_\rho = 1.082$)
	C max-var	0.00	2.391	0.003	0.602	yes ($T_\rho = 0.545$)
		0.25	2.955	0.602	0.997	yes ($T_\rho = 0.683$)
		0.45	3.557	0.602	0.997	yes ($T_\rho = 1.082$)
RKHS (Ch. 5)	Itô	0.00	1.760 ± 0.687	0.048 ± 0.062	0.720 ± 0.160	70%
		0.25	2.112 ± 0.888	0.412 ± 0.208	0.850 ± 0.148	90%
		0.45	2.626 ± 1.031	0.437 ± 0.202	0.694 ± 0.279	70%
	$\|\cdot\|_{L_2}$	0.00	2.339	0.183	0.733	yes ($T_\rho = 1.355$)
		0.25	2.737	0.549	0.599	yes ($T_\rho = 1.446$)
		0.45	5.053	0.552	0.599	yes ($T_\rho = 2.822$)
	C max-var	0.00	3.694	0.000	0.599	yes ($T_\rho = 1.193$)
		0.25	4.598	0.599	0.997	yes ($T_\rho = 1.231$)
		0.45	5.528	0.599	0.997	yes ($T_\rho = 1.857$)

8. Concluding remarks and future work

Summary of contributions

This dissertation develops nonparametric methodology for detecting *epidemic* (changed-segment) departures in functional data. Three complementary families of scan statistics are proposed and analysed:

(a) *antisymmetric-kernel* scans of the Wilcoxon type, applied to features of functional observations through Brownian and related projections (Chapter 3);

(b) *L_p-type* (Cramér–von Mises) scans of empirical process increments, over start index and window length jointly (Chapter 4);

(c) *RKHS-based* scans using kernel mean embeddings (Chapter 5).

For each family we (i) establish a functional central limit theorem in a Hölder-type space $\mathcal{H}^o_\rho$ tailored to the weighting class $\mathcal{R}$; (ii) derive the null limit distribution of the scan statistic and tabulate its quantiles by Monte Carlo; and (iii) study finite-sample power under heavy-tailed and Gaussian-vs.-Pareto alternatives. Chapter 7 exercises the three procedures on Lithuanian electricity balancing prices as an exploratory application (the data are dependent and thus outside the i.i.d. assumptions of the theory, so we treat the application as illustrative rather than confirmatory).

Future work

Several open directions remain.

Data-driven choice of ρ. All three scans depend on the weighting function $\rho \in \mathcal{R}$; simulations (Chapters 3, 4, 5) suggest that $\gamma = 0.25$ provides a favourable trade-off between short- and long-segment sensitivity. Developing an objective, data-driven selection rule for ρ – for instance through cross-validation of empirical power or through an information criterion on segment width – is a concrete and tractable open problem.

Power as a function of segment length. It is currently unclear how the power of the test depends on the length of the changed segment $|I^*|$ and the magnitude of the distributional shift. Chapter 3 gives heuristic arguments pointing to thresholds of order $\log n$, but a rigorous minimax-type lower bound tied to the weighting exponent γ would complete the theoretical picture.

Dependent data. The theoretical analysis assumes i.i.d. samples. Extending the functional limit theorems of Chapters 3–5 to weakly dependent (e.g.,

α-mixing or near-epoch dependent) functional sequences would make the tests directly applicable to the balancing-price data of Chapter 7 without the i.i.d. caveat.

Alternative projections. Chapter 7 introduces a simple point-wise "C projection" (sampling the path at the argmax of the sample variance) as a complement to L_2-norm and Itô-integral projections. More systematic projection rules – driven by the local geometry of the sample path or by a specific alternative of interest – would help localise changes that are confined to a narrow time window.

Broader applications. Balancing-price data are one of many possible domains for the methodology; further empirical studies, particularly on biomedical signals and high-frequency finance, would test the robustness and interpretability of the proposed scans.

9. APPENDIX

This chapter collects the tables of simulated rejection rates supporting Chapter 6, in turn for the Pareto-curve scenarios F1–F3 of Section 6.1.1, the F4 cross-method comparison of Section 6.1.2, the random-projection stability scan of Section 6.1.3, and the scalar scenarios S1–S5 of Section 6.2.

9.1. Functional data: Pareto scenarios

Table 9.1: Wilcoxon test power on *F1: Normal vs centred Pareto*, segment length $\ell^* = \lfloor \log n \rfloor + 1$. $N_{\text{rep}} = 20$, $n = 400$, $\alpha = 0.05$.

Projection	m	γ	$a = 1.5$	$a = 2$	$a = 2.5$	$a = 3$	$a = 5$	$a = 10$
Itô	1	0	0.05	0.00	0.05	0.10	0.05	0.10
		0.25	0.00	0.00	0.00	0.00	0.00	0.00
		0.45	0.00	0.00	0.00	0.00	0.00	0.00
	2	0	0.00	0.00	0.00	0.00	0.00	0.05
		0.25	0.00	0.00	0.00	0.00	0.00	0.00
		0.45	0.00	0.00	0.00	0.00	0.00	0.00
	4	0	0.00	0.00	0.00	0.00	0.00	0.05
		0.25	0.00	0.00	0.00	0.00	0.00	0.00
		0.45	0.00	0.00	0.00	0.00	0.00	0.00
$\|\cdot\|_{L_2}$	1	0	0.00	0.05	0.00	0.00	0.00	0.15
		0.25	0.00	0.00	0.00	0.00	0.00	0.00
		0.45	0.00	0.00	0.00	0.00	0.00	0.00
	2	0	0.00	0.10	0.00	0.00	0.05	0.05
		0.25	0.00	0.00	0.00	0.00	0.00	0.00
		0.45	0.00	0.00	0.00	0.00	0.00	0.00
	4	0	0.00	0.00	0.00	0.00	0.05	0.05
		0.25	0.00	0.00	0.00	0.00	0.00	0.00
		0.45	0.00	0.00	0.00	0.00	0.00	0.00
C max-var	1	0	0.05	0.05	0.00	0.00	0.00	0.15
		0.25	0.00	0.00	0.00	0.00	0.00	0.00
		0.45	0.00	0.00	0.00	0.00	0.00	0.00
	2	0	0.00	0.00	0.00	0.00	0.00	0.00
		0.25	0.00	0.00	0.00	0.00	0.00	0.00
		0.45	0.00	0.00	0.00	0.00	0.00	0.00
	4	0	0.00	0.00	0.05	0.00	0.00	0.00
		0.25	0.00	0.00	0.00	0.00	0.00	0.00
		0.45	0.00	0.00	0.00	0.00	0.00	0.00

Table 9.2: Wilcoxon test power on *F1: Normal vs centred Pareto*, segment length $\ell^* = n/5$. $N_{\text{rep}} = 20$, $n = 400$, $\alpha = 0.05$.

Projection	m	γ	$a = 1.5$	$a = 2$	$a = 2.5$	$a = 3$	$a = 5$	$a = 10$
Itô	1	0	1.00	0.50	0.05	0.15	1.00	1.00
		0.25	0.10	0.00	0.00	0.00	0.00	1.00
		0.45	0.00	0.00	0.00	0.00	0.00	0.00
	2	0	0.95	0.10	0.00	0.15	1.00	1.00
		0.25	0.00	0.00	0.00	0.00	0.00	0.00
		0.45	0.00	0.00	0.00	0.00	0.00	0.00
	4	0	0.95	0.10	0.00	0.05	0.90	1.00
		0.25	0.00	0.00	0.00	0.00	0.00	0.00
		0.45	0.00	0.00	0.00	0.00	0.00	0.00
$\|\cdot\|_{L_2}$	1	0	1.00	1.00	0.00	0.80	1.00	1.00
		0.25	0.65	0.00	0.00	0.00	1.00	1.00
		0.45	0.00	0.00	0.00	0.00	0.00	0.00
	2	0	1.00	0.55	0.00	0.45	1.00	1.00
		0.25	0.00	0.00	0.00	0.00	0.00	0.40
		0.45	0.00	0.00	0.00	0.00	0.00	0.00
	4	0	1.00	0.35	0.00	0.35	1.00	1.00
		0.25	0.00	0.00	0.00	0.00	0.05	0.85
		0.45	0.00	0.00	0.00	0.00	0.00	0.00
C max-var	1	0	0.95	0.20	0.15	0.55	1.00	1.00
		0.25	0.00	0.00	0.00	0.00	0.10	1.00
		0.45	0.00	0.00	0.00	0.00	0.00	0.00
	2	0	0.90	0.05	0.00	0.15	1.00	1.00
		0.25	0.00	0.00	0.00	0.00	0.00	0.00
		0.45	0.00	0.00	0.00	0.00	0.00	0.00
	4	0	0.70	0.00	0.00	0.05	1.00	1.00
		0.25	0.00	0.00	0.00	0.00	0.00	0.00
		0.45	0.00	0.00	0.00	0.00	0.00	0.00

Table 9.3: L_p test power on *F1: Normal vs centred Pareto*, segment length $\ell^* = \lfloor \log n \rfloor + 1$. $N_{\text{rep}} = 20$, $n = 400$, $\alpha = 0.05$.

Projection	p	γ	$a = 1.5$	$a = 2$	$a = 2.5$	$a = 3$	$a = 5$	$a = 10$
Itô	2	0	0.15	0.05	0.00	0.00	0.10	0.00
		0.25	0.15	0.10	0.10	0.05	0.05	0.05
		0.45	0.00	0.00	0.10	0.05	0.05	0.00
$\|\cdot\|_{L_2}$	2	0	0.00	0.20	0.15	0.00	0.15	0.15
		0.25	0.10	0.10	0.25	0.25	0.20	0.20
		0.45	0.50	0.05	0.05	0.05	0.60	0.95
C max-var	2	0	0.10	0.00	0.00	0.00	0.15	0.15
		0.25	0.10	0.25	0.15	0.10	0.05	0.00
		0.45	0.10	0.10	0.10	0.05	0.10	0.00

Table 9.4: L_p test power on *F1: Normal vs centred Pareto*, segment length $\ell^* = n/5$. $N_{\text{rep}} = 20$, $n = 400$, $\alpha = 0.05$.

Projection	p	γ	$a = 1.5$	$a = 2$	$a = 2.5$	$a = 3$	$a = 5$	$a = 10$
		0	0.20	0.05	0.00	0.05	0.60	1.00
Itô	2	0.25	0.90	0.15	0.15	0.00	0.90	1.00
		0.45	0.50	0.00	0.05	0.15	0.45	1.00
		0	1.00	1.00	0.00	1.00	1.00	1.00
$\lVert \cdot \rVert_{L_2}$	2	0.25	1.00	1.00	0.15	1.00	1.00	1.00
		0.45	1.00	0.95	0.15	0.90	1.00	1.00
		0	0.35	0.00	0.15	0.15	0.60	1.00
C max-var	2	0.25	0.50	0.10	0.00	0.20	0.90	1.00
		0.45	0.20	0.00	0.05	0.15	0.75	1.00

Table 9.5: RKHS test power on *F1: Normal vs centred Pareto*, segment length $\ell^* = \lfloor \log n \rfloor + 1$. $N_{\text{rep}} = 20$, $n = 400$, $\alpha = 0.05$.

Projection	Kernel	γ	$a = 1.5$	$a = 2$	$a = 2.5$	$a = 3$	$a = 5$	$a = 10$
		0	0.00	0.00	0.05	0.00	0.00	0.00
Itô	Gaussian	0.25	0.05	0.10	0.10	0.05	0.15	0.05
		0.45	0.00	0.00	0.00	0.00	0.05	0.00
		0	0.00	0.00	0.00	0.00	0.00	0.00
$\lVert \cdot \rVert_{L_2}$	min	0.25	0.00	0.00	0.00	0.00	0.00	0.00
		0.45	0.50	0.10	0.00	0.00	0.45	0.90
		0	0.05	0.00	0.00	0.00	0.05	0.00
C max-var	Gaussian	0.25	0.05	0.10	0.05	0.05	0.05	0.15
		0.45	0.00	0.00	0.00	0.00	0.00	0.00

Table 9.6: RKHS test power on *F1: Normal vs centred Pareto*, segment length $\ell^* = n/5$. $N_{\text{rep}} = 20$, $n = 400$, $\alpha = 0.05$.

Projection	Kernel	γ	$a = 1.5$	$a = 2$	$a = 2.5$	$a = 3$	$a = 5$	$a = 10$
		0	0.60	0.15	0.00	0.00	0.45	1.00
Itô	Gaussian	0.25	1.00	0.50	0.10	0.05	1.00	1.00
		0.45	1.00	0.20	0.05	0.10	1.00	1.00
		0	1.00	0.10	0.00	0.00	1.00	1.00
$\lVert \cdot \rVert_{L_2}$	min	0.25	1.00	0.75	0.00	0.55	1.00	1.00
		0.45	1.00	1.00	0.10	1.00	1.00	1.00
		0	0.30	0.00	0.00	0.00	0.60	1.00
C max-var	Gaussian	0.25	1.00	0.05	0.05	0.10	1.00	1.00
		0.45	0.95	0.00	0.00	0.00	1.00	1.00

Table 9.7: Wilcoxon test power on *F2: Pareto vs Pareto*, segment length $\ell^* = \lfloor \log n \rfloor + 1$. $N_{\text{rep}} = 20$, $n = 400$, $\alpha = 0.05$.

Projection	m	γ	$a = 0.5$	$a = 1$	$a = 1.5$	$a = 2$	$a = 5$
		0	0.00	0.00	0.00	0.05	0.10
	1	0.25	0.00	0.00	0.00	0.00	0.00
		0.45	0.00	0.00	0.00	0.00	0.00
		0	0.00	0.00	0.00	0.10	0.00
Itô	2	0.25	0.00	0.00	0.00	0.00	0.00
		0.45	0.00	0.00	0.00	0.00	0.00
		0	0.00	0.00	0.00	0.05	0.05
	4	0.25	0.00	0.00	0.00	0.00	0.00
		0.45	0.00	0.00	0.00	0.00	0.00
		0	0.05	0.10	0.05	0.05	0.05
	1	0.25	0.00	0.00	0.00	0.00	0.00
		0.45	0.00	0.00	0.00	0.00	0.00
		0	0.00	0.05	0.05	0.00	0.00
$\|\cdot\|_{L_2}$	2	0.25	0.00	0.00	0.00	0.00	0.00
		0.45	0.00	0.00	0.00	0.00	0.00
		0	0.00	0.00	0.00	0.00	0.00
	4	0.25	0.00	0.00	0.00	0.00	0.00
		0.45	0.00	0.00	0.00	0.00	0.00
		0	0.00	0.00	0.05	0.00	0.05
	1	0.25	0.00	0.00	0.00	0.00	0.00
		0.45	0.00	0.00	0.00	0.00	0.00
		0	0.00	0.05	0.05	0.00	0.00
C max-var	2	0.25	0.00	0.00	0.00	0.00	0.00
		0.45	0.00	0.00	0.00	0.00	0.00
		0	0.00	0.00	0.00	0.00	0.00
	4	0.25	0.00	0.00	0.00	0.00	0.00
		0.45	0.00	0.00	0.00	0.00	0.00

Table 9.8: Wilcoxon test power on *F2: Pareto vs Pareto*, segment length $\ell^* = n/5$. $N_{\text{rep}} = 20$, $n = 400$, $\alpha = 0.05$.

Projection	m	γ	$a = 0.5$	$a = 1$	$a = 1.5$	$a = 2$	$a = 5$
		0	1.00	0.95	0.10	0.70	1.00
	1	0.25	1.00	0.00	0.00	0.00	1.00
		0.45	0.00	0.00	0.00	0.00	0.00
		0	1.00	0.95	0.00	0.35	1.00
Itô	2	0.25	0.00	0.00	0.00	0.00	0.00
		0.45	0.00	0.00	0.00	0.00	0.00
		0	1.00	0.60	0.00	0.05	1.00
	4	0.25	0.05	0.00	0.00	0.00	0.00
		0.45	0.00	0.00	0.00	0.00	0.00
		0	1.00	1.00	0.05	1.00	1.00
	1	0.25	1.00	0.10	0.00	0.00	1.00
		0.45	0.00	0.00	0.00	0.00	0.00
		0	1.00	1.00	0.00	0.75	1.00
$\Vert \cdot \Vert_{L_2}$	2	0.25	0.25	0.00	0.00	0.00	0.40
		0.45	0.00	0.00	0.00	0.00	0.00
		0	1.00	1.00	0.00	0.70	1.00
	4	0.25	0.75	0.00	0.00	0.00	0.35
		0.45	0.00	0.00	0.00	0.00	0.00
		0	1.00	1.00	0.00	0.65	1.00
	1	0.25	1.00	0.00	0.00	0.00	0.85
		0.45	0.00	0.00	0.00	0.00	0.00
		0	1.00	0.65	0.00	0.45	1.00
C max-var	2	0.25	0.05	0.00	0.00	0.00	0.00
		0.45	0.00	0.00	0.00	0.00	0.00
		0	1.00	0.50	0.00	0.05	1.00
	4	0.25	0.05	0.00	0.00	0.00	0.00
		0.45	0.00	0.00	0.00	0.00	0.00

Table 9.9: L_p test power on *F2: Pareto vs Pareto*, segment length $\ell^* = \lfloor \log n \rfloor + 1$. $N_{\text{rep}} = 20$, $n = 400$, $\alpha = 0.05$.

Projection	p	γ	$a = 0.5$	$a = 1$	$a = 1.5$	$a = 2$	$a = 5$
		0	0.10	0.10	0.00	0.05	0.05
Itô	2	0.25	0.10	0.05	0.10	0.00	0.05
		0.45	0.15	0.05	0.00	0.10	0.05
		0	0.15	0.10	0.05	0.05	0.10
$\Vert \cdot \Vert_{L_2}$	2	0.25	0.25	0.25	0.10	0.20	0.25
		0.45	0.95	0.05	0.10	0.00	1.00
		0	0.00	0.15	0.00	0.05	0.05
C max-var	2	0.25	0.15	0.10	0.05	0.10	0.15
		0.45	0.10	0.05	0.05	0.05	0.15

Table 9.10: L_p test power on *F2: Pareto vs Pareto*, segment length $\ell^* = n/5$. $N_{\text{rep}} = 20$, $n = 400$, $\alpha = 0.05$.

Projection	p	γ	$a = 0.5$	$a = 1$	$a = 1.5$	$a = 2$	$a = 5$
		0	1.00	0.15	0.00	0.20	1.00
Itô	2	0.25	1.00	0.65	0.10	0.15	1.00
		0.45	1.00	0.25	0.00	0.05	1.00
		0	1.00	1.00	0.10	1.00	1.00
$\|\cdot\|_{L_2}$	2	0.25	1.00	1.00	0.00	1.00	1.00
		0.45	1.00	1.00	0.05	1.00	1.00
		0	1.00	0.10	0.10	0.05	1.00
C max-var	2	0.25	1.00	0.40	0.05	0.15	1.00
		0.45	1.00	0.15	0.05	0.15	1.00

Table 9.11: RKHS test power on *F2: Pareto vs Pareto*, segment length $\ell^* = \lfloor \log n \rfloor + 1$. $N_{\text{rep}} = 20$, $n = 400$, $\alpha = 0.05$.

Projection	Kernel	γ	$a = 0.5$	$a = 1$	$a = 1.5$	$a = 2$	$a = 5$
		0	0.00	0.00	0.00	0.00	0.00
Itô	Gaussian	0.25	0.00	0.05	0.10	0.00	0.10
		0.45	0.10	0.00	0.05	0.00	0.00
		0	0.00	0.00	0.00	0.00	0.00
$\|\cdot\|_{L_2}$	min	0.25	0.00	0.05	0.00	0.00	0.00
		0.45	0.90	0.00	0.05	0.00	0.85
		0	0.05	0.05	0.00	0.05	0.00
C max-var	Gaussian	0.25	0.15	0.10	0.05	0.05	0.05
		0.45	0.10	0.00	0.00	0.00	0.05

Table 9.12: RKHS test power on *F2: Pareto vs Pareto*, segment length $\ell^* = n/5$. $N_{\text{rep}} = 20$, $n = 400$, $\alpha = 0.05$.

Projection	Kernel	γ	$a = 0.5$	$a = 1$	$a = 1.5$	$a = 2$	$a = 5$
		0	1.00	0.40	0.00	0.10	1.00
Itô	Gaussian	0.25	1.00	1.00	0.05	0.30	1.00
		0.45	1.00	0.85	0.00	0.00	1.00
		0	1.00	0.85	0.00	0.15	1.00
$\|\cdot\|_{L_2}$	min	0.25	1.00	1.00	0.00	0.85	1.00
		0.45	1.00	1.00	0.05	1.00	1.00
		0	1.00	0.15	0.05	0.00	1.00
C max-var	Gaussian	0.25	1.00	0.90	0.05	0.20	1.00
		0.45	1.00	0.85	0.00	0.10	1.00

Table 9.13: Wilcoxon test power on *F3: Normal vs heavy-tailed (piecewise)*, segment length $\ell^* = \lfloor \log n \rfloor + 1$. $N_{\text{rep}} = 100$, $n = 400$, $\alpha = 0.05$.

Projection	m	γ	$a = 0.5$	$a = 1$	$a = 1.5$	$a = 2$	$a = 2.5$	$a = 5$
		0	0.06	0.06	0.05	0.03	0.03	0.04
	1	0.25	0.00	0.00	0.00	0.00	0.00	0.00
		0.45	0.00	0.00	0.00	0.00	0.00	0.00
		0	0.03	0.03	0.02	0.04	0.02	0.04
Itô	2	0.25	0.00	0.00	0.00	0.00	0.00	0.00
		0.45	0.00	0.00	0.00	0.00	0.00	0.00
		0	0.01	0.01	0.01	0.01	0.00	0.03
	4	0.25	0.00	0.00	0.00	0.00	0.00	0.00
		0.45	0.00	0.00	0.00	0.00	0.00	0.00
		0	0.04	0.04	0.01	0.04	0.06	0.05
	1	0.25	0.00	0.00	0.00	0.00	0.00	0.00
		0.45	0.00	0.00	0.00	0.00	0.00	0.00
		0	0.04	0.04	0.01	0.03	0.01	0.02
$\|\cdot\|_{L_2}$	2	0.25	0.00	0.00	0.00	0.00	0.00	0.00
		0.45	0.00	0.00	0.00	0.00	0.00	0.00
		0	0.01	0.02	0.03	0.00	0.02	0.01
	4	0.25	0.00	0.00	0.00	0.00	0.00	0.00
		0.45	0.00	0.00	0.00	0.00	0.00	0.00
		0	0.10	0.05	0.06	0.05	0.00	0.05
	1	0.25	0.00	0.00	0.00	0.00	0.00	0.00
		0.45	0.00	0.00	0.00	0.00	0.00	0.00
		0	0.03	0.04	0.02	0.04	0.00	0.01
C max-var	2	0.25	0.00	0.00	0.00	0.00	0.00	0.00
		0.45	0.00	0.00	0.00	0.00	0.00	0.00
		0	0.00	0.01	0.01	0.00	0.00	0.01
	4	0.25	0.00	0.00	0.00	0.00	0.00	0.00
		0.45	0.00	0.00	0.00	0.00	0.00	0.00

Table 9.14: Wilcoxon test power on *F3: Normal vs heavy-tailed (piecewise)*, segment length $\ell^* = n/5$. $N_{\text{rep}} = 100$, $n = 400$, $\alpha = 0.05$.

Projection	m	γ	$a = 0.5$	$a = 1$	$a = 1.5$	$a = 2$	$a = 2.5$	$a = 5$
Itô	1	0	1.00	1.00	1.00	0.87	0.11	1.00
		0.25	1.00	1.00	0.07	0.00	0.00	0.03
		0.45	0.00	0.00	0.00	0.00	0.00	0.00
	2	0	1.00	1.00	1.00	0.43	0.04	1.00
		0.25	0.30	0.04	0.00	0.00	0.00	0.00
		0.45	0.00	0.00	0.00	0.00	0.00	0.00
	4	0	1.00	1.00	0.97	0.26	0.01	0.86
		0.25	0.93	0.00	0.00	0.00	0.00	0.00
		0.45	0.00	0.00	0.00	0.00	0.00	0.00
$\|\cdot\|_{L_2}$	1	0	1.00	1.00	1.00	0.98	0.10	1.00
		0.25	1.00	1.00	0.91	0.00	0.00	0.80
		0.45	0.00	0.00	0.00	0.00	0.00	0.00
	2	0	1.00	1.00	1.00	0.89	0.01	1.00
		0.25	0.39	0.18	0.00	0.00	0.00	0.00
		0.45	0.00	0.00	0.00	0.00	0.00	0.00
	4	0	1.00	1.00	1.00	0.73	0.02	1.00
		0.25	1.00	0.38	0.00	0.00	0.00	0.00
		0.45	0.00	0.00	0.00	0.00	0.00	0.00
C max-var	1	0	1.00	1.00	0.98	0.62	0.07	1.00
		0.25	1.00	0.97	0.18	0.00	0.00	0.02
		0.45	0.00	0.00	0.00	0.00	0.00	0.00
	2	0	1.00	1.00	0.98	0.38	0.04	1.00
		0.25	0.20	0.00	0.00	0.00	0.00	0.00
		0.45	0.00	0.00	0.00	0.00	0.00	0.00
	4	0	1.00	1.00	0.98	0.27	0.00	0.97
		0.25	0.90	0.00	0.00	0.00	0.00	0.00
		0.45	0.00	0.00	0.00	0.00	0.00	0.00

Table 9.15: L_p test power on *F3: Normal vs heavy-tailed (piecewise)*, segment length $\ell^* = \lfloor \log n \rfloor + 1$. $N_{\text{rep}} = 100$, $n = 400$, $\alpha = 0.05$.

Projection	p	γ	$a = 0.5$	$a = 1$	$a = 1.5$	$a = 2$	$a = 2.5$	$a = 5$
Itô	2	0	0.08	0.07	0.02	0.08	0.05	0.05
		0.25	0.10	0.09	0.08	0.16	0.12	0.12
		0.45	0.09	0.07	0.05	0.07	0.04	0.04
$\|\cdot\|_{L_2}$	2	0	0.09	0.04	0.04	0.06	0.12	0.16
		0.25	0.29	0.24	0.16	0.16	0.10	0.17
		0.45	1.00	0.91	0.32	0.10	0.04	0.30
C max-var	2	0	0.08	0.06	0.07	0.05	0.04	0.05
		0.25	0.13	0.10	0.06	0.10	0.07	0.07
		0.45	0.09	0.08	0.05	0.09	0.07	0.07

Table 9.16: L_p test power on *F3: Normal vs heavy-tailed (piecewise)*, segment length $\ell^* = n/5$. $N_{\text{rep}} = 100$, $n = 400$, $\alpha = 0.05$.

Projection	p	γ	$a = 0.5$	$a = 1$	$a = 1.5$	$a = 2$	$a = 2.5$	$a = 5$
		0	1.00	1.00	0.79	0.10	0.03	0.39
Itô	2	0.25	1.00	1.00	0.98	0.23	0.08	0.83
		0.45	1.00	1.00	0.79	0.18	0.08	0.32
		0	1.00	1.00	1.00	0.99	0.20	1.00
$\|\cdot\|_{L_2}$	2	0.25	1.00	1.00	1.00	1.00	0.34	1.00
		0.45	1.00	1.00	1.00	1.00	0.16	1.00
		0	1.00	1.00	0.67	0.08	0.03	0.55
C max-var	2	0.25	1.00	1.00	0.86	0.17	0.07	0.77
		0.45	1.00	1.00	0.82	0.10	0.03	0.32

Table 9.17: RKHS test power on *F3: Normal vs heavy-tailed (piecewise)*, segment length $\ell^* = \lfloor \log n \rfloor + 1$. $N_{\text{rep}} = 100$, $n = 400$, $\alpha = 0.05$.

Projection	Kernel	γ	$a = 0.5$	$a = 1$	$a = 1.5$	$a = 2$	$a = 2.5$	$a = 5$
		0	0.02	0.02	0.01	0.01	0.02	0.01
Itô	Gaussian	0.25	0.09	0.04	0.06	0.04	0.08	0.06
		0.45	0.75	0.16	0.08	0.01	0.01	0.01
		0	0.00	0.00	0.00	0.00	0.00	0.00
$\|\cdot\|_{L_2}$	min	0.25	0.00	0.00	0.00	0.00	0.00	0.01
		0.45	1.00	0.79	0.23	0.07	0.02	0.12
		0	0.00	0.02	0.02	0.03	0.01	0.04
C max-var	Gaussian	0.25	0.06	0.07	0.09	0.05	0.07	0.04
		0.45	0.76	0.29	0.03	0.02	0.01	0.01

Table 9.18: RKHS test power on *F3: Normal vs heavy-tailed (piecewise)*, segment length $\ell^* = n/5$. $N_{\text{rep}} = 100$, $n = 400$, $\alpha = 0.05$.

Projection	Kernel	γ	$a = 0.5$	$a = 1$	$a = 1.5$	$a = 2$	$a = 2.5$	$a = 5$
		0	1.00	1.00	0.99	0.07	0.02	0.27
Itô	Gaussian	0.25	1.00	1.00	1.00	0.72	0.04	0.99
		0.45	1.00	1.00	1.00	0.63	0.02	0.92
		0	1.00	1.00	1.00	0.16	0.00	1.00
$\|\cdot\|_{L_2}$	min	0.25	1.00	1.00	1.00	0.91	0.01	1.00
		0.45	1.00	1.00	1.00	0.99	0.13	1.00
		0	1.00	1.00	0.82	0.08	0.02	0.30
C max-var	Gaussian	0.25	1.00	1.00	1.00	0.56	0.11	1.00
		0.45	1.00	1.00	0.98	0.51	0.02	0.95

Table 9.19: Wilcoxon test power on F4 scenario, segment length $\ell^* = \lfloor \log n \rfloor + 1$. $N_{\text{rep}} = 100$, $n = 400$, $\alpha = 0.05$.

Projection	m	γ	$a = 0$	$a = 0.25$	$a = 0.5$	$a = 1$	$a = 2$	$a = 4$	$a = 8$
		0	0.13	0.20	0.21	0.28	0.26	0.40	0.40
	1	0.25	0.00	0.00	0.00	0.00	0.00	0.00	0.00
		0.45	0.00	0.00	0.00	0.00	0.00	0.00	0.00
		0	0.17	0.18	0.19	0.23	0.23	0.30	0.23
Itô	2	0.25	0.00	0.00	0.00	0.00	0.00	0.00	0.00
		0.45	0.00	0.00	0.00	0.00	0.00	0.00	0.00
		0	0.12	0.12	0.12	0.15	0.17	0.19	0.23
	4	0.25	0.00	0.00	0.00	0.00	0.00	0.00	0.00
		0.45	0.00	0.00	0.00	0.00	0.00	0.00	0.00
		0	0.22	0.31	0.30	0.35	0.46	0.43	0.55
	1	0.25	0.00	0.00	0.00	0.00	0.00	0.00	0.00
		0.45	0.00	0.00	0.00	0.00	0.00	0.00	0.00
		0	0.27	0.24	0.29	0.35	0.31	0.37	0.39
$\|\cdot\|_{L_2}$	2	0.25	0.00	0.00	0.00	0.00	0.00	0.00	0.00
		0.45	0.00	0.00	0.00	0.00	0.00	0.00	0.00
		0	0.22	0.17	0.21	0.23	0.22	0.33	0.28
	4	0.25	0.00	0.00	0.00	0.00	0.00	0.00	0.00
		0.45	0.00	0.00	0.00	0.00	0.00	0.00	0.00
		0	0.23	0.18	0.16	0.24	0.23	0.24	0.40
	1	0.25	0.00	0.00	0.00	0.00	0.00	0.00	0.00
		0.45	0.00	0.00	0.00	0.00	0.00	0.00	0.00
		0	0.20	0.14	0.22	0.19	0.16	0.19	0.21
C max-var	2	0.25	0.00	0.00	0.00	0.00	0.00	0.00	0.00
		0.45	0.00	0.00	0.00	0.00	0.00	0.00	0.00
		0	0.18	0.06	0.17	0.07	0.11	0.17	0.22
	4	0.25	0.00	0.00	0.00	0.00	0.00	0.00	0.00
		0.45	0.00	0.00	0.00	0.00	0.00	0.00	0.00

Table 9.20: Wilcoxon test power on F4 scenario, segment length $\ell^* = n/5$. $N_{\text{rep}} = 100$, $n = 400$, $\alpha = 0.05$.

Projection	m	γ	$a=0$	$a=0.25$	$a=0.5$	$a=1$	$a=2$	$a=4$	$a=8$
		0	0.25	0.27	0.57	0.84	0.94	0.97	0.98
	1	0.25	0.00	0.00	0.00	0.45	0.76	0.95	0.97
		0.45	0.00	0.00	0.00	0.00	0.00	0.00	0.00
		0	0.21	0.23	0.62	0.94	0.99	1.00	1.00
Itô	2	0.25	0.00	0.00	0.00	0.04	0.45	0.67	0.88
		0.45	0.00	0.00	0.00	0.00	0.00	0.00	0.00
		0	0.15	0.21	0.50	0.95	0.97	1.00	1.00
	4	0.25	0.00	0.00	0.00	0.02	0.69	0.98	0.99
		0.45	0.00	0.00	0.00	0.00	0.00	0.00	0.00
		0	0.27	0.42	0.80	1.00	1.00	1.00	1.00
	1	0.25	0.00	0.00	0.01	0.92	1.00	1.00	1.00
		0.45	0.00	0.00	0.00	0.00	0.00	0.00	0.00
		0	0.33	0.31	0.75	1.00	1.00	1.00	1.00
$\lVert\cdot\rVert_{L_2}$	2	0.25	0.00	0.00	0.00	0.07	0.65	0.83	0.96
		0.45	0.00	0.00	0.00	0.00	0.00	0.00	0.00
		0	0.24	0.27	0.72	1.00	1.00	1.00	1.00
	4	0.25	0.00	0.00	0.00	0.03	1.00	1.00	1.00
		0.45	0.00	0.00	0.00	0.00	0.00	0.00	0.00
		0	0.19	0.21	0.68	1.00	1.00	1.00	1.00
	1	0.25	0.00	0.00	0.01	0.43	0.99	1.00	1.00
		0.45	0.00	0.00	0.00	0.00	0.00	0.00	0.00
		0	0.15	0.24	0.54	0.98	1.00	1.00	1.00
C max-var	2	0.25	0.00	0.00	0.01	0.04	0.39	0.63	0.72
		0.45	0.00	0.00	0.00	0.00	0.00	0.00	0.00
		0	0.10	0.22	0.50	0.95	1.00	1.00	1.00
	4	0.25	0.00	0.00	0.00	0.00	0.63	1.00	1.00
		0.45	0.00	0.00	0.00	0.00	0.00	0.00	0.00

Table 9.21: L_p test power on F4 scenario, segment length $\ell^* = \lfloor \log n \rfloor + 1$. $N_{\text{rep}} = 100$, $n = 400$, $\alpha = 0.05$.

Projection	p	γ	$a=0$	$a=0.25$	$a=0.5$	$a=1$	$a=2$	$a=4$	$a=8$
		0	0.84	0.83	0.84	0.83	0.81	0.86	0.80
Itô	2	0.25	0.86	0.91	0.96	0.94	0.97	0.96	0.98
		0.45	0.95	0.98	0.98	0.99	1.00	1.00	0.99
		0	0.33	0.36	0.41	0.43	0.54	0.55	0.59
$\lVert\cdot\rVert_{L_2}$	2	0.25	0.57	0.61	0.53	0.69	0.79	0.90	1.00
		0.45	0.64	0.67	0.53	0.72	0.99	1.00	1.00
		0	0.71	0.71	0.64	0.74	0.72	0.73	0.74
C max-var	2	0.25	0.83	0.79	0.88	0.84	0.85	0.88	0.86
		0.45	0.85	0.79	0.85	0.83	0.93	1.00	1.00

Table 9.22: L_p test power on F4 scenario, segment length $\ell^* = n/5$. $N_{\text{rep}} = 100$, $n = 400$, $\alpha = 0.05$.

Projection	p	γ	$a=0$	$a=0.25$	$a=0.5$	$a=1$	$a=2$	$a=4$	$a=8$
		0	0.79	0.88	0.94	0.98	1.00	1.00	1.00
Itô	2	0.25	0.99	0.96	0.99	1.00	1.00	1.00	1.00
		0.45	0.97	0.96	0.99	1.00	0.99	1.00	1.00
		0	0.36	0.50	0.87	1.00	1.00	1.00	1.00
$\|\cdot\|_{L_2}$	2	0.25	0.54	0.71	0.93	1.00	1.00	1.00	1.00
		0.45	0.74	0.78	0.95	1.00	1.00	1.00	1.00
		0	0.70	0.82	0.99	1.00	1.00	1.00	1.00
C max-var	2	0.25	0.79	0.89	0.99	1.00	1.00	1.00	1.00
		0.45	0.89	0.93	1.00	1.00	1.00	1.00	1.00

Table 9.23: RKHS test power on F4 scenario, segment length $\ell^* = \lfloor \log n \rfloor + 1$. $N_{\text{rep}} = 100$, $n = 400$, $\alpha = 0.05$.

Projection	Kernel	γ	$a=0$	$a=0.25$	$a=0.5$	$a=1$	$a=2$	$a=4$	$a=8$
		0	0.03	0.01	0.02	0.01	0.02	0.01	0.02
Itô	Gaussian	0.25	0.05	0.02	0.06	0.07	0.02	0.01	0.01
		0.45	0.02	0.03	0.06	0.04	0.06	0.28	0.39
		0	0.02	0.06	0.04	0.09	0.06	0.05	0.36
$\|\cdot\|_{L_2}$	min	0.25	0.03	0.06	0.08	0.05	0.45	1.00	1.00
		0.45	0.06	0.02	0.05	0.12	0.88	1.00	1.00
		0	0.03	0.05	0.06	0.08	0.03	0.02	0.03
C max-var	Gaussian	0.25	0.03	0.04	0.03	0.01	0.04	0.03	0.03
		0.45	0.06	0.05	0.06	0.05	0.08	0.03	0.01

Table 9.24: RKHS test power on F4 scenario, segment length $\ell^* = n/5$. $N_{\text{rep}} = 100$, $n = 400$, $\alpha = 0.05$.

Projection	Kernel	γ	$a=0$	$a=0.25$	$a=0.5$	$a=1$	$a=2$	$a=4$	$a=8$
		0	0.03	0.05	0.02	0.04	0.20	0.51	0.75
Itô	Gaussian	0.25	0.07	0.03	0.08	0.12	0.28	0.74	0.89
		0.45	0.04	0.06	0.07	0.34	0.53	0.82	0.85
		0	0.08	0.07	0.26	1.00	1.00	1.00	1.00
$\|\cdot\|_{L_2}$	min	0.25	0.03	0.19	0.77	1.00	1.00	1.00	1.00
		0.45	0.02	0.09	0.67	1.00	1.00	1.00	1.00
		0	0.08	0.12	0.54	0.85	0.94	0.99	1.00
C max-var	Gaussian	0.25	0.06	0.10	0.48	0.86	0.94	1.00	1.00
		0.45	0.09	0.12	0.47	0.87	0.98	1.00	1.00

Table 9.25: Empirical quantiles of $T_{n,\rho}^{(\kappa)}$ on F4 (FAR(1) null), $n = 400$, $N_{\text{rep}} = 1000$. Used as critical values for the F4 power tabulations of Tables 9.23 and 9.24.

Projection / kernel	γ	2.5%	5%	25%	50%	75%	95%	97.5%
Itô / Gaussian	0	1.387	1.392	1.406	1.408	1.410	1.410	1.410
	0.25	1.393	1.397	1.407	1.409	1.411	1.411	1.411
	0.45	1.394	1.399	1.408	1.410	1.411	1.412	1.412
$\lVert \cdot \rVert_{L_2}$ / min	0	0.719	0.754	0.903	1.009	1.115	1.206	1.239
	0.25	0.763	0.793	0.937	1.040	1.143	1.239	1.275
	0.45	1.155	1.179	1.318	1.461	1.639	2.001	2.111
C max-var / Gaussian	0	0.975	1.044	1.200	1.298	1.371	1.576	1.723
	0.25	1.104	1.163	1.292	1.370	1.532	2.021	2.164
	0.45	1.303	1.333	1.486	1.925	2.294	2.805	2.976

Table 9.26: Birbilas's epidemic statistic $E_{n,\beta_1,\gamma}$ ($\beta_1(t) = 0.7\sqrt{t}$, c.v. adjusted, see eq. (6.1)) power on F4 scenario, segment length $\ell^* = \lfloor \log n \rfloor + 1$. $N_{\text{rep}} = 100$, $n = 400$, $\alpha = 0.05$.

γ	$a = 0$	$a = 0.25$	$a = 0.5$	$a = 1$	$a = 2$	$a = 4$	$a = 8$
0	0.06	0.07	0.05	0.03	0.08	0.54	1.00
0.25	0.06	0.02	0.08	0.06	0.26	0.99	1.00
0.45	0.05	0.06	0.01	0.11	0.80	1.00	1.00

Table 9.27: Birbilas's epidemic statistic $E_{n,\beta_1,\gamma}$ ($\beta_1(t) = 0.7\sqrt{t}$, c.v. adjusted, see eq. (6.1)) power on F4 scenario, segment length $\ell^* = n/5$. $N_{\text{rep}} = 100$, $n = 400$, $\alpha = 0.05$.

γ	$a = 0$	$a = 0.25$	$a = 0.5$	$a = 1$	$a = 2$	$a = 4$	$a = 8$
0	0.06	0.19	0.82	1.00	1.00	1.00	1.00
0.25	0.05	0.23	0.84	1.00	1.00	1.00	1.00
0.45	0.02	0.20	0.80	1.00	1.00	1.00	1.00

9.3. Functional data: stability of random projections

Summary statistics of the antisymmetric-kernel Wilcoxon scan over N independent Itô trajectories on a fixed sample, supporting Section 6.1.3.

Table 9.28: Stability of the antisymmetric-kernel Wilcoxon scan under repeated draws of the Itô projector. For each scenario and value of a, $K = 100$ independently drawn samples of size $n = 400$ are fixed and $N = 100$ Itô trajectories are drawn against each; the table reports the mean, standard deviation, and coefficient of variation CV $=$ sd/mean of $\widehat{R}_N = N^{-1} \sum_i \mathbf{1}\{T_n(\omega_i) > c_\alpha\}$ across the K fixed samples at $\alpha = 0.05$. We write "–" in the CV column when the mean equals zero.

Scenario	a	γ	mean $\widehat{R}_N$	sd $\widehat{R}_N$	CV $\widehat{R}_N$
F1	2.5	0	0.053	0.045	0.849
		0.25	0.000	0.000	–
		0.45	0.000	0.000	–
	5	0	1.000	0.001	0.001
		0.25	0.031	0.044	1.419
		0.45	0.000	0.000	–
	10	0	1.000	0.000	0.000
		0.25	0.999	0.002	0.002
		0.45	0.000	0.000	–
F2	1.5	0	0.038	0.070	1.842
		0.25	0.000	0.000	–
		0.45	0.000	0.000	–
	2	0	0.696	0.217	0.312
		0.25	0.000	0.000	–
		0.45	0.000	0.000	–
	5	0	1.000	0.000	0.000
		0.25	0.978	0.035	0.036
		0.45	0.000	0.000	–
F3	2.5	0	0.081	0.122	1.506
		0.25	0.000	0.000	–
		0.45	0.000	0.000	–
	5	0	1.000	0.000	0.000
		0.25	0.013	0.043	3.308
		0.45	0.000	0.000	–
F4	0	0	0.198	0.164	0.828
		0.25	0.000	0.000	–
		0.45	0.000	0.000	–
	1	0	0.859	0.043	0.050
		0.25	0.440	0.190	0.432
		0.45	0.000	0.000	–
	4	0	0.970	0.016	0.016
		0.25	0.923	0.027	0.029
		0.45	0.000	0.000	–

9.4. Scalar data

L_p **test.**

Table 9.29: Scalar Wilcoxon test power, segment length $\ell^* = \lfloor \log n \rfloor + 1$. $N_{\text{rep}} = 100$, $n = 400$, $\alpha = 0.05$.

Scenario	m	γ	$a=0$	$a=0.25$	$a=0.5$	$a=1$	$a=2$	$a=4$	$a=8$
S1	1	0	0.01	0.01	0.02	0.03	0.05	0.07	0.09
		0.25	0.00	0.00	0.00	0.00	0.00	0.00	0.00
		0.45	0.00	0.00	0.00	0.00	0.00	0.00	0.00
	2	0	0.03	0.03	0.03	0.02	0.03	0.01	0.02
		0.25	0.00	0.00	0.00	0.00	0.00	0.00	0.00
		0.45	0.00	0.00	0.00	0.00	0.00	0.00	0.00
	4	0	0.01	0.01	0.01	0.01	0.00	0.01	0.02
		0.25	0.00	0.00	0.00	0.00	0.00	0.00	0.00
		0.45	0.00	0.00	0.00	0.00	0.00	0.00	0.00
S2	1	0	0.03	0.03	0.02	0.07	0.05	0.06	0.06
		0.25	0.00	0.00	0.00	0.00	0.00	0.00	0.00
		0.45	0.00	0.00	0.00	0.00	0.00	0.00	0.00
	2	0	0.01	0.01	0.04	0.00	0.02	0.01	0.03
		0.25	0.00	0.00	0.00	0.00	0.00	0.00	0.00
		0.45	0.00	0.00	0.00	0.00	0.00	0.00	0.00
	4	0	0.00	0.00	0.01	0.01	0.00	0.00	0.02
		0.25	0.00	0.00	0.00	0.00	0.00	0.00	0.00
		0.45	0.00	0.00	0.00	0.00	0.00	0.00	0.00
S3	1	0	0.02	0.07	0.05	0.06	0.14	0.09	0.05
		0.25	0.00	0.00	0.00	0.00	0.00	0.00	0.00
		0.45	0.00	0.00	0.00	0.00	0.00	0.00	0.00
	2	0	0.03	0.02	0.02	0.03	0.02	0.02	0.04
		0.25	0.00	0.00	0.00	0.00	0.00	0.00	0.00
		0.45	0.00	0.00	0.00	0.00	0.00	0.00	0.00
	4	0	0.00	0.01	0.00	0.01	0.02	0.02	0.02
		0.25	0.00	0.00	0.00	0.00	0.00	0.00	0.00
		0.45	0.00	0.00	0.00	0.00	0.00	0.00	0.00
S4	1	0	0.03	0.02	0.00	0.05	0.10	0.06	0.11
		0.25	0.00	0.00	0.00	0.00	0.00	0.00	0.00
		0.45	0.00	0.00	0.00	0.00	0.00	0.00	0.00
	2	0	0.01	0.04	0.01	0.01	0.05	0.08	0.02
		0.25	0.00	0.00	0.00	0.00	0.00	0.00	0.00
		0.45	0.00	0.00	0.00	0.00	0.00	0.00	0.00
	4	0	0.01	0.00	0.00	0.00	0.00	0.02	0.00
		0.25	0.00	0.00	0.00	0.00	0.00	0.00	0.00
		0.45	0.00	0.00	0.00	0.00	0.00	0.00	0.00
S5	1	0	0.02	0.05	0.02	0.03	0.05	0.08	0.06
		0.25	0.00	0.00	0.00	0.00	0.00	0.00	0.00
		0.45	0.00	0.00	0.00	0.00	0.00	0.00	0.00
	2	0	0.03	0.03	0.02	0.01	0.01	0.02	0.05
		0.25	0.00	0.00	0.00	0.00	0.00	0.00	0.00
		0.45	0.00	0.00	0.00	0.00	0.00	0.00	0.00
	4	0	0.00	0.00	0.01	0.01	0.00	0.01	0.02
		0.25	0.00	0.00	0.00	0.00	0.00	0.00	0.00
		0.45	0.00	0.00	0.00	0.00	0.00	0.00	0.00

Table 9.30: Scalar Wilcoxon test power, segment length $\ell^* = n/5$. $N_{\text{rep}} = 100$, $n = 400$, $\alpha = 0.05$.

Scenario	m	γ	$a = 0$	$a = 0.25$	$a = 0.5$	$a = 1$	$a = 2$	$a = 4$	$a = 8$
		0	0.04	0.19	0.68	1.00	1.00	1.00	1.00
	1	0.25	0.00	0.00	0.00	0.01	1.00	1.00	1.00
		0.45	0.00	0.00	0.00	0.00	0.00	0.00	0.00
		0	0.05	0.08	0.31	0.97	1.00	1.00	1.00
S1	2	0.25	0.00	0.00	0.00	0.00	0.03	0.29	0.35
		0.45	0.00	0.00	0.00	0.00	0.00	0.00	0.00
		0	0.02	0.02	0.13	0.94	1.00	1.00	1.00
	4	0.25	0.00	0.00	0.00	0.00	0.00	0.98	1.00
		0.45	0.00	0.00	0.00	0.00	0.00	0.00	0.00
		0	0.03	0.05	0.06	0.61	1.00	1.00	1.00
	1	0.25	0.00	0.00	0.00	0.00	0.80	1.00	1.00
		0.45	0.00	0.00	0.00	0.00	0.00	0.00	0.00
		0	0.02	0.02	0.05	0.27	1.00	1.00	1.00
S2	2	0.25	0.00	0.00	0.00	0.00	0.00	0.31	0.31
		0.45	0.00	0.00	0.00	0.00	0.00	0.00	0.00
		0	0.01	0.00	0.00	0.11	1.00	1.00	1.00
	4	0.25	0.00	0.00	0.00	0.00	0.00	0.95	1.00
		0.45	0.00	0.00	0.00	0.00	0.00	0.00	0.00
		0	0.02	1.00	1.00	1.00	1.00	1.00	1.00
	1	0.25	0.00	0.00	0.86	1.00	1.00	1.00	1.00
		0.45	0.00	0.00	0.00	0.00	0.00	0.00	0.00
		0	0.02	0.96	1.00	1.00	1.00	1.00	1.00
S3	2	0.25	0.00	0.00	0.00	0.04	0.16	0.36	0.37
		0.45	0.00	0.00	0.00	0.00	0.00	0.00	0.00
		0	0.01	0.86	1.00	1.00	1.00	1.00	1.00
	4	0.25	0.00	0.00	0.00	0.00	0.56	0.96	1.00
		0.45	0.00	0.00	0.00	0.00	0.00	0.00	0.00
		0	0.01	0.17	0.80	1.00	1.00	1.00	1.00
	1	0.25	0.00	0.00	0.00	0.03	0.99	1.00	1.00
		0.45	0.00	0.00	0.00	0.00	0.00	0.00	0.00
		0	0.01	0.06	0.34	0.99	1.00	1.00	1.00
S4	2	0.25	0.00	0.00	0.00	0.00	0.01	0.12	0.34
		0.45	0.00	0.00	0.00	0.00	0.00	0.00	0.00
		0	0.00	0.05	0.22	0.94	1.00	1.00	1.00
	4	0.25	0.00	0.00	0.00	0.00	0.00	0.58	1.00
		0.45	0.00	0.00	0.00	0.00	0.00	0.00	0.00
		0	0.02	0.77	1.00	1.00	1.00	1.00	1.00
	1	0.25	0.00	0.00	0.00	0.16	0.99	1.00	1.00
		0.45	0.00	0.00	0.00	0.00	0.00	0.00	0.00
		0	0.02	0.43	0.89	1.00	1.00	1.00	1.00
S5	2	0.25	0.00	0.00	0.00	0.00	0.00	0.02	0.08
		0.45	0.00	0.00	0.00	0.00	0.00	0.00	0.00
		0	0.01	0.18	0.78	1.00	1.00	1.00	1.00
	4	0.25	0.00	0.00	0.00	0.00	0.00	0.03	0.16
		0.45	0.00	0.00	0.00	0.00	0.00	0.00	0.00

Table 9.31: L_p-type test power, segment length $\ell^* = \lfloor \log n \rfloor + 1$. $N_{\text{rep}} = 100$, $n = 400$, $\alpha = 0.05$.

Scenario	γ	$a = 0$	$a = 0.25$	$a = 0.5$	$a = 1$	$a = 2$	$a = 4$	$a = 8$
	0	0.36	0.43	0.50	0.42	0.58	0.65	0.62
S1	0.25	0.38	0.31	0.30	0.38	0.54	0.52	0.64
	0.45	0.07	0.10	0.15	0.24	0.63	1.00	1.00
	0	0.44	0.53	0.30	0.44	0.51	0.53	0.59
S2	0.25	0.32	0.27	0.38	0.39	0.46	0.53	0.54
	0.45	0.09	0.12	0.04	0.11	0.38	1.00	1.00
	0	0.38	0.43	0.50	0.60	0.59	0.57	0.54
S3	0.25	0.36	0.36	0.51	0.54	0.52	0.57	0.61
	0.45	0.14	0.18	0.39	0.89	1.00	1.00	1.00
	0	0.44	0.49	0.50	0.49	0.64	0.64	0.53
S4	0.25	0.34	0.30	0.31	0.36	0.47	0.53	0.62
	0.45	0.04	0.05	0.11	0.21	0.50	1.00	1.00
	0	0.38	0.41	0.40	0.51	0.46	0.55	0.57
S5	0.25	0.36	0.35	0.30	0.43	0.48	0.41	0.62
	0.45	0.14	0.07	0.08	0.25	0.47	0.87	0.97

Table 9.32: L_p-type test power, segment length $\ell^* = n/5$. $N_{\text{rep}} = 100$, $n = 400$, $\alpha = 0.05$.

Scenario	γ	$a = 0$	$a = 0.25$	$a = 0.5$	$a = 1$	$a = 2$	$a = 4$	$a = 8$
	0	0.46	0.72	0.98	1.00	1.00	1.00	1.00
S1	0.25	0.31	0.63	1.00	1.00	1.00	1.00	1.00
	0.45	0.11	0.35	0.90	1.00	1.00	1.00	1.00
	0	0.41	0.46	0.51	0.98	1.00	1.00	1.00
S2	0.25	0.33	0.29	0.42	0.97	1.00	1.00	1.00
	0.45	0.13	0.08	0.19	0.93	1.00	1.00	1.00
	0	0.44	1.00	1.00	1.00	1.00	1.00	1.00
S3	0.25	0.34	1.00	1.00	1.00	1.00	1.00	1.00
	0.45	0.06	1.00	1.00	1.00	1.00	1.00	1.00
	0	0.40	0.81	0.99	1.00	1.00	1.00	1.00
S4	0.25	0.33	0.72	1.00	1.00	1.00	1.00	1.00
	0.45	0.11	0.47	0.97	1.00	1.00	1.00	1.00
	0	0.44	1.00	1.00	1.00	1.00	1.00	1.00
S5	0.25	0.34	1.00	1.00	1.00	1.00	1.00	1.00
	0.45	0.06	0.99	1.00	1.00	1.00	1.00	1.00

Table 9.33: RKHS test power, segment length $\ell^* = \lfloor \log n \rfloor + 1$. $N_{\text{rep}} = 100$, $n = 400$, $\alpha = 0.05$.

Scenario	γ	$a=0$	$a=0.25$	$a=0.5$	$a=1$	$a=2$	$a=4$	$a=8$
S1 with $\exp\{-\frac{(x-y)^2}{2}\}$	0	0.06	0.06	0.03	0.00	0.02	0.02	0.03
	0.25	0.07	0.04	0.09	0.08	0.07	0.07	0.11
	0.45	0.03	0.03	0.00	0.03	0.28	1.00	1.00
S2 with $\min(x, y)$	0	0.03	0.06	0.06	0.10	0.08	0.39	1.00
	0.25	0.06	0.06	0.09	0.11	0.51	1.00	1.00
	0.45	0.04	0.06	0.02	0.09	0.65	1.00	1.00
S4 with $2 - \max(x, y)$	0	0.00	0.00	0.00	0.01	0.00	0.00	0.00
	0.25	0.01	0.01	0.00	0.00	0.01	0.00	0.00
	0.45	0.02	0.01	0.06	0.00	0.00	0.00	0.00

Table 9.34: RKHS test power, segment length $\ell^* = n/5$. $N_{\text{rep}} = 100$, $n = 400$, $\alpha = 0.05$.

Scenario	γ	$a=0$	$a=0.25$	$a=0.5$	$a=1$	$a=2$	$a=4$	$a=8$
S1 with $\exp\{-\frac{(x-y)^2}{2}\}$	0	0.08	0.06	0.29	0.97	1.00	1.00	1.00
	0.25	0.07	0.16	0.68	1.00	1.00	1.00	1.00
	0.45	0.00	0.07	0.39	1.00	1.00	1.00	1.00
S2 with $\min(x, y)$	0	0.06	0.08	0.06	0.68	1.00	1.00	1.00
	0.25	0.05	0.05	0.10	0.93	1.00	1.00	1.00
	0.45	0.02	0.04	0.02	0.68	1.00	1.00	1.00
S4 with $2 - \max(x, y)$	0	0.02	0.00	0.00	0.00	0.00	0.00	1.00
	0.25	0.01	0.00	0.00	0.00	0.00	1.00	1.00
	0.45	0.06	0.00	0.00	0.00	0.95	1.00	1.00

Bibliography

[1] J. Antoch and M. Hušková. Estimators for epidemic alternatives. *Commentationes Mathematicae Universitatis Carolinae*, 36.2:279–291, 1996.

[2] Sylvain Arlot, Alain Celisse, and Zaid Harchaoui. A kernel multiple change-point algorithm via model selection. *Journal of Machine Learning Research*, 20(162):1–56, 2019.

[3] J. A. D. Aston and C. Kirch. Evaluating stationarity via change-point alternatives with applications to fMRI data. *The Annals of Applied Statistics*, 6(4):1906 – 1948, 2012.

[4] J. A. D. Aston and C. Kirch. High dimensional efficiency with applications to change point tests. *Electronic Journal of Statistics*, 12(1):1901–1947, 2018.

[5] A. Aue, R. Gabrys, L. Horváth, and P. Kokoszka. Estimation of a change-point in the mean function of functional data. *Journal of Multivariate Analysis*, 100(10):2254–2269, 2009.

[6] P. Avery and A. Henderson. Detecting a changed segment in DNA sequences. *Journal of the Royal Statistical Society: Series C (Applied Statistics)*, 48(4):489–503, 1999.

[7] P. J. Avery. The effect of dependence in a binary sequence on tests for a changepoint or a changed segment. *Journal of the Royal Statistical Society: Series C (Applied Statistics)*, 50(2):243–246, 2001.

[8] I. Berkes, E. Gombay, L. Horváth, and P. Kokoszka. Sequential change-point detection in GARCH(p, q) models. *Econometric Theory*, 20(6):1140–1167, 2004.

[9] A. Berlinet and C. Thomas-Agnan. *Reproducing Kernel Hilbert Spaces in Probability and Statistics*. Springer, New York, 2004.

[10] P.J. Bickel. A distribution-free version of the Smirnov two-sample test in the p-variate case. *Ann. Math. Statist.*, 40(1):1–23, 1969.

[11] Algimantas Birbilas. *Functional Data Analysis in Telecommunications*. Phd dissertation, Vilnius University, 2025. Supervisor: prof. habil. dr. Alfredas Račkauskas.

[12] E. Carlstein. Nonparametric change-point estimation. *The Annals of Statistics*, 16(1):188–197, 1988.

[13] Z. Ciesielski. On the isomorphisms of the spaces H^α and m. *Bull. Acad. Polon. Sci. Sér. Sci. Math. Astron. Phys.*, 8:217–222, 1960.

[14] D. Commenges, J. Seal, and F. Pinatel. Inference about a change point in experimental neurophysiology. *Math. Biosci.*, 80:81–108, 1986.

[15] M. Csörgö and L. Horváth. *Limit Theorems in Change-Point Analysis*. John Wiley & Sons, Inc., 1997.

[16] M. L. Diop and W. Kengne. Epidemic change-point detection in general causal time series. *Statistics & Probability Letters*, 184:109416, 2022.

[17] M. L. Diop and W. Kengne. Epidemic change-point detection in general integer-valued time series. *Journal of Applied Statistics*, 51(6):1131–1150, 2023.

[18] David L. Donoho and Iain M. Johnstone. Ideal spatial adaptation by wavelet shrinkage. *Biometrika*, 81(3):425–455, 1994.

[19] R. M. Dudley. *Real Analysis and Probability*. Cambridge University Press, 2002.

[20] R. M. Dudley and R. Norvaiša. *Concrete Functional Calculus*. Springer Monographs in Mathematics. Springer New York, NY, 1 edition, 2011. 978-1-4419-6950-7 (2010). Series ISSN: 1439-7382, E-ISSN: 2196-9922. Copyright: Springer Science+Business Media, LLC 2011.

[21] U. Einmahl and I. W. McKeague. Empirical likelihood-based hypothesis testing. *Bernoulli*, 9(2):267–290, 2003.

[22] A. T. M. Fisch, I. A. Eckley, and P. Fearnhead. A linear time method for the detection of collective and point anomalies. *Statistical Analysis and Data Mining*, 15(4):494–508, 2022.

[23] E. Gombay. Testing for change-points with rank and sign statistics. *Statist. Probab. Lett.*, 20(1):49–55, 1994.

[24] A. Gretton, K.M. Borgwardt, M. Rasch, B. Schölkopf, and A. Smola. A kernel method for the two-sample problem. In B. Schölkopf, J. Platt, and

T. Hoffman, editors, *Advances in Neural Information Processing Systems 19*, pages 513–520. MIT Press, 2007.

[25] A. Gretton, K.M. Borgwardt, M.J. Rasch, B. Schölkopf, and A. Smola. A kernel two-sample test. *J. Mach. Learn. Res.*, 13:723–773, 2012.

[26] C. Inclan and G. C. Tiao. Use of cumulative sums of squares for retrospective detection of changes of variance. *Journal of the American Statistical Association*, 89(427):913–923, 1994.

[27] B. Jin, Y. Han, and Y. Wu. Simultaneous estimation of change-points in epidemic change models. *Sankhyā B*, 87(1):1–25, 2025.

[28] J. Juodakis and S. Marsland. Epidemic change point detection in the presence of nuisance changes. *Statistical Papers*, 64(1):17–39, 2023.

[29] G. Kerkyacharian and D. Picard. Density estimation in Besov spaces. *Statistics & Probability Letters*, 13(1):15–24, 1992.

[30] Piotr Kokoszka and Matthew Reimherr. *Introduction to Functional Data Analysis*. Chapman and Hall/CRC, 1 edition, 2017.

[31] B. Levin and J. Kline. The CUSUM test of homogeneity with an application in spontaneous abortion epidemiology. *Statistics in Medicine*, 4(4):469–488, 1985.

[32] F. Lombard. Rank tests for change point problems. *Biometrika*, 74(3):615–624, 1987.

[33] Fermín Mallor, José A. Moler, and Henar Urmeneta. Simulation of household electricity consumption by using functional data analysis. *Journal of Simulation*, 12(4):1–12, 2018.

[34] W. Ning. Empirical likelihood ratio test for a mean change point model with a linear trend followed by an abrupt change. *Journal of Applied Statistics*, 39(5):947–961, 2012.

[35] W. Ning, J. Pailden, and A. Gupta. Empirical likelihood ratio test for the epidemic change model. *Journal of Data Science*, 10(1):107–127, 2012.

[36] A. N. Pettitt. A non-parametric approach to the change-point problem. *Journal of the Royal Statistical Society. Series C (Applied Statistics)*, 28(2):126–135, 1979.

[37] A. Račkauskas and C. Suquet. Estimating a changed segment in a sample. *Acta Applicandae Mathematicae*, 97(1–3):189–210, 2007.

[38] Alfredas Račkauskas and Charles Suquet. Necessary and sufficient condition for the functional central limit theorem in hölder spaces. *Journal of Theoretical Probability*, 17(1):221–243, January 2004.

[39] A. Račkauskas and M. Wendler. Convergence of U-processes in Hölder spaces with application to robust detection of a changed segment. *Stat Papers*, 61:1409–1435, 2020.

[40] Alfredas Račkauskas and Charles Suquet. Hölder norm test statistics for epidemic change. *Journal of Statistical Planning and Inference*, 126(2):495–520, 2004.

[41] G.R. Shorack. *Probability for Statisticians*. Springer, New York, 2000.

[42] D. Siegmund. Boundary crossing probabilities and statistical applications. *Ann. Statist.*, 14(2):361–404, 1986.

[43] N. Smirnov. On the estimation of the discrepancy between empirical curves of distribution for two independent samples. *Moscow University Mathematics Bulletin*, 2:3–26, 1939.

[44] Hoseung Song and Hao Chen. Practical and powerful kernel-based change-point detection. *IEEE Transactions on Signal Processing*, 72:5174–5186, 2024.

[45] Novri Suhermi and Rahida Rihhadatul Aisy. Functional data analysis for household appliance energy consumption prediction. In *2024 International Conference on Computer, Control, Informatics and its Applications (IC3INA)*, pages 468–471, 2024.

[46] Q. Yao. Tests for change-points with epidemic alternatives. *Biometrika*, 80(1):179–191, 1993.

[47] Z. Zhao and C. Y. Yau. Alternating pruned dynamic programming for multiple epidemic change-point estimation. *Journal of Computational and Graphical Statistics*, 30(3):808–821, 2021.

[48] D. Zuokas. Testing for a changed segment in variance with application. *Liet. matem. rink.*, 45 (spec. nr.):385–389, 2005.

Santrauka (summary in Lithuanian)

Daugelis šiuolaikinių duomenų aibių pateikiamos kaip sekos: matavimai laike, stebėjimai erdvėje arba kokybės užtikrinimo sistemų generuojami įrašai. Esminis statistinis uždavinys tokiose sekose yra nustatyti, ar duomenis generuojantis mechanizmas išlieka stabilus, ar tam tikram momente (arba intervale) pasikeičia. Daugelyje taikymų nuokrypis nėra nuolatinis: sistema gali laikinai nukrypti nuo bazinės elgsenos ir vėliau sugrįžti į pradinį režimą. Pavyzdžiai: trumpalaikės anomalijos jutiklių tinkluose, laikini poslinkiai finansų rinkose, trumpi pokyčiai biomedicinos signaluose, klasikinės „epidemijos“ laiko eilutėse. Tokie scenarijai kelia poreikį *pasikeitusio segmento* (arba *epideminio tipo*) modeliams, kai pasiskirstymas nuo bazinio skiriasi tik nežinomame vientisame intervale.

Pasikeitusio segmento modelis. Tegu $(\mathbb{S}, \mathcal{S})$ yra mati erdvė ir $X_1, \ldots, X_n$ yra nepriklausomi atsitiktiniai elementai, įgyjantys reikšmes $\mathbb{S}$ ir turintys skirstinius $P_{X_1}, \ldots, P_{X_n}$. Disertacijos atspirties taškas yra testas su hipoteze

$$H_0 : \quad P_{X_1} = \cdots = P_{X_n} = P, \tag{9.1}$$

prieš epideminę alternatyvą

$$\begin{aligned} H_1 : \quad & \exists\, I^* = \{k^* + 1, \ldots, k^* + \ell^*\} \subset \{1, \ldots, n\} \ \text{ tokią, kad} \\ P_{X_i} &= \begin{cases} P, & i \notin I^*, \\ Q, & i \in I^*, \end{cases} \quad \text{kur } P \neq Q. \end{aligned} \tag{9.2}$$

Esant H_1, stebiniai intervale I^* sudaro vientisą segmentą, generuotą iš kito skirstinio. Jei k^* ir ℓ^* būtų žinomi, uždavinys redukuotųsi į dviejų imčių testą, lyginant „vidinę“ ir „išorinę“ imtis. Tačiau praktikoje tiek segmento pradžia, tiek ilgis yra nežinomi, todėl efektyvus metodas turi „skenuoti“ daug kandidatinių intervalų ir kartu išlaikyti korektišką I rūšies klaidos kontrolę esant H_0.

Kontekstas ir motyvacija. Klasikiniai pokyčio taško metodai ilgą laiką buvo parametriniai, tačiau plečiantis taikymams išaugo paklausa neparametriniams metodams, leidžiantys aptikti poslinkius skirstinio prasme ir dirbti su didelės ar begalinės dimensijos duomenimis. Ankstyvieji neparametriniai darbai apima ranginius metodus [36], neparametrinius įvertinius, užtikrinančius stiprų pokyčio taško įverčių suderinamumą silpniausiomis prielaidomis [12], bei metodus, paremtus dalinėmis sumomis ar empirinio tikėtinumo idėjomis [26, 21, 34]. Epideminio tipo alternatyva yra aktuali problema [31, 14, 46, 23, 1, 15, 7, 48, 35] ir išlieka aktyvi tyrimų kryptis [4, 28, 16, 17].

Šiai disertacijai ypač svarbūs du aspektai. Pirmas, *integralinės tikimybinės metrikos* tapo standartiniu metodu lyginti skirstinius be parametrinių prielaidų; žinomi pavyzdžiai yra Kolmogorovo–Smirnovo tipo testai [43, 10, 41] ir branduoliniai atstumai, paremti maksimalia vidurkio neatitiktimi (MMD) [24, 25]. Antras, *funkcinių duomenų analizė* (FDA) tiria atsitiktinius objektus begalinės dimensijos erdvėse (kreives, paviršius, trajektorijas). Funkciniai stebiniai sustiprina metodologinius iššūkius: reikia kontroliuoti I rūšies klaidą esant sudėtingoms struktūroms ir išlaikyti galią prieš subtilias alternatyvas.

Tikslas ir vedančios idėjos. Disertacijoje kuriami neparametriniai metodai epideminio tipo pasiskirstymo pokyčiams aptikti, pabrėžiant procedūras, kurios

- formuluojamos be griežtų parametrinių prielaidų,
- leidžia spręsti nežinomos pradžios ir ilgio uždavinį skenavimo (angl. scan) principu,
- natūraliai išplečiamos į Hilberto erdves ir funkcinius stebinius.

Vienijantis požiūris: skenavimas pagal integralinius skirtumus. Pasikeitusio segmento aptikimą galima formuluoti maksimizuojant per visus intervalus $I(k,\ell) = \{k+1, \ldots, k+\ell\}$ tinkamai normuotą empirinio skirstinio skirtumą „viduje“ ir „išorėje“. Pažymėkime

$$P_n^I = \frac{1}{|I|} \sum_{i \in I} \delta_{X_i}, \qquad \widehat{P}_n := P_n^{\{1,\ldots,n\}}.$$

Tuomet natūralus heterogeniškumo matas yra atstumas (arba seminorma) tarp $P_n^{I(k,\ell)}$ ir $P_n^{I^c(k,\ell)}$. Tai veda į skenavimo statistikas

$$\max_{k,\ell} \frac{\mathcal{N}\Big(\sum_{i=k+1}^{k+\ell} (\delta_{X_i} - \widehat{P}_n)\Big)}{\rho(\ell/n)},$$

kur $\mathcal{N}$ yra seminorma krūvių erdvėje (gali priklausyti nuo n), o ρ yra svorio funkcija, stabilizuojanti skirtingų ilgių intervalų įtaką ribinei skirstinių formai ir galiai. Parenkant $\mathcal{N}$ tinkamai, į epideminį kontekstą perkeliami įvairūs dviejų imčių atstumai, tačiau atsiranda naujų techninių klausimų dėl maksimizavimo pagal (k, ℓ) ir dėl to, kad „išorinė“ imtis priklauso nuo pasirinkto intervalo.

Žymėjimai ir svorinė funkcija. Toliau santraukoje naudojame klasę $\mathcal{R}$ svorinių funkcijų $\rho : (0, 1) \to (0, \infty)$, tenkinančių:

i) egzistuoja $0 < \alpha \leq 1/2$ ir lėtai begalybėje kintanti funkcija L tokia, kad $\rho(s) = s^\alpha L(1/s), 0 < s \leq 1$;

ii) $\theta(t) = t^{1/2}\rho(1/t)$ yra C^1 funkcija intervale $[1, \infty)$;

iii) egzistuoja $\beta > 1/2$ ir $a > 0$ tokie, kad $\theta(t) \log^{-\beta}(t)$ yra nemažėjanti funkcija intervale $[a, \infty)$.

Klasei $\mathcal{R}$ priklauso, pavyzdžiui, $\rho_\gamma(t) = t^\gamma$ su $0 \leq \gamma < 1/2$ ir $\rho_{0.5,\beta}(t) = t^{1/2} \log^\beta(c/t)$ su $\beta > 1/2$ (žr. [39]). Šis žymėjimas naudojamas vienodai visuose santraukos skyriuose.

Nuo baigtinės prie begalinės dimensijos. Funkciniams ir Hilberto erdvės stebiniams disertacijoje kuriamos Wilcoxon tipo statistikos, paremtos antisimetriškais branduoliais, jungiančios ranginius testus, U-statistikas ir pokyčių analizę. *Brown'o projekcijos* yra naudojamos begalinės dimensijos objektų sumažinimui iki informatyvios vienmatės sekos. Šis metodas papildo skenavimo idėją: gaunami įgyvendinami testai epideminiams pasiskirstymo pokyčiams Hilberto erdvėse ir įrodoma jų asimptotinė teorija.

Disertacijos indėlis. Disertacija remiasi dviem publikuotais straipsniais ir jų plėtiniais. Pagrindinis indėlis – bendras neparametrinis epideminių pokyčių testavimo karkasas, paremtas empirinio mato skirtumo seminormomis ir pasvertomis normomis, kartu su trimis vienas kitą papildančiomis statistikų klasėmis: (i) Wilcoxon tipo antisimetriškų branduolių skenavimu; (ii) L_p tipo (Cramér–von Mises) integraliniais atstumais; (iii) RKHS branduoliniais atstumais. Visiems metodams rasti ribiniai skirstiniai, o Brown'o projekcijų metodika apjungia juos funkciniams stebiniams. Teorija papildyta modeliavimo tyrimais ir pritaikymu Lietuvos elektros balansavimo kainoms. Tikslios formuluotės pateikiamos žemiau skyriuose *Mokslinis naujumas* ir *Ginamieji teiginiai*.

Tikslai ir uždaviniai

Šios disertacijos tikslas - sukurti ir ištirti neparametrinius metodus *pasikeitusio segmento* (epideminio tipo pokyčio) aptikimui nepriklausomų stebinių sekoje, akcentuojant pokyčius *visame pasiskirstyme* ir metodų išplėtimą į Hilberto erdves bei funkcinius duomenis. Siūloma metodika remiasi skenavimo principu (dviejų imčių skirtumų maksimizavimu per visus intervalus) ir projekcijomis, tinkamomis begalinės dimensijos kontekstui.

Tikslui pasiekti sprendžiami šie uždaviniai:

1. Suformuluoti epideminio pokyčio problemą kaip skirstinių homogeniškumo testą prieš alternatyvą su nežinomu vientisu segmentu ir susieti ją su neparametriniais dviejų imčių testais.

2. Sukurti skenavimo statistikas, paremtas empirinio mato skirtumo seminormomis, ir parinkti svorio funkcijas, leidžiančias apimti platų segmentų ilgių spektrą ir gauti korektišką asimptotinę elgseną esant H_0.

3. Pritaikyti integralinius dviejų imčių skirtumus epideminio segmento aptikimui, ypač nagrinėjant L_p tipo ir RKHS/branduolinius atstumus, bei gauti jų asimptotines savybes ir nuoseklumą esant alternatyvai.

4. Sukurti nuo skirstinio nepriklausomus (angl. distribution-free) Wilcoxon tipo skenavimo testus Hilberto erdvėms, naudojant antisimetriškus branduolius, ir rasti jų ribinius skirstinius bei galią.

5. Pasiūlyti Brown'o projekcijų metodą funkciniams stebiniams ir ištirti jo tinkamumą epideminiams pasiskirstymo pokyčiams.

6. Įvertinti galią baigtinėse imtyse modeliavimo tyrimais, tiriant segmento ilgį, pokyčio stiprumą ir funkcijų formą.

7. Parodyti praktinį metodų pritaikomumą realiems duomenims, Lietuvos elektros balansavimo kainų analize.

Mokslinis ir praktinis naujumas

1. **Vieningas skenavimo karkasas empirinio mato seminormoms.** Epideminis testavimas formuluojamas maksimizuojant normalizuotą dalinių sumų krūvio $\sum_{i\in I(k,\ell)}(\delta_{X_i} - \widehat{P}_n)$ seminormą; tai vienoje konstrukcijoje sujungia kelias neparametrines atstumų klases.

2. **Trys viena kitą papildančios statistikų klasės.** Į skenavimo karkasą įterpiami antisimetriškų branduolių (Wilcoxon tipo), L_p tipo ir RKHS branduolinių atstumų testai. Visiems išvestos ribinės skirstinio formos ir pateikiami nuoseklumo rezultatai.

3. **Brown'o projekcijų metodika funkciniams stebiniams.** Pasiūlomas projekcinis metodas, jungiantis funkcinių duomenų įrankius su epideminių pokyčių testavimu; taip procedūros pritaikomos kreivėms Hilberto erdvėse be griežtų kovariacijos prielaidų.

4. **Empirinis patvirtinimas.** Teoriniai rezultatai papildyti modeliavimo tyrimais su lengvų ir sunkių uodegų alternatyvomis bei taikymu Lietuvos elektros balansavimo kainoms.

Darbo struktūra

Disertaciją sudaro santrauka ir įvadinė dalis, pagrindiniai skyriai, baigiamosios pastabos su tolesnių tyrimų kryptimis ir literatūros sąrašas. Struktūra atspindi metodinę eigą: pirmiausia įvedami funkciniai ir tikimybiniai pagrindai, tuomet aptariami dimensijos mažinimo/projekcijų įrankiai, o vėliau pateikiamos trys neparametrinių pasikeitusio segmento testų klasės bei jų empiriniai tyrimai ir taikymas.

* **Santrauka ir įvadinė dalis** (Santrauka; Įvadas; Tikslas ir uždaviniai; Mokslinis ir praktinis naujumas; Disertacijos struktūra; Ginamieji teiginiai; Rezultatų sklaida; Pagrindiniai rezultatai; Modeliavimas ir taikymas) apžvelgia problemą, pagrindžia epideminių alternatyvų poreikį ir apibendrina indėlį bei empirinius pastebėjimus.

* **1 skyrius: Įvadas.** Pateikiama bendroji problemos formuluotė ir apžvelgiami reikalingi pagrindai: (i) funkciniai duomenys, rekonstrukcija ir glodinimas (įskaitant Faber–Schauder bazę), (ii) pasikeitusio segmento aptikimas ir sąsajos su dviejų imčių testais, (iii) svorinės funkcijos apibrėžimas.

* **2 skyrius: Dimensijos mažinimas.** Aprašomi projekcijų ir dimensijos mažinimo metodai funkciniams stebiniams: Brown'o projekcijos ir taškinės projekcijos $C[0,1]$ erdvėje.

* **3 skyrius: Testai su antisimetriškais branduoliais.** Kuriami Wilcoxon tipo skenavimo testai Hilberto erdvėms; gaunami ribiniai rezultatai ir pateikiamos Brown'o projekcijos realizacijos.

* **4 skyrius: L_p tipo testai.** Pritaikomi L_p (Cramér–von Mises) integraliniai skirtumai epideminiam aptikimui ir pateikiama teorija.

* **5 skyrius: RKHS testai.** Nagrinėjamos RKHS procedūros: branduoliniai atstumai ir jų skenavimo versijos; pateikiami teoriniai rezultatai.

* **6 skyrius: Testų galios tyrimas.** Pateikiami simuliacijų scenarijai, empiriniai palyginimai ir aptarimas bei taikymo rekomendacijos.

* **7 skyrius: Taikymas Lietuvos elektros balansavimo kainoms.** Pateikiamas duomenų aprašas, funkcinė reprezentacija ir testų taikymo rezultatai bei jų interpretacija.

* **8 skyrius: Baigiamosios pastabos.** Apibendrinamos išvados ir nurodomos tolesnių tyrimų kryptys.

Ginamieji teiginiai

1. Sukurtos projekcijos ir dimensijos mažinimo priemonės išplečia klasikinius metodus funkcinių duomenų analizės kontekste.

2. Surasti sukonstruotų testinių statistikų ribiniai skirstiniai.

3. Sukurtos statistinės procedūros epideminio tipo (pasikeitusio segmento) pokyčiams aptikti.

4. Metodų taikymas Lietuvos elektros balansavimo kainoms parodo praktinį siūlomų testų naudingumą.

Disertacijos rezultatų aprobavimas

Disertacijos tema paskelbti du straipsniai:

Publikacijos

A1 Bartkus, K.; Račkauskas, A. Changed segment tests via norm and Brownian projection. *Lith Math J* **2025**, *65*, 481–499. doi.org/10.1007/s10986-025-09699-7.

A2 Bartkus, K.; Račkauskas, A. Nonparametric changed segment detection in functional data. *Nonlinear Analysis: Modelling and Control* **2026**, *31(1)*, 194–211. doi.org/10.15388/namc.2026.31.44489.

Disertacijos keliami klausimai ir rezultatai pristatyti dviejose tarptautinėse konferencijose ir dviejose konferencijose Lietuvoje:

Konferencijos

C1 Bartkus, K. Change segment detection in functional sample via projections to Wiener process. *64-oji Lietuvos matematikų draugijos konferencija, Vilnius* **2023 birželis**.

C2 Bartkus, K. Nonparametric changed segment detection in functional data. *66-oji Lietuvos matematikų draugijos konferencija, Klaipėda* **2025 birželis**.

C3 Bartkus, K. Changed segment tests via norm and Brownian projection. *1-oji tarptautinė Vilniaus statistikos ir jos taikymų konferencija (ICSA 2025), Vilnius* **2025 rugpjūtis 27–29**.

C4 Bartkus, K. Changed segment tests via C-type projection. *25-asis Europos jaunųjų statistikų susitikimas (EYSM 2026), Vilnius* **2026 liepa 7–10**.

Pasikeitusio segmento testai paremti antisimetriškais branduoliais

Uždavinys ir motyvacija

Tegu $X_1, \dots, X_n$ yra nepriklausomi atsitiktiniai $\mathbb{S}$-reikšmiai elementai, čia $(\mathbb{S}, \mathcal{S})$ yra mati erdvė. Testuojame homogeniškumą

$$H_0: \quad P_{X_1} = P_{X_2} = \cdots = P_{X_n} = P,$$

prieš *pasikeitusio segmento* (epideminę) alternatyvą

$$H_1: \quad \exists\, I^* = \{k^*+1, \dots, k^*+\ell^*\} \subset I_n := \{1, \dots, n\} \text{ tokią, kad}$$
$$P_{X_i} = \begin{cases} P, & i \notin I^*, \\ Q, & i \in I^*, \end{cases} \qquad P \neq Q.$$

Pagal H_1 tik nežinomame gretimame intervale I^* pasiskirstymas pakinta į Q, o už intervalo ribų grįžta į bazinį P. Tokie laikini "išsiveržimai" natūraliai atsiranda monitoringo, finansų, energetikos, biomedicinos ir kt. sričių taikymuose.

Šiame skyriuje konstruojame testus, kurie remiasi *antisimetriškais branduoliais* ir skenavimo (angl. scan) idėja: intervalo kandidatų atžvilgiu maksimizuojamas dviejų imčių heterogeniškumo matas. Pagrindinis privalumas yra tas, kad tinkamai parinkus branduolius gaunami *pasiskirstymo atžvilgiu stabilūs* (angl. distribution-free) testai, kurie ypač konkurencingi sunkių uodegų (angl. heavy-tailed) situacijose; žr. [39].

Antisimetriški branduoliai ir skenavimo statistika

Pažymėkime $I(k,m) = \{k+1, \dots, m\}$, kur $0 \le k < m \le n$, ir $I^c(k,m) = I_n \setminus I(k,m)$. Bet kuriam poslinkiui (kandidatiniam segmentui) $I(k,m)$ lyginame empirinį pasiskirstymą intervalo viduje ir išorėje. Tegu $h: \mathbb{S} \times \mathbb{S} \to \mathbb{R}$ yra matus branduolys. Apibrėžiame

$$\Delta_{n,h}(k,m) := \sum_{i \in I(k,m)} \sum_{j \in I^c(k,m)} h(X_i, X_j).$$

Tai yra U-tipo statistika, kuri matuoja „kryžminį“ skirtumą tarp intervalo ir jo papildinio.

Branduolį vadiname *antisimetrišku*, jei

$$h(x,y) = -h(y,x) \qquad \forall x, y \in \mathbb{S}.$$

Tokiu atveju, esant n.a.d. porai (X, Y) su tuo pačiu pasiskirstymu, paprastai gauname $E\,h(X, Y) = 0$ (kai egzistuoja vidurkis), todėl $\Delta_{n,h}(k, m)$ pagal H_0 „centravosi“ natūraliai. Kaip ir [39], skenavimo statistiką apibrėžiame su svorio funkcija ρ:

$$T_{n,\rho}(h; X_1, \dots, X_n) := \max_{0 \le k < m \le n} \frac{|\Delta_{n,h}(k, m)|}{\rho\Big(\frac{m-k}{n}\Big(1 - \frac{m-k}{n}\Big)\Big)}.$$

Svoris ρ kontroliuoja skirtingo ilgio segmentų įtaką: kai segmentas labai trumpas arba labai ilgas, normalizavimas turi užtikrinti stabilų ribinį pasiskirstymą ir kartu išlaikyti galią.

Naudojame klasę $\mathcal{R}$, apibrėžtą santraukos įžangoje (žr. skyrelį apie svorinę funkciją ρ).

Kelių branduolių agregavimas ir blokinis skenavimas

Dažnai norime būti jautrūs skirtingoms alternatyvoms (pvz., pokyčiui projekcijoje, pokyčiui normoje, pokyčiui uodegose). Todėl imame baigtinę antisimetriškų branduolių šeimą $\mathcal{H} = \{h_1, \dots, h_d\}$ ir agreguojame:

$$T_{n,\rho}(\mathcal{H}) := \max_{h \in \mathcal{H}} T_{n,\rho}(h; X_1, \dots, X_n).$$

Papildomai naudojame blokinę idėją. Tarkime, kad $n = dN$ ir išskaidome seką į d nuoseklius blokus po N stebėjimų: $X_{i,1}, \dots, X_{i,N}$, kur $X_{i,k} = X_{(i-1)N+k}$. Tuomet skaičiuojame

$$T^{(d)}_{n,\rho}(\mathcal{H}) := \max_{1 \le i \le d} T_{N,\rho}(h_i; X_{i,1}, \dots, X_{i,N}).$$

Šis konstravimas motyvuotas tuo, kad jeigu tikrasis pasikeitęs segmentas yra trumpas (pvz., $\ell^* < N$), jis pilnai patenka į vieną bloką arba daugiausia į du gretimus blokus. Tuomet bent vieno bloko statistika turėtų „iššokti“, o tuo pačiu gauname paprastesnę ribinę analizę ir nepriklausomumą tarp blokų.

Ribiniai rezultatai

Toliau trumpai suformuluojame ribinių pasiskirstymų tipą. Esant H_0 ir tinkamoms momentinėms / uodegų sąlygoms (žr. [39]), laužčių procesas U konverguoja į Brauno tiltą atitinkamoje Hölder erdvėje. Tai duoda ir skenavimo statistikų ribinius dėsnius.

Kiekvienam branduoliui h, turime Brauno tiltą B_h su kovariacija, kuri priklauso nuo

$$\overline{h}(y) := E\,h(X,y), \qquad \sigma_h^2 = \mathrm{var}(\overline{h}(X)).$$

Tada gauname:

$$n^{-3/2} T_{n,\rho}(h) \ \Rightarrow \sup_{0\le s<t\le 1} \frac{|B_h(t) - B_h(s)|}{\rho((t-s)(1-(t-s)))}.$$

Baigtinei šeimai $\mathcal{H}$ ribinis objektas yra daugiamatis Brauno tiltas, o maksimizavimas per $h \in \mathcal{H}$ duoda $\max_{h\in\mathcal{H}}$ atitinkamų funkcionalų; analogiškai ir blokiniam variantui $T_{n,\rho}^{(d)}$, kur dėl blokų nepriklausomumo gaunamas d kartų sandaugos dėsnis.

Ši teorija pagrindžia asimptotinį kritinių reikšmių skaičiavimą ir leidžia konstruoti testą

$$\text{atmesti } H_0 \iff T_{n,\rho}^{(d)} \ge c_{\alpha,\rho}\, n^{3/2},$$

čia $c_{\alpha,\rho}$ parenkamas taip, kad ribiniame dėsyje reikšmė atitiktų lygmenį α.

Wilcoxon branduolių taikymas projekcijoms

Šiame darbe svarbus atvejis yra $X_i \in \mathbb{H}$, kur $\mathbb{H}$ yra reali separabili Hilberto erdvė (su skaliarine sandauga $\langle\cdot,\cdot\rangle$ ir norma $\|x\| = \sqrt{\langle x, x\rangle}$). Norėdami gauti antisimetriškus branduolius iš funkcinio objekto, naudojame projekcijas į $\mathbb{R}$.

Brauniškos projekcijos. Tegu $\mathrm{W} = \{\mathrm{W}(x) : x \in \mathbb{H}\}$ yra $\mathbb{H}$-izonormali Gauso šeima: $E[\mathrm{W}(x)\mathrm{W}(y)] = \langle x, y\rangle$. Kai $\mathbb{H} = L_2([0,1])$, tipinis pavyzdys yra Itô integralas $\mathrm{W}(x) = \int_0^1 x\,\mathrm{d}W$ su Wiener procesu W [19]; kai x turi pakankamą Hölder glodumą, integralas gali būti apibrėžtas ir trajektorijomis [20]. Prieš pradedant testavimą nepriklausomai traukiame d elementariųjų įvykių $\omega_1, \dots, \omega_d \in \Omega$ iš tikimybinės erdvės, kurioje apibrėžtas W; jie fiksuojami viso tolesnio testavimo laikui. Gauname d realių projekcijų $f_i : \mathbb{H} \to \mathbb{R}$, $f_i(x) := \mathrm{W}(x)(\omega_i)$, $i = 1, \dots, d$.

Wilcoxon branduolys. Skaliariniams duomenims naudojame standartinį antisimetrišką Wilcoxon branduolį

$$h(u,v) := \mathbf{1}\{u - v \le 0\} - \mathbf{1}\{v - u \le 0\}, \qquad u, v \in \mathbb{R}.$$

Tada Hilberto erdvėje apibrėžiame branduolį

$$h_i(x,y) := h(f_i(x), f_i(y)), \qquad i = 1, \dots, d,$$

ir normos branduolį

$$h_0(x, y) := h(\|x\|, \|y\|).$$

Praktinė interpretacija. Wilcoxon branduolys yra jautrus pokyčiams skirstinyje ir atsparus išskirtims. Normos branduolys dažnai gerai veikia, kai alternatyva labiau susijusi su bendru dispersijos/energijos pokyčiu (arba kai pasikeitęs segmentas sukuria amplitudės šuolį).

Įgyvendinimo pastabos

- **Skenavimas.** $\Delta_{n,h}(k, m)$ skaičiuoti visiems (k, m) brangu, naudojame dalines sumas.

- d **pasirinkimas.** Didelė d reikšmė reiškia daugiau projekcijų (didesnė galia), bet mažesni blokai $N = n/d$; dėl to blogėja konvergavimas ir gali mažėti galia baigtinėse imtyse. Šis kompromisas matomas simuliacijose.

- ρ **pasirinkimas.** γ arti $1/2$ prioritetizuoja trumpus segmentus, bet blogina konvergavimo greitį ($n^{1/2-\gamma}$); todėl per didelių γ reikšmių praktiškai verta vengti.

- **Kritinės reikšmės.** Ribinis dėsnis yra Brauno tilto funkcionalas, todėl $c_{\alpha,\rho}$ galima įvertinti Monte Karlo būdu (generuojant Brauno tiltą su smulkia diskretizacija ir maksimizuojant per (s, t)).

Apibendrinant, antisimetriškų branduolių skenavimo statistikos suteikia paprastą, stabilų ir teoriškai pagrįstą kelią pasikeitusio segmento aptikimui. Hilberto erdvės ar funkcinių duomenų atveju projekcijos (Brauno ar kitos) leidžia išlaikyti neparametrinį pobūdį ir gauti testus, kurių ribiniai dėsniai valdomi Brauno tilto funkcionalais [39, 19, 20].

Pasikeitusio segmento testai paremti L_p tipo statistikomis

Šiame skyriuje nagrinėjame pasikeitusio segmento (epideminio) aptikimo testus, paremtus L_p tipo empirinio proceso funkcionalais. Pagrindinė idėja yra skenuoti per visus kandidatinius intervalus $I(k,\ell) = \{k+1,\dots,k+\ell\}$ ir matuoti, kiek empirinė skirstinio funkcija intervale nukrypsta nuo visos imties empirinės skirstinio funkcijos. Tokia konstrukcija natūraliai apima Cramér–von Mises tipo kriterijų (kai $p=2$), tačiau $p \geq 2$ leidžia gauti lankstesnį testą, jautrų plačiam pasiskirstymo pokyčių spektrui (ne tik vidurkio ar dispersijos prasme).

Tarkime, stebime nepriklausomus realiuosius kintamuosius $X_1,\dots,X_n$ su skirstinio funkcijomis $F_{X_1},\dots,F_{X_n}$. Testuojame santraukoje apibrėžtą hipotezių porą (9.1)–(9.2), skirstinius P_{X_i} tapatinant su atitinkamomis skirstinio funkcijomis F_{X_i}. Toliau laikome, kad k^* ir ℓ^* yra nežinomi, o intervalas $I(k^*,\ell^*)$ yra nenutrūkstantis.

Skenavimo logika. Jei (k^*,ℓ^*) būtų žinomi, uždavinys susiprastintų į dviejų imčių testą (intervalas prieš likusią imtį). Kadangi k^*,ℓ^* nežinomi, statistika turi maksimizuoti dviejų imčių skirtumą per daug intervalų, tačiau išlaikyti korektišką I tipo klaidos kontrolę. Tam reikalinga normalizacija ir svorio funkcija $\rho \in \mathcal{R}$.

L_p tipo skenavimo statistika

Pažymėkime bendrąją empirinę skirstinio funkciją

$$F_n(x) = \frac{1}{n}\sum_{i=1}^{n} \mathbf{1}\{X_i \leq x\}, \qquad x \in \mathbb{R}.$$

Fiksavę intervalą $I(k,\ell)$, svarstome empirinio proceso prieaugį

$$G_{k,\ell}(x) := \sum_{i=k+1}^{k+\ell} \big(\mathbf{1}\{X_i \leq x\} - F_n(x)\big).$$

Tuomet L_p tipo funkcionalas apibrėžiamas kaip

$$\|G_{k,\ell}\|_{p,F_n} := \Big(\int_{-\infty}^{\infty} |G_{k,\ell}(x)|^p \, \mathrm{d}F_n(x)\Big)^{1/p}, \qquad p \geq 2.$$

Galiausiai, skenavimo statistika:

$$T_{n,\rho,p} := \max_{1\le\ell\le n/2}\max_{0\le k\le n-\ell}\frac{\|G_{k,\ell}\|_{p,F_n}}{\rho(\ell/n)}. \tag{9.3}$$

Pastaba (kodėl integruojama pagal F_n). Jei tikrasis skirstinys F būtų žinomas, integralą būtų galima skaičiuoti tiesiogiai pagal $\mathrm{d}F$. Praktikoje F nežinomas, todėl integruojame pagal empirinę F_n; tai palieka testą skirstinio prasme laisvą ir kartu išreiškia integralą per baigtinę sumą

$$\int |G_{k,\ell}(x)|^p\,\mathrm{d}F_n(x) = \frac{1}{n}\sum_{j=1}^{n}|G_{k,\ell}(X_{(j)})|^p,$$

čia $X_{(1)}\le\cdots\le X_{(n)}$.

Nulinės hipotezės asimptotika

Toliau darome standartinę prielaidą, kad F yra tolydi. Tada $U_i := F(X_i)\sim$ Unif$[0,1]$ ir statistikos riba gali būti išreikšta per dvimačio Wiener'io paklodės (angl. Wiener sheet) prieaugius.

Tegu $W^{(2)} = \{W(u,t) : (u,t)\in[0,1]^2\}$ yra standartinė Wiener'io paklodė su kovariacija

$$\mathrm{E}\big[W(u,t)W(u',t')\big] = \min\{u,u'\}\min\{t,t'\}.$$

Apibrėžkime prieaugį

$$\begin{aligned}\Delta_{t,s}(u) := \big(W(u,t)-W(u,s)\big)-(t-s)W(u,1)\\ -u\Big(\big(W(1,t)-W(1,s)\big)-(t-s)W(1,1)\Big),\\ 0\le s<t\le 1,\;\; u\in[0,1].\end{aligned} \tag{9.4}$$

Teorema 1 . *Tegu ρ priklauso klasei $\mathcal{R}$ (žr. skyrelį apie svorinę funkciją ρ santraukos įžangoje), ir $p\ge 2$. Jei $X_1,\dots,X_n$ yra n.a.d. su tolydžiu skirstiniu F, tai*

$$n^{-1/2}T_{n,\rho,p}\xrightarrow{\mathscr{D}} T_{\rho,p},$$

kur

$$T_{\rho,p} := \sup_{0<t-s\le 1/2}\frac{\Big(\int_0^1|\Delta_{t,s}(u)|^p\,\mathrm{d}u\Big)^{1/p}}{\rho(t-s)}, \tag{9.5}$$

o $\Delta_{t,s}(u)$ apibrėžtas (9.4).

Įrodymo eskizas. Taikome integralinę transformaciją $U_i = F(X_i)$ ir identifikuojame su $L_p(0,1)$ elementais $Z_i(t) = \mathbf{1}\{U_i \le t\} - t$. Skenavimo statistika yra tolydžių prieaugių funkcionalas

$$\max_{k,\ell} \frac{\big\| \sum_{i=k+1}^{k+\ell} Z_i \big\|_{L_p}}{\rho(\ell/n)},$$

o iš $n^{-1/2}$ normuotas ribinis procesas gaunamas iš funkcinės centrinės ribinės teoremos L_p erdvėje (Hölder tipo topologijoje, suderintoje su ρ), ir galiausiai pritaikoma tolydaus atvaizdžio teorema tolydžių prieaugių funkcionalui, duoda (9.4). □

Testas. Pasirinkus $\alpha \in (0,1)$, apibrėžiame kritinę reikšmę C_α iš $\mathbb{P}(T_{\rho,p} > C_\alpha) = \alpha$, ir atmetame H_0, jei

$$T_{n,\rho,p} > \sqrt{n}\, C_\alpha. \tag{9.6}$$

Kadangi $T_{\rho,p}$ neturi išreikštinių kvantilių, C_α praktikoje skaičiuojamas Monte Karlo būdu, simuliuojant $U_i \sim \mathrm{Unif}[0,1]$ ir skaičiuojant $T_{n,\rho,p}$ dideliems n.

Pastabos apie galią ir segmento lokalizaciją

Galia

Jei intervale $I(k^*, \ell^*)$ skirstinys pasikeičia, tuomet $G_{k^*,\ell^*}(x)$ turi nenulinį vidurkį kaip x funkcija. L_p funkcionalas tampa didelis, kai pokytis matomas pakankamai plačiai per x. Skirtingai nei vidurkio testai, L_p tipas jautrus ir formos pokyčiams: asimetrijai, uodegoms, multimodalumui.

Lokalizacija

Pažymėkime

$$(\hat{k}, \hat{\ell}) \in \arg \max_{1\le \ell \le n/2,\ 0 \le k \le n-\ell} \frac{\|G_{k,\ell}\|_{p,F_n}}{\rho(\ell/n)}.$$

Tuomet pora $(\hat{k}, \hat{\ell})$ natūraliai interpretuojama kaip epideminio intervalo įverčiai. Esant fiksuotam signalui ir pakankamam atotrūkiui tarp F ir F', $(\hat{k}, \hat{\ell})$ lokalizuoja (k^*, ℓ^*) su tikimybe, artėjančia prie 1 (su paklaida, priklausančia nuo tinklelio ir ρ). Formaliai, tam reikalingos papildomos prielaidos apie signalo dydį (pvz., skirtumo integralinę normą) ir apie minimalią segmento trukmę.

Santrauka

Šiame skyriuje apibrėžėme L_p tipo skenavimo statistiką (9.3), kuri matuoja empirinio proceso prieaugių „energiją“ (integruotą pagal F_n) ir maksimizuoja ją per visus kandidatinius intervalus. Pagal H_0 gavome ribinį skirstinį (9.5), išreikštą per Wiener'io paklodės prieaugius, ir nurodėme, kaip pagal šį ribinį skirstinį kalibruoti testą (9.6).

Kitame skyriuje analogiška skenavimo logika bus taikoma RKHS (branduolio) atstumams.

Pasikeitusio segmento testai paremti reprodukuojančia Hilberto erdve

Šiame skyriuje nagrinėjami pasikeitusio segmento (epideminio tipo) testai, paremti reprodukuojančia Hilberto erdve (RKHS). Pagrindinė idėja yra perkelti dviejų imčių atstumo matą į pasikeitusio segmento situaciją: kiekvienam kandidatiniam intervalui $I(k,\ell) = \{k+1,\dots,k+\ell\}$ lyginame empirinį pasiskirstymą intervalo viduje ir už jo ribų, o tada skenuojame per visus (k,ℓ). RKHS metodai leidžia konstruoti jautrius testus bendriems skirstinių pokyčiams (ne tik vidurkio ar dispersijos prasme), remiantis branduoliniais vidurkiais ir MMD (angl. maximum mean discrepancy) atstumu [24, 25].

RKHS įterpimas ir MMD atstumas

Tarkime, kad $(\mathbb{S},\mathcal{S})$ yra stebinių erdvė, o $\kappa : \mathbb{S}\times\mathbb{S}\to\mathbb{R}$ simetriška teigiamai apibrėžta branduolinė funkcija. Pagal Moore–Aronszajn teoremą egzistuoja atitinkama RKHS erdvė $(\mathcal{H}_\kappa, \langle\cdot,\cdot\rangle_\kappa)$ su savybe $f(x) = \langle f, \kappa(\cdot,x)\rangle_\kappa$, $f\in\mathcal{H}_\kappa$, $x\in\mathbb{S}$.

Tikimybinį matą $P\in\mathcal{P}(\mathbb{S})$ įterpiame į RKHS per branduolinį vidurkį

$$\mu_\kappa(P) = \int_{\mathbb{S}} \kappa(\cdot,x)\, P(\mathrm{d}x) \in \mathcal{H}_\kappa,$$

kai integralas egzistuoja (pvz., jei $\int \kappa(x,x)^{1/2} P(\mathrm{d}x) < \infty$). Tuomet dviejų skirstinių skirtumą matuojame:

$$\mathrm{MMD}_\kappa(P,Q) := \|\mu_\kappa(P) - \mu_\kappa(Q)\|_\kappa.$$

Jei κ yra charakteristinis branduolys, tai $\mathrm{MMD}_\kappa(P,Q) = 0$ tada ir tik tada, kai $P = Q$; todėl MMD_κ tampa tikru atstumu skirstinių erdvėje [25].

Pasikeitusio segmento skenavimo statistika

Duota nepriklausoma imtis $X_1,\dots,X_n$ su skirstiniais $P_{X_1},\dots,P_{X_n}$. Testuojame santraukoje apibrėžtą hipotezių porą (9.1)–(9.2). Kiekvienam intervalui $I = I(k,\ell)$ empiriniai matai yra $P_n^I = \frac{1}{\ell}\sum_{i\in I}\delta_{X_i}$ ir $P_n^{I^c} = \frac{1}{n-\ell}\sum_{i\notin I}\delta_{X_i}$. Naudojame ekvivalentų centravimą pagal visos imties empirinį matą $\widehat{P}_n := P_n^{I_n}$:

$$\sum_{i=k+1}^{k+\ell}\Big(\mu_\kappa(\delta_{X_i}) - \mu_\kappa(\widehat{P}_n)\Big) = \sum_{i=k+1}^{k+\ell}\kappa(\cdot,X_i) - \frac{\ell}{n}\sum_{j=1}^{n}\kappa(\cdot,X_j).$$

Tada apibrėžiame skenavimo statistiką:

$$T_{n,\rho}^{(\kappa)} := \max_{1\le\ell\le n/2}\max_{0\le k\le n-\ell}\frac{\left\|\sum_{i=k+1}^{k+\ell}\left(\mu_\kappa(\delta_{X_i})-\mu_\kappa(\widehat{P}_n)\right)\right\|_\kappa}{\rho(\ell/n)}. \tag{9.7}$$

Svorio funkcija $\rho\in\mathcal{R}$ (žr. skyrelį apie svorinę funkciją ρ santraukos įžangoje) stabilizuoja indėlį skirtingiems segmento ilgiams: pvz., $\rho_\gamma(t)=t^\gamma$ su $0\le\gamma<1/2$ arba $\rho_{0.5,\beta}(t)=t^{1/2}\log^\beta(c/t)$ su $\beta>1/2$.

Normą (9.7) galima apskaičiuoti tik per branduolio reikšmes. Pažymėkime

$$S_1(k,\ell)=\sum_{i,j=k+1}^{k+\ell}\kappa(X_i,X_j),\qquad S_2(k,\ell)=\sum_{i=k+1}^{k+\ell}\sum_{j=1}^{n}\kappa(X_i,X_j),$$
$$S_3=\sum_{i,j=1}^{n}\kappa(X_i,X_j).$$

Tada

$$\Delta_{k,\ell}^2 := \left\|\sum_{i=k+1}^{k+\ell}\left(\mu_\kappa(\delta_{X_i})-\mu_\kappa(\widehat{P}_n)\right)\right\|_\kappa^2 = S_1(k,\ell)-2\frac{\ell}{n}S_2(k,\ell)+\left(\frac{\ell}{n}\right)^2 S_3, \tag{9.8}$$

ir

$$T_{n,\rho}^{(\kappa)} = \max_{1\le\ell\le n/2}\max_{0\le k\le n-\ell}\frac{\Delta_{k,\ell}}{\rho(\ell/n)}.$$

Ši forma leidžia efektyviai realizuoti skenavimą, ypač jei galima iš anksto paruošti dalines sumas (pvz., branduolio matricai).

Asimptotinė teorija galiojant H_0

Galiojant H_0, vektoriai $\kappa(\cdot,X_i)$ yra n.a.d. atsitiktiniai elementai RKHS erdvėje $\mathcal{H}_\kappa$ su vidurkiu $\mu_\kappa(P)$. Tuomet (9.7) statistika yra tolydžių prieaugių (UI) tipo funkcionalas Hilberto erdvėje, analogiškai kaip L_p skyriuje. Esant uodegų/momentų sąlygai (pvz., [38, 40]), gauname silpną konvergavimą į Q–Wiener procesą RKHS erdvėje.

Teorema 2 . *Tarkime $\rho\in\mathcal{R}$ ir tenkina sąlygą*

$$\lim_{t\to\infty} t\,\mathbb{P}\big(\kappa(X,X)^{1/2}>A\theta(t)\big)=0\quad \textit{visiems } A>0,\qquad \theta(t)=t^{1/2}\rho(1/t),$$

kur $X \sim P$. Tada, galiojant H_0,

$$n^{-1/2} T_{n,\rho}^{(\kappa)} \xrightarrow{\mathscr{D}} \sup_{0<t-s\le 1/2} \frac{\|W_Q(t) - W_Q(s) - (t-s)W_Q(1)\|_\kappa}{\rho(t-s)},$$

kur W_Q yra Q–Wiener procesas RKHS erdvėje $\mathcal{H}_\kappa$.

Praktikoje Teoremos 2 riba naudojama tik kaip teorinis pagrindas; kritines reikšmes patogu gauti Monte Karlo būdu (simuliuojant nulinės hipotezės imtis), nes ribinis skirstinys priklauso nuo P ir nuo κ.

Testo realizavimas ir kalibravimas

Kritinės reikšmės

Apibrėžiame testą:

$$\text{Atmesti } H_0 \iff T_{n,\rho}^{(\kappa)} \ge c_{\alpha,n}, \tag{9.9}$$

kur $c_{\alpha,n}$ parenkamas taip, kad $\mathbb{P}_{H_0}(T_{n,\rho}^{(\kappa)} \ge c_{\alpha,n}) \approx \alpha$.

Kvantilius galima suskaičiuoti atliekant Monte Karlo simuliacijas prie H_0 generuojant n.a.d. imtis.

Branduolio pasirinkimas ir pastabos funkciniams duomenims

Branduolio κ pasirinkimas lemia, kokio tipo pokyčiams testas bus jautrus. Realių skaičių atveju populiarūs Gauso (RBF) branduoliai $\kappa(x,y) = \exp\{-(x-y)^2/(2\sigma^2)\}$. Funkciniams duomenims $X_i \in C[0,1]$ dažnai naudojami branduoliai, priklausantys nuo funkcijų normos, pvz.

$$\kappa(x,y) = \exp\Big\{-\frac{\|x-y\|_{L_2}^2}{2\sigma^2}\Big\}, \qquad \kappa(x,y) = \exp\Big\{-\frac{\|x-y\|_{\infty}^2}{2\sigma^2}\Big\},$$

kai duomenys prieš tai rekonstruojami (pvz., per Faber–Schauder bazę). Parametras σ parenkamas euristiškai (pvz., pagal imties medianą); šiame darbe $\sigma = 1$.

IŠVADOS

Pagrindinės išvados. Disertacijoje sukurta neparametrinė metodika epideminio (segmento pokyčio) tipo nukrypimams aptikti funkciniuose duomenyse. Pasiūlytos trys viena kitą papildančios skenavimo statistikos šeimos: (a) antisimetriškų branduolių (Wilcoxon tipo) testai, taikomi funkcinių stebinių sekai per Brown'o projekcijas; (b) L_p tipo (Cramér–von Mises) testai, skenuojami tiek pagal pradžios indeksą, tiek pagal ilgį; (c) RKHS/branduoliniai testai, naudojantys branduolinio vidurkio įterpinius. Kiekvienai šeimai įrodyta funkcinė ribinė teorema Hölderio erdvėje $\mathcal{H}_\rho^o$, suderintoje su svorių klase $\mathcal{R}$, iš jos išvestas nulinės hipotezės ribinis skirstinys, Monte Karlo metodu suskaičiuoti kvantiliai ir ištirta galia baigtinėse imtyse. Lietuvos elektros balansavimo kainų taikymas parodo, kaip procedūros veikia praktiškai; kadangi duomenys nėra n.a.d., šis taikymas vertinamas kaip iliustracinis.

Tolesni tyrimai.

Svorio funkcijos ρ parinkimas. Visos trys procedūros priklauso nuo $\rho \in \mathcal{R}$; simuliacijos rodo, kad $\gamma = 0.25$ yra geras kompromisas tarp jautrumo trumpiems ir ilgiems segmentams. Duomenimis paremtos ρ parinkimo taisyklės kūrimas – pavyzdžiui, per kryžminį empirinės galios patikrinimą – yra konkretus atviras uždavinys.

Galia ir segmento ilgis. Nėra tikslios testo galios priklausomybės nuo $|I^*|$ ir pokyčio dydžio; euristiniai argumentai rodo slenksčius $\log n$ eilės, bet griežtas minimaksinio tipo rezultatas, susietas su γ, teoriją užbaigtų.

Priklausomi duomenys. Teorija remiasi n.a.d. prielaida; jos praplėtimas silpnai priklausomoms funkcinėms sekoms (pvz., α-maišomoms) leistų tiesiogiai taikyti testus prie balansavimo kainų duomenų be šios prielaidos.

Alternatyvios projekcijos. Be L_2 normos ir Itô tipo projekcijų, aptariama taškinė C projekcija. Labiau pritaikytos projekcinės taisyklės, atsižvelgiančios į kelio geometriją ar į konkrečią alternatyvą, padėtų rasti siaurai lokalizuotus pokyčius.

Platesni taikymai. Balansavimo kainos – tik vienas iš daugelio galimų taikymų; biomedicinos signalai ir didelio dažnio finansų duomenys būtų natūralus kitas žingsnis patikrinti metodų tvirtumą ir interpretuojamumą.

ACKNOWLEDGMENTS

I would like to thank my supervisor, Prof. Habil. Dr. Alfredas Račkauskas, for his guidance and patience throughout this work. His advice has shaped this dissertation in ways both obvious and less so, and I have benefited greatly from his judgement and from the time he has given me.

I am grateful to my late grandparents, Liudvikas and Ona Barauskai, thanks to whom I began this work. I would also like to thank my sister, Paulina, and my fiancée, Gražvilė, for their support over the years this work has taken, and Gražvilė especially, for her patience with the share of that time it has cost us both.

Karolis Bartkus
Vilnius
May 2026

CURRICULUM VITAE

Name: Karolis

Surname: Bartkus

E-mail: karolis.bartkus@mif.vu.lt

Education:

2013–2017	Vilnius University, Faculty of Mathematics and Informatics *Bachelor's degree in Financial and Actuarial Mathematics*
2017–2019	Vilnius University, Faculty of Mathematics and Informatics *Master's degree in Data Science*
2019–2025	Vilnius University, Faculty of Mathematics and Informatics *Ph.D. studies in Mathematics*

Work experience:

2025–to date	Software Engineer, Inbalance Grid
2023–2024	Data Scientist, Exacaster
2018–2023	Data Analyst, Exacaster
2017–2018	Data Analyst, State Tax Inspectorate

Teaching experience:

2025–to date	Lecturer, Vilnius University

PUBLICATIONS BY THE AUTHOR

A1 Bartkus, K.; Račkauskas, A. Changed segment tests via norm and Brownian projection. *Lith Math J* **2025**, *65*, 481–499. doi.org/10.1007/s10986-025-09699-7.

A2 Bartkus, K.; Račkauskas, A. Nonparametric changed segment detection in functional data. *Nonlinear Analysis: Modelling and Control* **2026**, *31(1)*, 194–211. doi.org/10.15388/namc.2026.31.44489.

NOTES

Vilniaus universiteto leidykla
Saulėtekio al. 9, III rūmai, LT-10222 Vilnius
El. p. info@leidykla.vu.lt, www.leidykla.vu.lt
bookshop.vu.lt, journals.vu.lt
Tiražas 15 egz.